THE UNIVERSITY OF CHICAGO

THE ROLE OF THE MICROBIOTA IN RETROVIRAL PATHOGENESIS

A DISSERTATION SUBMITTED TO

THE FACULTY OF THE DIVISION OF THE BIOLOGICAL SCIENCES

AND THE PRITZKER SCHOOL OF MEDICINE

IN CANDIDACY FOR THE DEGREE OF

DOCTOR OF PHILOSOPHY

COMMITTEE ON MICROBIOLOGY

BY

JESSICA SPRING

CHICAGO, ILLINOIS

JUNE 2022

TABLE OF CONTENTS

LIST OF FIGURES

LIST OF TABLES

ACKNOWLEDGEMENTS

My accomplishments over the past six years would not have been possible without the following people. These individuals contributed to my education, scientific advancements, and well-being.

The way that I think about, conduct, and evaluate science I owe to my PhD advisor and PhD mentor, Drs. Tanya Golovkina and Sasha Chervonsky. The dedication Tanya and Sasha have to science and teaching the next generation of scientists is awe inspiring. I have been lucky to be a part of Tanya's lab and given the opportunity to contribute to a project investigating host-pathogen interactions. I am immensely grateful to Tanya for her support over the last six years, enabling me to earn a PhD and produce a body of work I am proud of.

The efforts of two collaborators, Drs. Aly Khan and Sandeep Gurbuxani, were instrumental for this project. Aly analyzed the RNA-sequencing data and Sandeep analyzed the histology slides described in this document. I would like to thank them for their time and expertise.

I would like to thank those involved with the metabolomics project including collaborator Dr. Michael Fischbach from Stanford University and Dr. Brian DeFelice who conducted the mass spectrometry. Furthermore, I owe a large thanks to Vera Beilinson who analyzed the mass spectrometry data and created most of the figures in Chapter 4.

The generation of Rnf128- and Serpinb9b-deficient mice was done with the assistance of Dr. Steven Erickson, a previous member of the Bendelac lab at the University of Chicago. His knowledge and advice related to the generation of CRISPR-Cas9 genetically modified mice was instrumental to my project and I have no doubt will also be vital for my career.

A huge thank you to ARC workers and those that manage the gnotobiotic facility including Carrie Murczek, Jamie Kasper, and Kim Campbell. This project would have been impossible without them.

Members of my committee, Drs. Eugene Chang, Sasha Chervonsky, and Dominique Missiakas have provided support and rigorous scientific discussion during my committee meetings. Many thanks for their encouragement and assistance during this journey. Further thanks to Sasha, who has provided additional insight into my project.

During my tenure in the Golovkina lab, I have had the privilege of working with many bright and talented undergraduate students, including Yunisse Gonzalez, Zoe Strong, Grace Ryan, and Donna Tong. Isabelle Preddy was my first mentee and a constant source of laughs over her wild tales and mispronounced words. Many aspects of my project were made possible with the assistance of another mentee, Sophie Lara. She has been a pleasure to train and work with and I'm happy to be leaving my project in her very capable hands.

I had the pleasure of working with other scientists within the Golovkina and Chervonsky labs including Drs. Renee DePooter and Andrey Kuznetsov. Labmates Matt Funsten, Dr. Helen Beilinson, Jean Lee, and Emily Cullum helped make my time in lab a fun and enjoyable experience. I am grateful to Helen and Jean for their constant kindness, advice, and conversations. I owe much of my sanity to Emily Cullum whose jokes and comments kept me going day to day and reminded me to not take myself so seriously.

When I arrived at the University of Chicago, I met the other seven students, all women, pursuing PhDs in microbiology. The 'Micro girls' immediate friendship and support was, and still is, invaluable. Some of my favorite memories from our first year are spending time between classes solving the New York Times crossword puzzles Dr. Andrea Watson subscribed to. I am indebted to Dr. Andrea Watson, Rebecca Reis, and Taryn Serman for the nights of trivia and dancing that made for a fun and eventful PhD.

I owe all my achievements to my incredible, loving parents, Lynette Spring and Dr. Robert Spring. My parents have always encouraged me to pursue my dreams and offered me every opportunity available. They instilled in me a sense of wonder and curiosity that has carried

over into my career as a scientist. Their unwavering support for all my endeavors cannot be expressed in words.

Finally, I would like to thank my husband Aaron Shrader for his unconditional support of me and all my goals.

ABSTRACT

The influence of the microbiota on viral transmission and replication is well appreciated. However, its impact on retroviral pathogenesis outside of transmission/replication control remained unknown. Using Murine Leukemia Virus (MuLV), we found that some commensal bacteria promoted the development of leukemia induced by this retrovirus. The promotion of leukemia development by commensals was due to suppression of the adaptive immune response through upregulation of several negative regulators of immunity. These negative regulators included Serpinb9b and Rnf128, which are associated with a poor prognosis of some spontaneous human cancers. Upregulation of Serpinb9b was mediated by sensing of bacteria by NOD1/NOD2/RIPK2 pathway. Using an unbiased metabolomics approach, we also identified various metabolites whose presence and abundances in the periphery is mediated by both bacterial colonization and MuLV infection. Highlighting the potential for metabolites to also influence virally induced leukemia development. This work describes a novel mechanism by which the microbiota enhances tumorigenesis within gut-distant organs and points at potential new targets for cancer therapy.

INTRODUCTION

Commensal microbiota

From birth, humans are colonized with a diverse and complex population of microorganisms including bacteria, viruses, fungi, archaea, and protozoans, collectively called the microbiota. Every surface of the human body exposed to the external world is colonized with microbes including the skin, genitourinary tract, and gastrointestinal tract. The human gastrointestinal tract is major site of colonization and is estimated to house over 10^{14} microbial organisms (Singh et al., 2017). Composition of the microbiota established during initial colonization can be affected by birth route and feeding method (Thursby & Juge, 2017). While microbial communities are stable in adult humans (David et al., 2014), factors encountered throughout a person's lifetime such as infection, antibiotic use, diet, sanitation, and urban/rural living can affect microbial composition (Carmody et al., 2015; David et al., 2014; Dethlefsen et al., 2008; Singh et al., 2017; Sonnenburg et al., 2016). However, the microbial composition generally returns to the pre-perturbed state after exposure with the exception of some microbial species (David et al., 2014; Sonnenburg et al., 2016). Additionally, host genetics also contribute to the composition of the microbiota. In humans, monozygotic twins have more similar microbiotas than dizygotic twins (Goodrich et al., 2014). Furthermore, mice of different genetic backgrounds associated with the same complex microbial input exhibit differences in what bacterial species stably colonize the gastrointestinal tract (Khan et al., 2019).

The majority of these microorganisms are non-pathogenic, coexisting as symbionts and supporting host health. Bacteria assist in breaking down nutrients and producing vitamins for the host to utilize (Thursby & Juge, 2017). One well studied example is the production of short chain fatty acids (SCFAs) via commensal bacteria and its influence on intestinal epithelial cellular processes and metabolization by colonocytes for energy (Thursby & Juge, 2017; Topping & Clifton, 2001). Intestinal barrier function, encompassing intestinal epithelial cell turnover and renewal, mucus and antimicrobial peptide production, and antibody secretion, is also supported by the microbiota. Germ-free (GF) mice, which lack all microorganisms, exhibit reduced epithelial cell

turnover and have lower production of mucus that prevents penetration of intestinal bacteria into the underlying epithelium (Natividad & Verdu, 2013; Thursby & Juge, 2017). Antimicrobial peptides exert a wide range of antimicrobial activity and can directly kill bacterial cells (Thursby & Juge, 2017). Baseline expression of antimicrobial proteins are maintained in GF mice, but expression of certain antimicrobials are increased in conventionally housed mice, suggesting the expression of these factors is modulated by the microbiota (Natividad & Verdu, 2013). GF mice also present with underdeveloped Peyer's patches and other lymphoid organs including spleen, thymus, and gut-associated lymphoid structures, resulting in reduced $CD4^+$/$CD8^+$ cells (Gensollen et al., 2016; Jandhyala et al., 2015). Needless to say, the microbiota plays a vital role in maintaining host health and supporting the development and maturation of the immune system.

Commensal microbiota and pathogens

Finally, one of the most important properties the commensal microbiota confers is the resistance of colonization by pathogenic microorganisms. The commensal microbiota support colonization resistance of pathogens by occupying the space, utilizing available nutrients, and activating the production of antimicrobial peptides and other host defenses (Buffie et al., 2015). This is clearly shown in GF mice, where the absence of the microbiota increases susceptibility to enteric pathogens including *Shigella flexneri, Citrobacter rodentium, Listeria monocytogenes,* and *Salmonella enterica* (Bäumler & Sperandio, 2016).

The interplay between the microbiota and bacterial pathogens has been well appreciated and studied for decades. However, it was recently discovered that the microbiota also influences viral infections. The Golovkina lab demonstrated dependence of the microbiota for transmission of a mucosally transmitted mouse retrovirus (Kane et al., 2011). It was determined MMTV binds to lipopolysaccharide (LPS) derived from commensal bacteria through incorporation of LPS-binding proteins into the viral envelope upon budding from the host cell. MMTV bound LPS initiates immune tolerance through production of cytokine IL-10 to inhibit the anti-viral response. Therefore, in the absence of microbiota derived LPS, the anti-viral immune response mediated by

neutralizing antibodies, prevents transmission of the virus from infected mothers to nursing progeny (Kane et al., 2011; Wilks et al., 2015).

Concurrently published, the Pfeiffer lab showed the influence of the microbiota on transmission and pathogenesis of two enteric viruses, poliovirus and reovirus (Kuss et al., 2011). Replication of the virus was significantly hindered, and survival enhanced in antibiotic treated mice compared to untreated mice. Incubation of microbially derived components including LPS, lipoteichoic acid, peptidoglycan, and chitin with poliovirus prior to infection of cells *in vitro* significantly increased poliovirus infectivity. The authors were able to show that microbially derived factors enhanced the ability of poliovirus to adhere to host cells, and therefore, likely increased infectivity.

Another study found that while enteric norovirus did not rely upon the microbiota for initial intestinal infection, the microbiota was required for the virus to establish a persistent infection in mice (Baldridge et al., 2015). Furthermore, they found the IFN-λ pathway controlled the clearance of persistent norovirus infection in antibiotic treated mice. Based on these data, the authors suggest the microbiota suppresses the efficacy of the IFN-λ innate immune response enabling persistence (Baldridge et al., 2015). Additionally, rotavirus replication and shedding were reduced, and diarrhea incidence was ameliorated in antibiotic treated mice compared to untreated mice due to an enhanced antibody response (Uchiyama et al., 2014). And in stark contrast, it was demonstrated that microbially derived products such as LPS, and to a lesser extent peptidoglycan, promoted the generation of T cell specific responses against influenza A virus, suppressing viral titers in the lung (Ichinohe et al., 2010). Overall, these studies demonstrate not only that many factors derived from commensal microorganisms promote or suppress viral infection, but that the microbiota affects the pathogenesis and/or transmission of viruses from a range of families through a variety of mechanisms.

Cancer

Aside from its influence on bacterial and viral infections, the microbiota has been shown to contribute to other disease states such as cancer. For example, early studies using germ-free rats found the intestinal microbiota promoted chemically induced spontaneous colon tumor development (Reddy et al., 1975). Three steps of cancer development are widely accepted: initiation, promotion, and progression, and microorganisms have been suggested to impact cancer development at all three stages (Casasanta et al., 2020; Guidi et al., 2013; He et al., 2019; Lopez et al., 2021). Cancer initiates from genetic alterations through germline inheritance of mutations or sporadic mutations in tumor suppressor and/or activation of oncogenes leading to abnormal and uncontrolled proliferation of cells (Lee & Muller, 2010). Tumor suppresser genes regulate cell growth. Therefore, mutation of these genes leads to dysregulation of the cell cycle and cell proliferation (Lee & Muller, 2010). Oncogenes are genes that promote cellular replication (Lee & Muller, 2010). In cancer, the protein product of the oncogene exhibits a gain of function, promoting uncontrolled and unregulated cell replication (Lee & Muller, 2010).

The promotion stage of cancer development involves reduced cell death and sustained proliferation of the precancerous cells with an accumulation of mutations necessary for further cancer development. To accomplish this, inflammatory cytokines are produced and trigger transcription factors such as NF-κB, STAT3, and AP-1 to stimulate cell proliferation and survival (Grivennikov et al., 2010; Whiteside, 2008). Furthermore, reactive oxygen species produced by inflammatory cells support cell proliferation and cause double-stranded DNA breaks, promoting genetic instability (Liou & Storz, 2010). Additionally, tumor associated macrophages recruited to the tumor by chemokines, secrete epidermal growth factor to promote cell proliferation and vascular epidermal growth factor to support angiogenesis (Gonzalez et al., 2018; Grivennikov et al., 2010).

Finally, in the progression stage, the cancer continues to acquire mutations and produce factors, such as TGF-β, that promote tumor motility, intravasation into the circulatory and lymphatic system, and metastasization (Grivennikov et al., 2010).

Microbiota and cancer

Microbes contribute to cancer development via three general mechanisms: modulating cell proliferation and death, altering the function of the immune system, and influencing metabolism of various compounds (Garrett, 2015). The study of microbiota influence on carcinogenesis is vast and has been applied to cancers of various etiologies manifesting in many locations (Eslami-S et al., 2020; Jain et al., 2021; Rakoff-Nahoum & Medzhitov, 2007; Riquelme et al., 2019; Sivan et al., 2015; Vetizou et al., 2015; Yoshimoto et al., 2013; Yu & Schwabe, 2017). Models used for these studies are generally carcinogen induced tumors or genetically engineered mouse models with a pre-disposition for tumor development. Most of these studies have focused on cancers that develop proximal to the intestinal microbiota such as colon and liver cancers. Dysbiosis of the microbiota leading to metabolic alterations or chronic inflammation influences the incidence and progression of genetic and carcinogen induced intra-intestinal and intestinal proximal cancers (Zitvogel et al., 2015). A well-studied example of this phenomenon is colorectal cancer (CRC). CRC results from the accumulation of genetic mutations, with the microbiota as a major risk factor (Sabit et al., 2019). Many bacterial species in mouse models have been shown to modulate CRC initiation/progression through direct action disrupting the integrity of the intestinal epithelial barrier or production of compounds that induce DNA damage, modulate the immune response, or generate reactive oxygen species (ROS) which promote inflammation (Sabit et al., 2019). The liver is connected to the gut via the portal vein, allowing microbial associated molecular patterns (MAMPs) and microbial metabolites originating in the gut to reach the liver (Yu & Schwabe, 2017). As mentioned above, dysbiosis of the gut resulting in loss of intestinal barrier integrity and subsequent leaky gut can contribute to inflammation and the development of liver diseases leading to hepatocellular carcinoma (HCC) (Yu & Schwabe, 2017). Dextran sulfite sodium (DSS) induced gut leakage in mice leads to increased levels of systemic bacterial derived LPS and promotion of HCC (Achiwa et al., 2016). Furthermore, in a model of chemical carcinogen induced HCC, mice on a high-fat diet compared to mice on a normal fat diet, had increased levels of deoxycholic acid (DCA), a bacterial metabolite known to induce DNA damage (Yoshimoto et al.,

2013). DCA was found to promote inflammation and HCC development in mice after treatment with a chemical carcinogen (Yoshimoto et al., 2013). These brief examples illustrate how bacteria, and their microbial products, influence the host and can greatly affect development of tumors connected to the gut.

How the microbiota affects tumor development at site distal from the gut microbiota is an open field of investigation. Studies investigating the impact of the microbiota on tumor development distal from the gut often observe leakiness of the gut enabling translocation of bacteria or their products from the gut to the periphery or microbial modulation of the anti-tumor immune response (D'Alessandro et al., 2020; Meisel et al., 2018; Sivan et al., 2015). However, many studies investigating the impact of the microbiota on distal tumors rely on transplanted tumors/tumor cells in mice which often exhibit characteristics of progression, genetic heterogeneity, and response to therapies amongst many other factors different compared to the spontaneous or inborn cancers that develop in humans (Coffelt & de Visser, 2015; Guerin et al., 2020; Jain et al., 2021; Olson et al., 2018).

As described above, tumors can result from inborn mutations in tumor suppressor/oncogenes or spontaneously from carcinogens, radiation, or infections. Around 20% of all human cancers are caused by infections and around 12% are caused by viral infections (White et al., 2014). Namely, Epstein-Barr virus, Hepatitis B virus, Hepatitis C virus, Human papillomavirus, Kaposi’s sarcoma herpesvirus, Human T-cell lymphotrophic virus, and Merkel cell polyomavirus (White et al., 2014). All of these viruses encode their own viral oncogenes that confer genetic changes or regulate cell proliferation/death which contribute to carcinogenesis (White et al., 2014).

Due to the known influence of the microbiota on non-virally induced cancers, the influence of the microbiota on the development of cancers via oncogenic viral infections is of great interest. However, it is very difficult to assign causality of the microbiota in human oncogenic viral infections. Studies examining a role of the microbiota in carcinogenesis induced by these human viruses are limited in number and rely upon transgenic mice or *in vitro* experiments (Fox et al.,

2010; Imai et al., 2012; Morris et al., 2007). Therefore, an alternative method of studying the role of the microbiota on carcinogenesis induced by viral infections is through the use of animal models paired with animal viruses. While such studies do not directly address how human commensals contribute to human oncogenic viral infections, pathways identified using animal models of virally induced tumors many prove useful therapeutic targets for both virally and non-virally induced cancers.

Retroviruses

Investigations into microbial influence on virally induced tumorigenesis using animal models began to be thoroughly tested in the 1960s with the advent of GF animals (Mishra et al., 2021). Studies at this time made use of murine retroviruses. Retroviruses are enveloped, positive sense single-stranded RNA (ssRNA) viruses belonging to group VI of the Baltimore classification system (Maeda et al., 2008). Upon entry of the virus into a host cell, the ssRNA is reverse transcribed by a virally encoded reverse transcriptase to double-stranded DNA (dsDNA). The dsDNA is subsequently integrated into the host genome as a provirus. Integration is necessary for viral replication. From the provirus, the viral genetic material is transcribed and translated by host machinery to produce virions which upon exiting from the host cell can infect other susceptible cells (Robinson, 1982).

Retroviruses that confer tumorigenesis fall into two categories: acute and non-acute transforming. Acute transforming viruses have virally encoded oncogenes that promote carcinogenesis (Robinson, 1982). Viral oncogenes are derived from host cellular proto-oncogenes and are constitutively active through loss or mutation of sequences required for its regulation (Robinson, 1982; Vogt, 2012). Tumors that develop from these infections typically arise very quickly and are polyclonal (Coffin et al., 1997). Non-acute transforming viruses do not encode viral oncogenes. Rather, they induce tumorigenesis via proviral insertional mutagenesis. This involves proviral integration near a cellular proto-oncogene and its subsequent upregulation. This is accomplished by promoter and enhancer elements within the proviral long terminal repeats (LTRs)

which drive upregulation of the cellular proto-oncogene (Coffin et al., 1997; Maeda et al., 2008). As integration near a cellular proto-oncogene is a rare and stochastic event, monoclonal tumors arise after a latent period (Coffin et al., 1997).

While retroviruses can generally infect many cell types, those that are oncogenic preferentially induce a single type of tumor. For retroviruses carrying viral oncogenes, this is mediated by specific interactions between the viral oncogene and cell specific co-factors or transcription factors (Coffin et al., 1997). Retroviruses that cause cancer via insertional mutagenesis, confer cell specificity through components of the LTRs. Specifically, host factors such as transcription factors inherent to certain cell types interact with LTRs to direct transcription of the proviral sequence within specific cell types (Coffin et al., 1997). Enhanced expression of the provirus and consequently a nearby cellular protooncogene within a particular cell type may lead to unregulated cell cycling and eventually tumor development.

Proviral integration into the host genome and expression of viral oncogenes or upregulation of cellular proto-oncogenes are the first necessary step for retroviral induced tumorigenesis. As cancer development is a multi-step process, other events are required for retrovirally induced cancer (Coffin et al., 1997; Compere et al., 1988; Robinson, 1982). This is exemplified in the instance of transgenic mice expressing oncogenes. These mice generally develop spontaneous tumors in the tissues that express the oncogene. However, not all animals develop tumors, the rate of tumor development varies, and not all cells within the tissue expressing the oncogene become tumors. Indicating the expression of an oncogene is not sufficient for tumor development (Adams & Cory, 1991). Therefore, it is likely that additional factors contribute to virally induced tumorigenesis.

Microbiota and retrovirally induced tumorigenesis

Beginning in the 1960s, researchers began studying the effect of the microbiota on the main pathogenesis of exogenous oncogenic retroviruses: tumor development. Due to the subject

matter of this dissertation, I will be focusing on those that utilized murine leukemia virus (MuLV) as a model oncogenic retrovirus. MuLVs do not encode viral oncogenes, and therefore initiate cancer through insertional mutagenesis. In 1963, disease development in conventionally housed and GF Hauschka-Mirand/ICR Swiss mice infected with Friend MuLV was determined. GF mice exhibited increased susceptibility and decreased latency to leukemia development, compared to conventionally housed mice (Mirand & Grace, 1963).

Nearly a decade later, a similar experiment was conducted using conventionally housed and GF BALB/c mice infected with Friend MuLV. Contrary to what was observed by Mirand and Grace, these authors observed increased resistance in GF mice compared to conventionally housed animals (Kouttab & Jutila, 1972). Nearly all (93%) infected conventionally housed mice died during the course of the experiment compared to only 13% of GF infected mice. Furthermore, necropsies of the infected conventionally housed mice revealed a loss of splenic architecture and an accumulation of lymphocytes within the spleen. GF infected mice exhibited a slight increase in lymphocyte counts and changes in the splenic architecture, but to a lesser degree than infected conventionally housed mice.

Another study also investigated the contribution of the microbiota to MuLV pathogenesis. This study utilized conventionally housed and GF BALB/c mice infected with Moloney MuLV (M-MuLV). Comparable to the study conducted in 1970, this investigation also found that GF mice were significantly more resistant to M-MuLV induced leukemia compared to conventionally housed mice (Isaak et al., 1988). Where conventionally housed mice succumbed to fatal leukemia by 18 weeks post infection, all GF mice were alive at 18 weeks and only started succumbing to virally induced tumorigenesis at 26 weeks post infection (Isaak et al., 1988). Interestingly, the researchers noted production of infectious M-MuLV in the spleen, lymph node, thymus, and bone marrow were not different between mice with or without a microbiota. Indicating the increased resistance to M-MuLV induced leukemia development observed in GF mice compared to conventionally housed mice was not due to a decreased number of viral permissive cells or their virus replicating capability (Isaak et al., 1988).

While it generally appears that the microbiota promotes MuLV induced tumorigenesis, these prior studies utilized different strains of mice and various MuLV variants. Making it difficult to conclude the effect of the microbiota on MuLV pathogenesis. Furthermore, these studies did not observe pathogenesis in mice infected with the virus via natural routes. Mice were infected through intraperitoneal injection rather than acquiring the virus through the blood or mucosa. Third, the researchers only investigated pathogenesis of the virus in injected mice. Therefore, it is unclear whether the microbiota effects transmission of MuLV as well as the pathogenesis. Additionally, these studies were conducted with viral preps that were likely contaminated with lactate dehydrogenase elevating virus (LDV) (Dittmer et al., 2019; Hanna et al., 1970). LDV has been shown to suppress and delay $CD8^+$ T cell response against Friend MuLV, prolonging acute viral infection (Robertson et al., 2008). Furthermore, at that pre-PCR and sequencing era, the sterility of the experimental isolators was tested only using culturing techniques (Kouttab & Jutila, 1972). Thus, unculturable bacteria could have been missed.

Based on the known influence of the commensal microbiota on cancer development and the potential impact it could have on virally induced tumorigenesis, we decided to undertake a study to fully understand the role of the microbiota in retroviral pathogenesis.

OUTLINE

In Chapter 1, we begin investigating the influence of the microbiota on MuLV pathogenesis. We determine that the commensal microbiota, specifically bacteria, promote MuLV induced leukemia development. Furthermore, we show that the microbiota suppresses the adaptive immune response enabling the development of leukemia in SPF infected mice.

Next, in Chapter 2, we explore the mechanism by which the microbiota supports leukemia development. From the results of an RNA-seq experiment we identify two negative immune regulators, whose expression is mediated by the presence of the microbiota and MuLV infection and contribute to MuLV induced leukemia development.

In Chapter 3, we examine the means by which the host detects tumor promoting microbially derived factors. Using a biased genetic approach, we found that innate immune sensor Capase1/11 and innate immune sensing adaptor RIPK2 modulate leukemia development through the upregulation of a negative immune regulator identified in Chapter 2.

As previously described, both microbially derived structural compounds as well as metabolites can influence cancer development. Therefore, in Chapter 4, we utilized an unbiased metabolomics approach to identify metabolites differentially abundant in the presence of MuLV and a bacterium with the goal of identifying metabolites that contribute to MuLV induced leukemogenesis.

Herein we demonstrate that the microbiota modulates virally induced tumorigenesis that manifests distal from the gut in a sterile organ. Therefore, we were interested in whether the microbiota influences tumorigenesis in models of inborn mutations where tumors also manifest distal from the gastrointestinal system. In Chapter 5, *Trp53* deficient mice, a model of tumor suppresser mutagenesis, and Wnt1 transgenic mice, a model of oncogene dysregulation, were rederived as GF and monitored for tumor development and compared to their conventionally housed counterparts. These data suggest the commensal microbiota may not impact the development of tumors distal from the gut in models of genetic predisposition.

MATERIALS AND METHODS

Mice

Mice utilized in this study were bred and maintained at the animal facility of The University of Chicago. B6.129S2-*Trp53*^{tm1Tyj}/J (B6.Trp53$^{-/-}$), FVB.Cg-Tg(Wnt1)1Hev/J (FBV.wnt1Tg), and C.129S7(B6)-*Rag1*^{tm1Mom}/J, were purchased from The Jackson Laboratory (TJL). CByJ.129S2(B6)-IL6^{tm1Kopf}/J, purchased from TJL were crossed to BALB/cJ mice and the resulting F1 mice were intercrossed to generated -/- and +/+ littermate mice used in the studies. Similarly, C.C3-*Tlr4*$^{Lps-d}$/J, C.129(B6)-*Tlr2*^{tm1Kir}/J, B6N.129S2-*Casp1*^{tm1Flv}/J, and B6.129S1-*Ripk2*^{tm1Flv}/J mice were purchased from TJL and backcrossed to BALB/cJ mice for 10 generations to create TLR4$^{-/-}$, TLR2$^{-/-}$, Caspsae1/11$^{-/-}$, and RIPK2$^{-/-}$ mice, respectively, on the BALB/cJ background.

Serpinb9b$^{-/-}$, Rnf128$^{-/-}$, VSig4$^{-/-}$, CD4$^{-/-}$, CD8$^{-/-}$, and CD4$^{-/-}$CD8$^{-/-}$ BALB/cJ mice were generated using a CRISPR/Cas9 approach. VSig4$^{-/-}$ mice were generated by TJL. To generate VSig4$^{-/-}$ mice, two guide RNAs targeting exon 1 (5'AGAAGTAGCTTCAAATAGGATGG3' and 5'TGAGCACTATTAGGTGGCCCAGG3') were used. Five distinct BALB/cJ VSig4$^{-/-}$ lines were produced. Primers flanking exon 1 (5'CCAGAACAAATGGTTTCCCTAG3' and 5'TTGGAGTCCTCTGACATCCC3') were used to genotype the founder mice and subsequent offspring.

The following mice generated via CRISPR/Cas9 technology were made at the University of Chicago transgenics core. Injection mixtures were provided to the core for injection into embryos at the single cell stage. For all injections conducted at the University of Chicago, crRNAs (IDT) were resuspended in 0.1X TE to 1µg/µl (resuspension volumes were calculated using IDT resuspension calculator). tracrRNA (IDT) was also resuspended in 0.1X TE to a concentration of 1µg/µl. Guide RNA (gRNA) was prepared by mixing 5µg of crRNA with 10µg of tracrRNA. These components were annealed in a thermocycler (95°C for five minutes, ramping down to 25°C at a rate of 5°C per minute). gRNAs were diluted in embryo water to a final concentration of 75ng/µl

per gRNA. For genetically modified mice generated using two gRNAs, the injection mixture contained Cas9 nuclease at a final concentration of 150ng/µl. For mice generated via CRISPR/Cas9 using four gRNAs, the injection mixture contained Cas9 nuclease at a final concentration of 300ng/µl. To form the ribonucleoprotein complex (RNP), the gRNA plus Cas9 mixture was incubated at room temperature for ten to fifteen minutes. The injection mixture was centrifuged at 20,000g for 10 minutes at 4°C. The top 65µl was transferred to a new tube and provided to the transgenics core for injection.

To generate Serpinb9b$^{-/-}$ mice, two guide RNAs were used to target exon 2 (5'TATGGTCCTCCTGGGTGCAA3' and 5'TTCCACCCTAGTTGTTACTC3'). Genotyping was performed using two primers flanking exon 2 (5'TTTCCCTCCAGACTCTGCA3' and 5'GAGAAGCATGAGGCCAAGAC3'). Two lines of Serpinb9b$^{-/-}$ mice were produced. For the generation of BALB/cJ Rnf128$^{-/-}$ mice, one guide RNA was used to target exon 4 (5'AGGATGCGCACCAAATCATT3'). Genotyping was accomplished with two primers surrounding exon 4 (5'AGTCACACCTCACTCTTTATCCA3' and 5' TCGAGAACAAACTGTACCGGA3') One line of Rnf128$^{-/-}$ mice was developed.

Two guides were used to target exon 3 (5' AAGGTGTATTAATTAGAGGT3' and 5' ACCCGCAAAGGATGGGACAT3') of CD4 to generate CD4$^{-/-}$ mice. CD4$^{-/-}$ mice were genotyped using primers flanking exon 3 (5'CATGCACTGAGGTGTGTGTG3' and 5' GGATGGGACATAGGGAGACA3'). One line of CD4$^{-/-}$ mice were generated. CD8$^{-/-}$ mice were generated using two guides targeting exon 1 of CD8 (5'TGAAGCCATATAGACAACGA3' and 5'AATTCTATCCTGGAGCCAAC3'). Genotyping of CD8$^{-/-}$ mice was conducted using primers flanking exon 1 (5' CCCCTAAAAGGTGGTTGACA3' and 5' GGATACGTGCTGGGCTACTC3'). Two lines of CD8$^{-/-}$ mice were produced. CD4$^{-/-}$CD8$^{-/-}$ mice were generated by using both CD4 and CD8 guide RNAs. The one line of CD4$^{-/-}$CD8$^{-/-}$ mice produced were genotyped using primers as listed above. Founder VSig4$^{-/-}$, Serpinb9b$^{-/-}$, Rnf128$^{-/-}$, CD4$^{-/-}$, CD8$^{-/-}$, and CD4$^{-/-}$CD8$^{-/-}$ mice were crossed to BALB/cJ mice for at least two generations. Heterozygous mice were then intercrossed

to produce homozygous knockout (KO) and wild-type (WT) littermate animals used in subsequent studies.

Mice were genotyped using tail or ear tissue. Tissue was digested in 150µl of tail solution (1X STE 0.05% lauryl sarcosine) supplemented with 0.2mg/ml of proteinase K. Tissue was digested in a water bath overnight at 55°C then incubated at 85°C for 45 minutes to inactivate the proteinase K. Digested samples were stored at 4°C until genotyping was completed.

The knockout allele in genetically modified mice was analyzed by sequencing. Genotyping PCR products were prepared for sequencing using the ExoSAP-IT PCR product Cleanup (Thermo Fisher Scientific) as per manufacturer's instructions.

Males and females were used at ~50:50 ratio in all experiments. The studies outlined here have been reviewed and approved by the Animal Care and Use Committee at The University of Chicago.

Antibiotic treatment

BALB/cJ females injected intraperitoneally (i.p.) with 1 x 10^3 plaque forming units (pfus) of RL-MuLV were bred with BALB/cJ males to produce infected generation 1 (G1) animals. The G1 mice were weaned onto water containing the following antibiotic mixture: kanamycin (4 mg/ml), gentamicin (3.5 mg/ml), colistin (8500 U/ml), metronidazole (2.15 mg/ml), and vancomycin (4.5 mg/ml) for the duration of the experiment. When the mice became symptomatic (anemic, lethargic, enlarged abdomen), they were sacrificed and assessed for leukemia development. All animals were sacrificed by 5 months of age. The efficacy of the antibiotic-treatment protocol was evaluated by periodical bacteriologic examination of feces. Fresh fecal samples from antibiotic-treated and control mice were vortexed in TSA broth (0.1g in 1ml) and plated on BBL plates. Plates were incubated for 48h at 37°C under both aerobic and anaerobic conditions. Anaerobic growth conditions were created using a COY anaerobic chamber (Grass Lake, MI). There were no detectable colony forming units (CFUs) on either aerobic or anaerobic plates from the antibiotic

treated animals. The plates from the untreated animals had 10^7 CFUs and 8 x 10^5 CFUs of anerobic and aerotolerant bacteria per 1g of feces, respectively.

Monitoring sterility in GF isolators

BALB/cJ, BALB/cJ RAG1$^{-/-}$, B6.Trp53$^{-/-}$, FVB.wnt1Tg, BALB/cJ CD4$^{-/-}$, BALB/cJ CD8$^{-/-}$, BALB/cJ CD4$^{-/-}$CD8$^{-/-}$, BALB/cJ RIPK2$^{-/-}$, and BALB/cJ Caspase1/11$^{-/-}$ mice were re-derived as germ-free (GF) at Taconic and housed in sterile isolators at the gnotobiotic facility at the University of Chicago. Sterility of GF isolators was assessed as previously described (Wilks et al., 2014). Briefly, fecal pellets were collected from isolators weekly and quickly frozen. DNA was extracted using a bead-beating/phenol-chloroform extraction protocol. A single fecal pellet was placed in an autoclaved 2ml screw-cap tube containing 0.1mm zirconium beads. 500µl of 2X buffer A (filter sterilized 200mM NaCl, 200mM Tris, 20mM EDTA), 210µl of 20% SDS, and 500ul of phenol:chloroform, were added to the screw cap tube. The tube was bead beat on high for 2 minutes followed by centrifugation at 8,000 rpm at 4°C for 3 minutes. The aqueous phase was removed and placed into a new Eppendorf tube. 500µl of phenol:chloroform was added to the aqueous phase and subsequently spun at 13,000 rpm at 4°C for 3 minutes. The aqueous phase was removed and mixed with 40µl of 3M sodium acetate pH 7 and 400µl of -20°C isopropanol. The suspension was spun at 13,000 rpm at 4°C for 10 minutes. The supernatant was dumped followed by the addition of 500µl of -20°C 80% ethanol. The sample was again centrifuged at 13,000 rpm at 4°C for 5 minutes. The supernatant was dumped, and the sample was vacuum dried for 10 minutes. The pellet was resuspended in 1,000µl of sterile water and left overnight at 4°C. A set of primers that broadly hybridize to bacterial 16S rRNA gene sequences (5'GACGGGCGGTGWGTRCA3' and 5'AGAGTTTGATCCTGGCTCAG3') were used to amplify isolated DNA. In addition, microbiological cultures were set up with GF fecal pellets, positive control SPF fecal pellets, sterile saline (sham), and sterile culture medium (negative control). BHI, Nutrient, and Sabbaroud Broth tubes were inoculated with samples and incubated at 37°C and

42°C aerobically and anaerobically. Cultures were followed for five days until cultures were deemed negative.

Colonization of GF mice

GF BALB/cJ mice were colonized with the ASF consortium (Sarma-Rupavtarm et al., 2004) via oral gavage of suspended cecal contents from donor mice. All but one species (ASF360, *Lactobacillus acidophilus*) was found in the ASF-colonized mice. *Lactobacillus murinus* (*L. murinus*, ASF361) and *Parabacteroides goldsteinii* (*P. goldsteinii*, ASF519) were isolated from the ASF consortium. *L. murinus* was isolated by plating suspended fecal matter from ASF-colonized mice onto de Man, Rogosa and Sharpe agar (MRS) (Thermo Fisher Scientific), a selective media for *Lactobacilli.* Growth of *L. murinus* was confirmed by PCR. *P. goldsteinii* was isolated by plating fecal matter from ASF colonized mice re-suspended in PBS onto brain heart infusion supplemented (BHIS) media, supplemented with hemin and vitamin K1, and grown in an anaerobic chamber. Growth of *P. goldsteinii* was confirmed by PCR. *Bacteroides thetaiotaomicron* (*B. theta*) was grown on tryptone yeast extract glucose (TYG) media in an anaerobic container. *Enterococcus faecalis (E. faecalis)* a gift from Dr. Gary Dunni (University of Minnesota) was grown on BHI. *Parabacteroides goldsteinii* strain CL02 and *Parabacteroides distasonis* strain ATCC 8503, a gift from Dr. Laurie Comstock, were grown in BHI supplemented with vitamin K1, hematin, and cysteine. *L. murinus, P. goldsteinii* (ASF519)*, E. faecalis,* and *B. theta* were introduced to GF BALB/cJ mice by oral gavage of 200μl of overnight liquid culture grown from single colonies. For *P. goldsteinii* (CL02) and *P. distasonis* (ATCC 8503), bacteria were grown on agar plates for two or three days respectively. Bacteria were scraped off the plate and resuspended in sterile PBS. 200μl of resuspended bacteria was introduced into GF BALB/cJ mice by oral gavage. Successful colonization was confirmed via PCR using primers specific for each individual bacterium or 16S rRNA primers followed by sequencing of the PCR product.

Virus isolation, infection, and leukemia monitoring

Rauscher-like Murine Leukemia Virus (RL-MuLV) which consists of N, B tropic ecotropic and mink cell focus forming (MCF) virus (Hook et al., 2002) was isolated from tissue culture supernatant of chronically infected SC-1 cells (ATCC CRL-1404). Supernatants from infected SC-1 cells were combined with 3X polyethylene glycol (PEG) at a ratio of 2:1 and stirred at 4°C overnight. The mixture was centrifuged at 10,000 rpm for forty minutes at 4°C in 250ml bottles using an SLA-3000 fixed angle rotor. Pellets were resuspended in PBS and spun through a 30% sucrose cushion at 31,000 rpm in a TW55.1 bucket rotor for 1 hr at 4°C. The pelleted fraction was resuspended in 1ml of PBS and spun at 5000 rpm for 5 minutes. Supernatant was transferred to a new tube and viral titer was determined using XC infectious center assay (see below). The virus was tested for hepatitis virus, mouse thymic virus, mouse parvovirus, pneumonia virus of the mouse, polyomavirus, mammalian orthoreovirus serotype 3, enzootic diarrhea virus of infant mice, Sendai virus, *Mycoplasma (M) pulmonis*, *M. arginine*, *M. arthritidis*, *M. bovis*, *M. cloacale*, *M. falconis*, *M. faucium, M. fermentans, M. genitalium, M. hominis, M. hyorhinis, M. hyosynoviae, M. opalescens, M. orale, M. pirum, M. pneumonia, M. salivarium, M. synoviae, Acholeplasma laidlawii*, *Ureaplasma urealyticum,* cilium-associated respiratory bacillus, ectromelia virus, encephalitozoon cuniculi, Theiler's murine encephalomyelitis virus, Hantaan virus (Korean hemorrhagic virus), lymphocytic choriomeningitis virus, lactate dehydrogenase enzyme, minute virus of the mouse, mouse adenovirus, and mouse cytomegalovirus and was found to be negative for all the pathogens.

Ecotropic virus titers in the RL-MuLV mixture were determined by an XC infectious center assay as described below (Rowe et al., 1970). 1 x 10^3 pfus of the virus isolated from supernatants of infected SC-1 cells were injected i.p. into 6-8 week-old BALB/cJ mice (G0 mice). Mice were bred to produce G1 animals which were used as a source of the virus for all experiments. The virus was not passaged beyond G1 *in vivo*. To isolate the virus, splenic homogenates of non-leukemic 2-3-month-old G1 mice were centrifuged at 2,000 rpm for 15 min at 4°C. The

supernatant was layered onto a 30% sucrose cushion and spun down at 31,000 rpm using a TW55.1 bucket rotor for 1 hr at 4°C. The pelleted fraction was resuspended in PBS, which was spun at 10,000 rpm at 4°C to remove insoluble material. The resulting supernatant was aliquoted and stored at -80°C.

Splenic derived RL-MuLV was diluted in sterile PBS and filtered through a sterile 0.22μm membrane in a laminar flow hood. 1 x 10^3 pfus were injected i.p. into GF and SPF BALB/cJ control females. For gnotobiotic experiments, females were injected i.p. with 1 x 10^3 pfus of filter sterilized virus. SPF BALB/cJ mice were also infected as control for experiments with gnotobiotic mice. For genetically altered mice, KO females were injected i.p. with 1 x 10^3 pfus. WT littermates and non-littermate BALB/cJ mice bred in the colony were infected as controls. Infected females were put in mating to generate G1 animals. G1 mice were aged and monitored for leukemia development which included signs of lethargy, hunched back, ruffled/unkempt fur, distended abdomen, and anemia. Symptomatic mice were sacrificed. All mice were sacrificed by 5 months, at the conclusion of the experiment. Survival curves indicate symptomatic mice that were closed during the experiment. The survival curve for SPF mice is a cumulative curve generated over the course of the entire studies using BALB/cJ mice. Wild-type littermates were used for each of the experimental groups of mice and their survival curves were compared with the curve for SPF mice to ensure that the leukemia development rate is the same (Figures 2.4D and 2.4E). Comparison between leukemia score and spleen weight indicate that spleen weights ≥ 0.35g have a leukemia score of 2 or higher, which was used for some mice as a proxy for denoting leukemia Figures 1.2C and 1.2D). Leukemia or lack of it in all gnotobiotic mice, TLR2$^{-/-}$, TRL4$^{-/-}$, TLR2$^{-/-}$TLR4$^{-/-}$, RIPK2$^{-/-}$, Caspase1/11$^{-/-}$, Rnf128$^{-/-}$, Serpinb9b$^{-/-}$, VSig4$^{-/-}$ mice was also confirmed histologically using splenic sections.

Plaque and infectious center assays

Blood from RL-MuLV infected BALB/cJ mice was collected in tubes containing heparin,

which was then spun at 10,000 rpm for 10 min at 4°C. The plasma was serially diluted in PBS, and was subjected to the XC plaque assay (Rowe et al., 1970). Data is represented as the number of infectious centers per milliliter of plasma.

Infection status of mice with spleens weighing less than 0.2g was conducted via infectious center assay or analysis of integrated provirus (see below Isolation of DNA from organs). To assess the frequency of infected cells, single cell suspensions (with red blood cells) from RL-MuLV infected mouse spleens were serially diluted in Clicks medium supplemented with 5% fetal calf serum, pen/strep, 0.04mM mercaptoethanol, and 200mM L-glutamine (Irvine Scientific). The dilutions were subjected to the infectious center assay (Rowe et al., 1970). Data is represented as the number of infectious centers per million splenocytes.

The infectious center assay was conducted as follows. On day 1, SC-1 cells, grown in supplemented Click's medium were plated in 60mm tissue culture treated dishes at a concentration of 2 x 10^5 cells per dish. Day 2, SC-1 cells were checked for confluency before proceeding. Cells should be 30-60% confluent on day 2. Media was changed to 4ml of supplemented Click's medium containing polybrene at a final concentration of 10µg/ml. To stop proliferation, splenocytes were irradiated with 2000 rads and plated on the SC-1 cells at a final concentration of 10^4 or 10^5 splenocytes per dish. To ensure the splenocytes were evenly distributed in the dish, the dishes were gently mixed. As polybrene is toxic to cells, on day 3 the media was changed using 4ml of supplemented Click's medium. The media was changed again on day 6 using 3ml of supplemented Click's medium. On day 7, the media was removed, and each dish was subjected to UV irradiation for 30 seconds (2 GE germicidal bulbs at 26cm). 4ml of XC (ATCC CCL-165) cells, grown in minimum essential medium (MEM) supplemented with 10% fetal calf serum and pen/strep (Gibco), were plated in the dishes at a concentration of 10^6 cells per dish. Media was changed on day 9 using 4ml of supplemented MEM medium. On day 11, the dishes were checked for confluency then stained. Media was removed and the dishes were stained with the XC plaque assay stain (3 parts 1% methylene blue [stains proteins] in methanol, 1

part 1% carbol fuchsin [stains lipids] in methanol, and 2 parts methanol) for ten minutes. The excess stain was washed off and plaques were counted.

Isolation of DNA from organs and testing for integrated provirus

Spleens were homogenized in 2ml of 1X STE containing 1% SDS and 200µg/ml of proteinase K. The homogenized sample was then incubated at 55°C overnight. DNA was isolated via phenol-chloroform extraction. Briefly, 200µl of homogenate was mixed with and equal volume of 1X STE and mixed. An equal volume of phenol-chloroform was added and mixed by hand followed by centrifugation for five minutes at 14,000 rpm. The aqueous layer was extracted and placed in a fresh tube. The phenol-chloroform step was repeated once. The aqueous layer from the second extraction was mixed with 2.5 volumes -20°C 200 proof ethanol and mixed to precipitate the DNA. The precipitated DNA was transferred to a new tube containing 80% ethanol using a pipet tip. The DNA was centrifuged for five minutes at 14,000 rpm and vacuumed dry. The pellet was resuspended in 200µl of 1X STE and the DNA precipitation step was repeated. DNA was resuspended at a final concentration of 1mg/ml in 1X TE.

To test for integrated provirus, primers specific for the long terminal repeats found only in RL-MuLV integrated provirus (5'ATGAACGACCCCACCAAGT3' and 5'GAGACCCTCCCAAGGAACAG3') were used. Amplification of DNA from these primers denote the presence of integrated provirus and therefore indicates the mouse was infected with RL-MuLV.

Histology and immunohistochemistry

Mouse spleens were fixed in Telly's fixative (70ml 95% ethanol, 30ml water, 5ml glacial acid, 10ml 37-40% formaldehyde), sectioned, and stained with hematoxylin and eosin. Leukemia was scored using the following criteria: maintenance of splenic architecture, level of cellular mitotic activity and degree of cell maturation (Figure 1.2B). Visible tumors were excised from SPF and GF Trp53 deficient and Wnt1 transgenic mice and were fixed in Telly's fixative. Tumor diagnosis was

based on morphologic assessment of hematoxylin and eosin stained 4-micron sections.

For VSig4 and F4/80 immunohistochemistry, spleens were embedded in OCT (Tissue Tek; Torrance, CA) and flash frozen in dry ice chilled methylbutane. Five-micron sections of spleen were cut using a cryostat, collected on a glass slide, and air dried for three hours. Sections that were not fixed immediately were stored at -80°C. Tissue sections were fixed in cold acetone for three minutes and dried at room temperature for 30 minutes. The tissue section was circled with a paraffin pen and rehydrated by washing in FACS buffer (1X PBS supplemented with 1% fetal calf serum and 0.1% sodium azide) for ten minutes. Non-specific binding was reduced by blocking in FACS buffer containing 10% goat serum and 1µg/µl of Fc block for 30 minutes. Tissues were incubated with rat anti-mouse F4/80 conjugated to fluorescein isothiocyanate (FITC) and goat anti-mouse VSig4 followed by rhodamine (TRITC) – conjugated donkey anti-goat diluted in FACS buffer for thirty minutes in a humidity chamber at 4°C. Unbound antibodies were removed by washing the slide in FACS buffer for five minutes. To prevent the tissue from drying, PBS containing 50% glycerol was dripped onto the slide and a coverslip was slowly placed on the slide. Clear nail polish was used to adhere the coverslip to the slide. A Leica microscope type 307-072.056 was used to analyze tissue sections. Images were captured using a Diagnostic Instruments SPOT RT Slider camera (Sterling Heights, MI).

Isolation of peritoneal macrophages

Mice were sacrificed and pinned down on their back. The skin over the abdomen was carefully cut, avoiding cutting through the peritoneum. The skin was pulled back exposing the abdomen and pinned down on either side. Small slits were made in the skin of the limbs, the skin was pulled away and pinned down. Using a 22-gauge needed attached to a 5ml syringe, 5ml of ice-cold supplemented Click's media (Irvine Scientific) was injected into the peritoneal cavity through the leg. A hemostatic clamp was used to gently clamp the peritoneum tissue and shake the peritoneum for a minimum of two minutes. The needle attached to the syringe was used to

puncture the peritoneum and collect the Click's media containing the peritoneal macrophages.

Fluorescence-activated cell sorting (FACS) analysis

For analysis of VSig4 deletion in VSig4 deficient mice, peritoneal macrophages were stained with FITC-conjugated anti-F4/80 mAb (Biolegend; San Diego, CA) and allophycocyanin (APC)-conjugated anti-VSig4 mAb (eBioscience; San Diego, CA). Propidium-iodide positive dead cells were excluded from the analysis.

Deletion of CD4 and CD8 cells in $CD4^{-/-}$, $CD8^{-/-}$, and $CD4^{-/-}CD8^{-/-}$ mice was confirmed via FACS analysis. Splenocytes were harvested and red blood cells were lysed. Remaining single cell suspensions were stained with APC-conjugated anti-CD3 mAb (ThermoFischer Scientific; Pittsburg, PA), phycoerythrin (PE)-conjugated anti-CD4 mAb (BioLegend; San Diego, CA), and FITC-conjugated anti-CD8 mAb (BioLegend; San Diego, CA). Propidium-iodide was used to identify dead cells to exclude them from the analysis. Samples were run on a BD LSR Fortessa and analyzed using FlowJo.

Expression of $F4/80^{+}VSig4^{+}$ splenocytes in uninfected and infected SPF BALB/c mice was accomplished via FACS. Red blood cell lysed splenocytes were stained with FITC-conjugated anti-F4/80 mAb (Biolegend; San Diego, CA) and APC-conjugated anti-VSig4 mAb (eBioscience; San Diego, CA). Dead cells labeled with propidium-iodide were excluded from the analysis.

RNA sequencing

RNAseq analysis was performed on splenic RNA from infected (preleukemic) and uninfected GF and SPF BALB/cJ males and females (4 groups of mice, 6-8 mice per group). Splenic RNA was subjected to Illumina Next Gen Sequencing to generate a Directional Total RNA library. Ribosomal RNA was removed using a Ribo-Zero rRNA removal kit (Epicentre; Madison, WI). Gene expression was quantified through the Kallisto software (Bray et al., 2016). To identify genes regulated specifically by both the microbiota and the virus, we performed a series of

heuristic gene set filtering operations. We identified gene expression changes between infected/microbiome conditions using log-fold change >0.5 and $p < 0.05$ Wilcoxon rank sum test. Briefly, the set of gene expression change between uninfected SPF or infected/uninfected GF conditions were removed from the set of gene expression changes common between MuLV SPF and other conditions. These operations resulted in a candidate gene set specifically influenced by the presence of the virus and the microbiota. Gene filtering and statistical analysis was conducted using MATLAB (R2019b) (Natick, MA).

Splenic RNA from infected (preleukemic) and uninfected SPF BALB/cJ RIPK2$^{-/-}$ and Caspase1/11$^{-/-}$ was isolated and submitted for RNAseq analysis. Ribo-Zero rRNA removal kit (Epicentre; Madison, WI) was used to remove ribosomal RNA. Illumina Next Gen Sequencing was used to generate a Directional Total RNA library. Quality of raw reads were assessed via FastQC software (Andrews, 2017). STAR (Dobin et al., 2013) was then used to create a genome index using the BALB/cJ reference genome and the BALB/cJ GTF annotation file (both downloaded from Ensembl). Raw paired-ends were aligned using STAR to the genome index. SubReads FeatureCounts (Liao et al., 2014) was then used to sum the number of exonic reads per gene. Deseq2 v 1.32.0 (Love et al., 2014) was utilized to analyze differential gene expression. Finally, gene expression levels were compared between uninfected and infected mice for each genotype. We focused on expression of the three negative immune regulators by pulling out normalized transcript counts for Rnf128, Serpinb9b, and VSig4 from the Deseq 2 output. Expression of each negative regulators was plotted by condition (genotype and infection status) using ggplot2 v 3.3.5 (Wickham, 2009). P-values were calculated using a Wald test.

Measurement of serum cytokines

Serum cytokine levels were assessed in uninfected, pre-leukemic, and leukemic mice using a Cytometric Bead Array for mouse Th1, Th2, and Th17 cytokines (BD Biosciences; San Jose, CA) as per manufacturer's instructions.

FITC permeability assay

Permeability of the mouse gut was assessed using a FITC permeability assay. Food and water were removed from mouse cages for four hours. After four hours, mice were gavaged with 80mg/100g of FITC-dextran (citation). Three hours post gavage, mice were bled into 100μl heparin, and plasma was separated by spinning the blood at 2,000rpm for ten minutes and 4°C. 50μl of each sample was loaded into a 96-well plate in duplicate. FITC-dextran standards were diluted in plasma from mice that were not gavaged with FITC-dextran. FITC concentration was measured using a TECAN fluorescence spectrophotometer and Magellan software at emission and excitation wavelengths of 520nm and 490nm respectively. Fluorescence from the negative control well (unmanipulated sera) was subtracted from fluorescence of the standards and experimental wells. FITC concentration in the plasma of experimental animals was determined by intercalation of the standard curve and expressed as the concentration of FITC per ml of plasma.

Cell sorting and RNA isolation from sorted cells

Cells were sorted using a FACS or magnetic-activated cell sorting (MACS) based approach. For FACS, splenocytes were isolated and RBCs lysed. Cells were stained with a combination of APC-Cy7 labeled anti-B220 (Biolegend; San Diego, CA), APC labeled anti-CD3 (Life Technologies Corp; Carlsbad, CA), and BV421 labeled anti-F4/80 (Biolegend; San Diego, CA) and subsequently sorted based on these markers. RNA from sorted cells was isolated and gene expression was analyzed as described in the section below. For cells sorted via MACS, RBC-depleted splenocytes were incubated with anti-F4/80 microbeads beads (Miltenyi Biotec; Bergisch Gladbach, Germany). $F4/80^+$ cells were positively selected using LS columns as recommended by the manufacturer (Miltenyi Biotec; Bergisch Gladbach, Germany). F4/80 positive cells underwent a second round of positive selection using MS columns. F4/80 negative cells were incubated with biotin-labeled CD3 antibodies (Life Technologies Corp; Carslbad, CA) then streptavidin conjugated microbeads (Miltenyi Biotec; Bergisch Gladbach, Germany). $CD3^+$ cells

were positively selected using LS columns. $CD4^+$, $CD8^+$, and NK^+ cells were isolated from RBC-depleted splenocytes. Cells were incubated with anti-CD4 microbeads (Miltenyi Biotec; Bergisch Gladbach, Germany). CD4 positive cells were positively selected using LS columns as detailed by the manufacturer (Miltenyi Biotec; Bergisch Gladbach, Germany). CD4 negative cells underwent a second round of positive selection using LS columns. Remaining CD4 negative cells were incubated with biotin-labeled CD8 antibodies (BioLegend; San Diego, CA) then streptavidin conjugated microbeads (Miltenyi Biotec; Bergisch Gladbach, Germany). $CD8^+$ cells were positively selected using LS columns. CD4/CD8 negative cells were incubated with an antibody cocktail conjugated to biotin (Miltenyi Biotec; Bergisch Gladbach, Germany) then incubated with anti-biotin microbeads (Miltenyi Biotec; Bergisch Gladbach, Germany). NK positive cells were negatively selected using LS columns. Isolated cells were centrifuged at 2000 rpm for five minutes and kept at -80°C until RNA isolation.

Purity of cells sorted by MACS was confirmed via FACS analysis. Briefly, sorted cells were stained with a cocktail of antibodies: APC conjugated anti-CD3 (eBioscience), Pacific Blue conjugated anti-CD4 (Biolegend), FITC conjugated anti-CD8 (Biolegend), and PE conjugated anti-DX5 (Invitrogen).

RNA was isolated from sorted cells via guanidine thiocyanate extraction and CsCl gradient centrifugation (Chirgwin et al., 1979). Briefly, cell pellets were lysed with 3ml of solution 1 (solution 1 per 100ml: 60g guanidine thiocyanate, 0.5g sodium lauryl sarcosine, 5ml autoclaved 1M sodium citrate, 0.5ml beta-ETSH. Volume raised to 100ml with water and filter sterilized). Cell lysate was gently layered onto 2ml of 5.7M filter sterilized CsCl in a SW 55.1 tube. Samples were centrifuged at 36,000 rpm for 16-20 hours at 25°C using a TW55.1 bucket rotor. After centrifugation, the top 4ml were removed using p1000 pipet tips. The last ml was dumped into a beaker by quickly inverting the tube. To dry the tube, a piece of filter paper was rolled up and carefully inserted into the tube being cautious not to touch the RNA pellet at the bottom of the tube. RNA at the bottom of the tube was collected with 100-200μl of water, being careful not to touch the side of the tube with the pipet tip. RNA was solubilized by heating the samples at 65°C for 15 minutes. RNA

concentration was measured using a Qubit per manufacturer's instructions. RNA was precipitated in 2.5 volumes -20°C ethanol and 0.1 volumes 3M sodium acetate pH 5 and stored at -20°C.

Contaminating DNA was eliminated using the DNase treatment and removal reagents kit (Life Technologies). Briefly, 5µg of RNA was centrifuged for 15 minutes at 15,000 rpm and vacuum dried. RNA was resuspended in 50µl of water and solubilized by heating at 65°C for ten minutes. 5µl of 10X DNase I buffer and 1µl of rDNase I was added to the RNA and incubated at 37°C for thirty minutes. DNase was inactivated by adding 5µl of the DNase inactivation reagent followed by two minutes incubation at room temperature. The inactivation reagent was removed from the RNA by centrifuging the sample at 10,000g for 1.5 minutes. The RNA in the supernatant was transferred to a new tube for downstream applications.

RNA isolation from spleens

RNA was isolated from spleens using the PureLink RNA Mini Kit as per manufacturer's instructions (Invitrogen). Contaminating DNA was removed using an on-column PureLink DNase treatment (Invitrogen) during RNA isolation. RNA concentration was measured using a Qubit per manufacturer's instructions. RNA was precipitated in 2.5 volumes -20°C ethanol and 0.1 volumes 3M sodium acetate pH 5 and stored at -20°C.

RNA gel

A northern gel was run to assess the quality of RNA. A 1% agarose gel made in 1X running buffer (200mM MOPS, 10mM EDTA pH 8, 50mM NaOAc) was supplemented with 37ml of 37% formaldehyde and 0.2µg/ml ethidium bromide once the agarose had cooled. Precipitated RNA was centrifuged, vacuum dried, and resuspended in 20µl of 1X sample buffer containing 50% formamide and 2.2M formaldehyde. The RNA was heated for ten minutes at 65°C, loaded into the gel and run overnight at a low voltage. RNA gel was analyzed for an ideal ratio 2.5 28S subunit to 1 18S subunit and for a lack of smearing between the two bands which would indicate RNA degradation.

cDNA synthesis and quantitative reverse transcription PCR (RT-qPCR)

Complementary DNA (cDNA) was generated using SuperScript IV Reverse Transcriptase (Life Technologies). Briefly, 5µg of precipitated RNA was centrifuged and vacuum dried. RNA was mixed with 4.6µM random primer mix and 0.75mM dNTPs in a total volume of 13µl and heated at 65°C for five minutes. Afterwards, RNA was mixed with SuperScript buffer at a final concentration of 1X, DTT at a final concentration of 5mM, 1U of RNase OUT Recombinant RNase Inhibitor, and 1U of SuperScript IV Reverse Transcription to a final volume of 20µl. The reaction was heated at 55°C for ten minutes followed by incubation at 80°C for ten minutes.

The presence of quality cDNA was determined by using PCR primers specific for the *Actb* gene (5' GTATCCTGACCCTGAAGTACC3' and 5'TGAAGGTCTCAAACATGATCTG3').

For RT-qPCR, primer pairs and probe (Applied Biosystems) were used to amplify VSig4 (primer and probe set Mm00625349_m1), Serpinb9b (primer and probe set Mm00488405_m1), Rnf128 (primer and probe set Mm00480990_m1), and Beta-Actin (Mm02619580_g1) from splenic RNA using the Applied Biosystems QuantStudio 3 (ThermoFisher). For sorted cells, primers were developed to amplify VSig4 (5' GGAGATCTCATCAGGCTTGC3' and 5'CCAGGTCCCTGTCACACTCT), Rnf128 (5'TAGCTGTGCTGTGTGCATTG3' and 5'GAATGTCACACTTGCACATGG3'), Serpinb9b (5'AGCAGACCGCAGTCCAGATA3' and 5'GTCTGGCTTGTTCAGCTTCC3'), and Beta-Actin (5'GTATCCTGACCCTGAAGTACC3' and 5'TGAAGGTCTCAAACATGATCTG3') using SYBR green master mix (Bio-Rad; Hercules, CA). Taqman based qPCR reactions were performed in duplicate 20µl reactions containing 1µl cDNA (generated as described above), 2X Gene Expression Master Mix (ThermoFisher), and 20X Taqman primer/probe assays (ThermoFisher). An Applied Biosystems QuantStudio3 instrument was used to amplify each product using the following cycling conditions (50°C for two minutes, 95°C for ten minutes, followed by 40 cycles of 95°C for 15 seconds and 60°C for one minute. SYBR Green based qPCR reactions were performed in duplicate 10µl reactions containing 1µl of cDNA (generated as described above), 2X iTaq Universal SYBR Green Supermix (BioRad), and

primers at 200nM each. Amplification was carried out on an Applied Biosystems QuantStudio3 machine with the following cycling conditions: 95°C for three minutes, followed by 40 cycles of 95°C for five seconds and 60°C for 15 seconds. A melt curve was also generated using the following cycling conditions: 95°C for 15 seconds, 60°C for one minute, and 95°C for 15 seconds. cDNA was quantified using the comparative Ct method. Data are represented as log_2 fold change compared to uninfected controls, normalized to the endogenous control (beta-actin).

ELISA

An enzyme-linked immunosorbent assay (ELISA) was used to detect anti-MuLV antibodies in MuLV-infected GF and SPF BALB/cJ mice as previously described (Case et al., 2008). Briefly, RL-MuLV virions isolated from infected SC-1 cells were treated with 0.1% Triton X-100 and bound to plastic in borate-buffered saline overnight. Two percent ovalbumin was used as blocking component. Sera samples were incubated at 4ºC for one hour at a 1 x 10^{-2} dilution, followed by goat anti-mouse IgG2a coupled to horseradish peroxidase (HRP) (SouthernBiotech, Birmingham, AL). The IgG2a specific antibody response is a specialized response against viruses in BALB/cJ mice (Kane et al., 2018). Background optical density (OD_{450}) values from incubation with secondary antibody alone were subtracted from values acquired from sera of infected mice.

Association of GF mice and 16S rRNA sequencing

Cecal contents were harvested from three Taconic C57BL/6 mice or three SPF RIPK2$^{-/-}$ mice from our colony, mixed, and snap frozen at -80°C. Cecal content from Taconic C57BL/6 mice or SPF RIPK2$^{-/-}$ mice was resuspended in PBS and 200µl was gavaged into GF BALB/cJ WT,

RIPK2$^{-/-}$, and Caspase1/11$^{-/-}$ mice. Two weeks post associated, mice were sacrificed. Using non-ridged forceps, small intestinal contents were squeezed into Eppendorf tubes. Cecal content was also collected into Eppendorf tube. All samples were snap frozen at -80°C. Cecal content was sent to the Environmental Sample Preparation and Sequencing Facility at Argonne National

Laboratory. Sample preparation and sequencing was conducted as described in ((Khan et al., 2019). Briefly, DNeasy PowerSoil HTP 96 Kit (QIAGEN, Germantown, MD) was used to extract DNA from the samples per manufacturer's instructions. PCR was used to amplify the V4 region of the 16A rRNA-encoding gene (515F-806R). Specifically, PCR reactions were carried out with the 5 PRIME HotMasterMix kit (Quantabio, Beverly, MA) in triplicates. PCR cycling conditions were as follows: 95 ºC for 30 seconds, 55 ºC for 45 seconds, 72 ºC for 1.5 minutes, followed by 72 ºC for 10 minutes. Triplicates were pooled and primer dimers removed with UltraClean 96 PCR Cleanup Kit (QIAGAN, Germantown, MD). DNA concentration was determined using the PicoGreen® dsDNA Assay (Invitrogen/Thermo Fisher Scientific, Carlsbad, CA) and resuspended at 2ng/μl. Amplicons were sequenced with 151 x 151 base pair paired-end sequencing on an Illumina MiSeq.

Raw sequence data was processed using the DADA2 v 1.2.0 analysis pipeline (Callahan et al., 2016). Reads were filtered to remove those with poor/low quality and trimmed using the standard DADA2 parameters. Paired reads were merged, then clustered into an amplicon sequence variant (ASV) table. Sequence chimeras were removed, and taxonomy was assigned at the genus level using the Silva reference database v138.1 (Quast et al., 2013). The taxonomy table produced by the DADA2 pipeline was further analyzed using the Phyloseq v 1.36 package (McMurdie & Holmes, 2013) to generate principal coordinate analysis (PCoA) calculated using the Bray-Curtis dissimilarity index. Differentially abundant bacteria between genotypes were identified with an unpaired Student's T-test with a cut-off of $p < 0.05$.

Metabolomics

As detailed above, 200μl of overnight *Lactobacillus murinus* (ASF 361) culture grown in MRS broth was gavaged into GF mice. Successful colonization of mice was confirmed by isolating

DNA from fecal samples via phenol-chloroform extraction (see above) followed by sequencing of the 16S PCR product. Two weeks after colonization, mice were infected with $1x10^3$ PFU (see above). Progeny of MuLV infected *L. murinus* colonized mice were closed at 3 months. Uninfected *L. murinus* colonized mice, uninfected GF mice, and progeny of MuLV infected GF mice were also closed at 3 months. Spleens and plasma were collected upon sacrifice and immediately frozen and kept at -80ºC. Samples were shipped to the Fischbach lab at Stanford University for hydrophilic interaction liquid chromatography (HILIC) untargeted metabolomics at the Chan Zuckerberg Biohub. Metabolites were identified based on mass to charge ratio (m/z) and retention time compared to the local and global library.

Metabolites with a relative standard deviation (RSD) greater than 30% between other samples in the same group were discarded. Metabolites with RSDs less than 30% were normalized with Log_{10}, quantile normalization, followed by determining the zscore. Normalized values for each group were averaged and constructed into a heat map where red color indicates high metabolite levels and blue color indicates lower metabolite levels. P-values were adjusted using Bonferroni correction followed by two-way ANOVA to identify metabolites influenced by two independent variables: the presence of *L. murinus* and the virus.

CHAPTER 1: COMMENSAL BACTERIA MEDIATE MULV INDUCED LEUKEMIA DEVELOPMENT VIA SUPPRESSION OF THE ADAPTIVE IMMUNE RESPONSE

Preface

The contents of this chapter were modified and adapted from J. Spring, S. Lara, A. Khan, K. O'Grady, J. Wilks, S. Gurbuxani, et al. bioRxiv 2022 Pages 2022.02.02478820. I performed most of the experiments reported in the paper. Kelly O'Grady performed experiments with IL-6 and RAG1-deficient mice. Jessica Wilks conducted experiments with antibiotic treated mice, experiments on erythroid differentiation, and monitored ASF colonized mice. Sandeep Gurbuxani generated the leukemia scoring system and scored splenic tissue sections and contributed to experimental design. Amy Jacobson cultivated *B. thetaiotaomicron*. Michael Fischbach and Alexander Chervonsky contributed to experimental design and the edit of the manuscript. Jessica Spring and Tatyana Golovkina wrote the manuscript. Tatyana Golovkina conceived the project and performed many of the experiments.

Abstract

The influence of the microbiota on viral transmission and replication is well appreciated. However, its impact on retroviral pathogenesis outside of transmission/replication control remained unknown. Using Murine Leukemia Virus (MuLV), we found that some commensal bacteria promoted the development of leukemia induced by this retrovirus, in the absence of decreased viral burden. The promotion of leukemia development by commensal bacteria was due to suppression of the adaptive immune response.

Introduction

The commensal microbiota plays a critical role in maintaining host health by providing nutrition, creating a hostile environment for incoming bacterial pathogens, and modulating maturation of secondary lymphoid organs (Kim et al., 2017; Littman & Pamer, 2011). Pathogens

also take advantage of the microbiota for their spread and replication. Previously, we demonstrated that transmission of Mouse Mammary Tumor Virus (MMTV) that causes mammary carcinomas in susceptible mice depends on the gut commensal bacteria (Kane et al., 2011). Orally transmitted MMTV binds bacterial lipopolysaccharide (LPS) through LPS binding receptors incorporated into the viral membrane during budding (Wilks et al., 2015). LPS attached to the viral membrane triggers TLR4 to induce inhibitory cytokine interleukin-10 (IL-10), thus generating a status of immunological tolerance to the virus (Kane et al., 2011). Therefore, the presence of the microbiota enables MMTV transmission by suppressing the anti-viral immune response. Commensal microbiota has also been shown to impact transmission, replication, and pathogenesis of enteric and respiratory viruses from *Caliciviridae, Picornaviridae, Reoviridae,* and *Orthomyxoviridae* families (Baldridge et al., 2015; Kuss et al., 2011; Uchiyama et al., 2014). In this study, we sought to determine whether the commensal microbiota influences replication and pathology induced by a retrovirus transmitted through the blood – MuLV (Buffett et al., 1969; Duggan et al., 2006).

Results and discussion

We have previously shown that the replication of a different retrovirus (Mouse Mammary Tumor Virus, MMTV) was dependent on the presence of the host microbiota, which served as a source of LPS used by MMTV to dampen the host's immune response. If a similar scenario (control of replication by the microbiota) was applicable to MuLV, it would be difficult to study a potential role of the microbiota in development of MuLV-induced pathology. To address the issue, we used BALB/cJ mice either treated with microbiota-depleting doses of antibiotics (Abx) (Kane et al., 2011) upon weaning or reared in germ-free (GF) conditions. It is necessary to utilize both approaches in parallel as each has pros and cons. While mice treated with Abx beginning at weaning will have developed normal secondary lymphoid structures, there is the possibility for outgrowth of Abx resistant bacteria during the course of the experiment as well as depletion of

non-bacterial microorganisms (Wilks et al., 2013). GF mice lack all microorganisms, but have underdeveloped lymphoid tissues (Wilks et al., 2013). To test whether the microbiota has an effect on RL-MuLV transmission, all groups of mice were infected by intraperitoneal (i.p.) injection of 0.22μM filter-sterilized MuLV as adults (G0 mice) and bred to produce offspring (G1 mice). G1 mice were examined for the presence of infectious virus. This experimental design allowed us to test whether the microbiota is required for both virus transmission and replication. Frequency of infected cells and viremia were compared *via* infectious center assay (Rowe et al., 1970). Abx treatment had no effect on viral replication compared to untreated mice (Figure 1.1A), Furthermore, GF MuLV-infected mice also showed similar levels of MuLV in the spleens (Figure 1.1A) or in the plasma (Figure 1.1B) compared to infected SPF mice. Thus, the system was robust for testing the role of the microbiota in leukemogenesis caused by MuLV.

Upon RL-MuLV infection, hematopoiesis within the bone marrow is blocked, resulting in compensatory extramedullary hematopoiesis (EMH) in the spleen (Hook *et al.*, 2002). EMH leads to expansion of target cells susceptible for infection. RL-MuLV readily replicates within the rapidly proliferating erythroid progenitor cells, increasing the likelihood of proviral integration near a cellular proto-oncogene, a step necessary for development of erythroid leukemia as this virus does not encode for an oncogene (Figure 1.2A).

To test whether the microbiota has an effect on RL-MuLV pathogenesis, all groups of mice were infected by i.p. injection of filter-sterilized MuLV as adults (G0 mice) and bred to produce infected offspring (G1 mice) that were further observed for leukemia development. G1 mice, which received a physiologically relevant infectious virus dose from their parents, were aged and monitored for leukemia for 150 days (unless indicated otherwise). Diseased mice removed from the cohorts and mice surviving up to 150 days were examined according to a leukemia scoring system based on histological analysis of the spleen. Uninfected mice retain splenic architecture and are given a score of 0. Pre-leukemic mice are defined as having increased extramedullary hematopoiesis and are given a score of 1. Leukemic mice exhibiting regions containing leukemic blasts with high mitotic activity are scored as 2, and more advanced cases, where the splenic

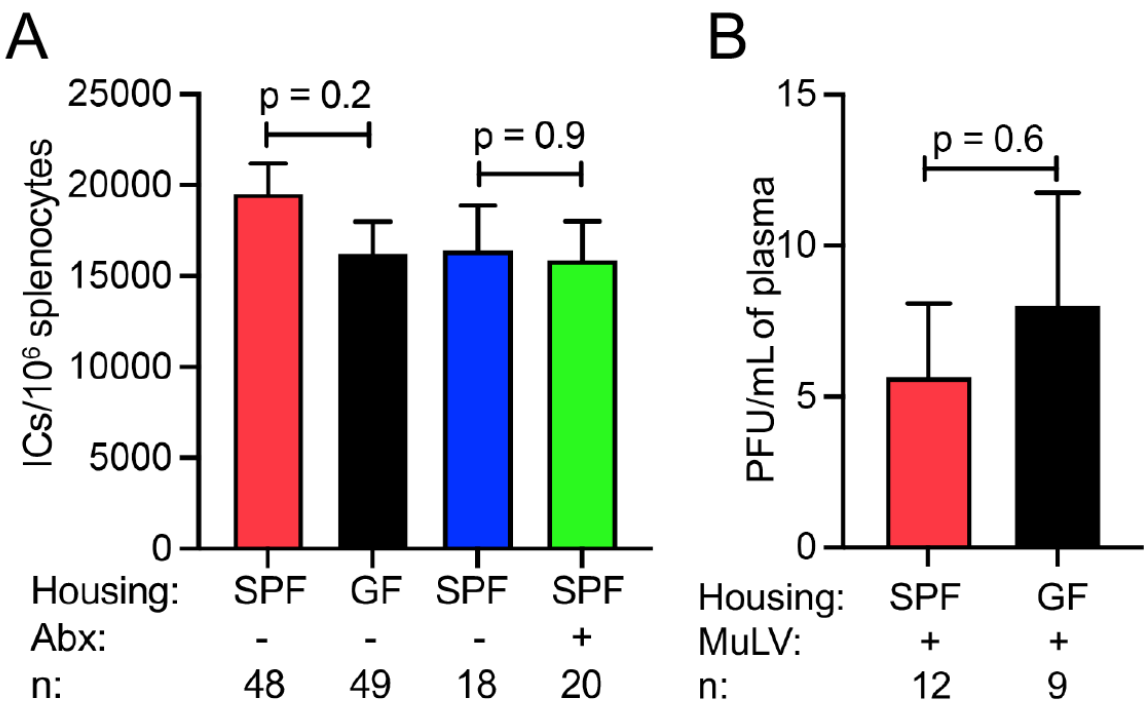

Figure 1.1. Commensal microbiota is not required for MuLV transmission and replication. Adult BALB/cJ females from different experimental groups were injected with MuLV and bred (G0 mice). Their offspring (G1 mice) were assayed for infectious virus. **(A)** Comparison of viral load [number of infectious centers (ICs) per 106 splenocytes] in SPF, GF, and Abx-treated animals. IC assay was done on preleukemic mice with a score of 1. **(B)** Plaque forming units (PFU) per mL of plasma in SPF and GF mice. Abx, antibiotic. n, number of mice used per group. p values were calculated using an unpaired t test. Error bars indicate standard error of the mean.

architecture is wholly disrupted by immature leukemic blasts, are scored as 3 (Figure 1.2B). Leukemia score directly correlated with spleen weight and all animals with spleen weight greater than or equal to 0.35g had leukemia (Figures 1.2C, 1.2D).

Infected SPF BALB/cJ mice exposed to water containing a broad-spectrum Abx cocktail since weaning as well as infected GF BALB/cJ mice had increased latency of the disease and markedly reduced spleen weights compared to infected untreated SPF mice (Figures 1.3A, 1.3B, and 1.3C). Leukemia latency was not significantly different between Abx treated and GF mice (Figure 1.3B). Therefore, the likelihood outgrowth of Abx-resistant bacteria influenced leukemia development in Abx treated mice is unlikely. As leukemia resistant phenotype of Abx-treated and GF mice was not due to a reduction in viral replication (Figures 1.1A and 1.1B), it became obvious that the microbiota significantly augmented viral pathogenesis.

The commensal microbiota is composed of various microorganisms including bacteria, viruses, archaea, fungi, and unicellular eukaryotes. To define a subset of the microbiota capable of enhancing leukemia susceptibility to SPF mice, GF mice were colonized with a defined consortium of mouse commensal bacteria, Altered Schaedler's Flora (ASF) (Dewhirst et al., 1999), bred, and infected with 0.22μM filtered RL-MuLV. Virus fate and pathogenesis was followed in G1 mice generated from infected G0 females. ASF restored high susceptibility of GF mice to leukemia (Figures 1.4A and 1.4B), proving that commensal bacteria can promote virally induced leukemogenesis. ASF contains seven bacterial species that include both gram-positive and gram-negative lineages (Sarma-Rupavtarm et al., 2004). A single gram-positive bacterium, *Lactobacillus murinus* (*L. murinus*), and a single gram-negative bacterium, *Parabacteroides goldsteinii* (*P. goldsteinii*), were isolated from ASF and used to colonize GF mice. Progeny from RL-MuLV infected *L. murinus* colonized females developed leukemia at a similar rate and incidence as SPF mice (Figures 1.4C and 1.4D). Conversely, progeny from RL-MuLV infected *P. goldsteinii* colonized females exhibited leukemia development similar to that of GF mice (Figures 1.4C and 1.4D). Importantly, infected *P. goldsteinii* colonized mice had a frequency of infected splenocytes

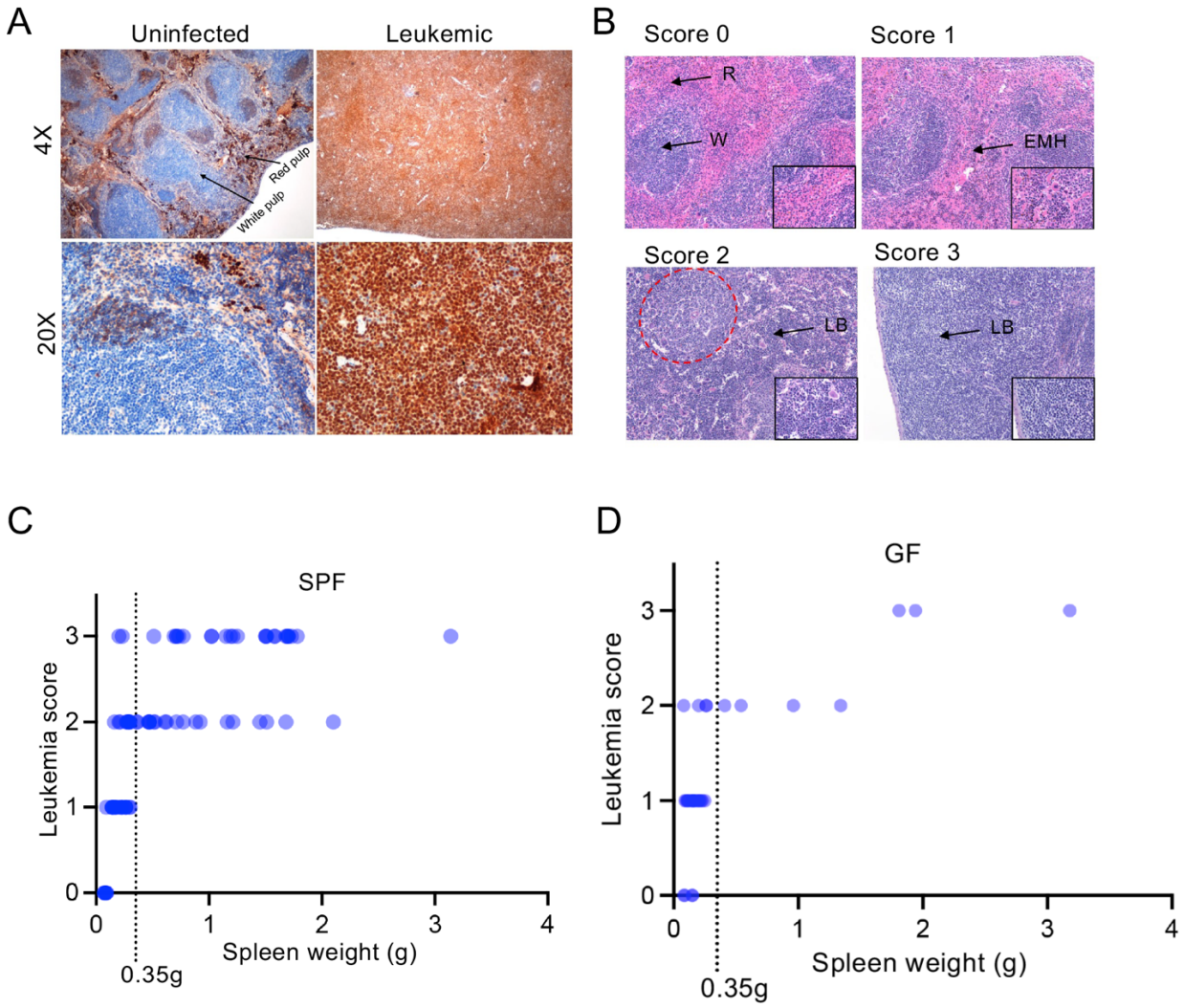

Figure 1.2. Leukemia development in infected SPF and GF BALB/c mice.
(A) Paraffin section of the spleen from an infected SPF mouse was stained with anti-GATA1 antibody and counterstained with hematoxylin. **(B)** Disease scoring system. Uninfected mice retain splenic architecture and were given a score of 0. R, red pulp; W, white pulp. Pre-leukemic mice were defined as having increased extramedullary hematopoiesis and were given a score of 1. Leukemic mice exhibiting regions containing leukemic blasts (LB) with high mitotic activity were scored as 2. Red dotted circle are the remnants of the white pulp. Score 3 was given to mice in which splenic architecture was wholly disrupted by immature LBs. Representative stained sections of spleens from SPF infected mice with indicated scores. Magnification - 10X, 40X magnification is shown in lower right corners. **(C, D)** Correlation of spleen weight with leukemia score in SPF **(C)** and GF **(D)** mice determined by histological examination of hematoxylin and eosin (H & E) stained spleen sections. 74 spleens from SPF infected, 6 spleens from SPF uninfected, 34 spleens from GF infected, and 4 spleens from GF uninfected mice were analyzed histologically. Vertical dotted line indicates spleen weight of 0.35g.

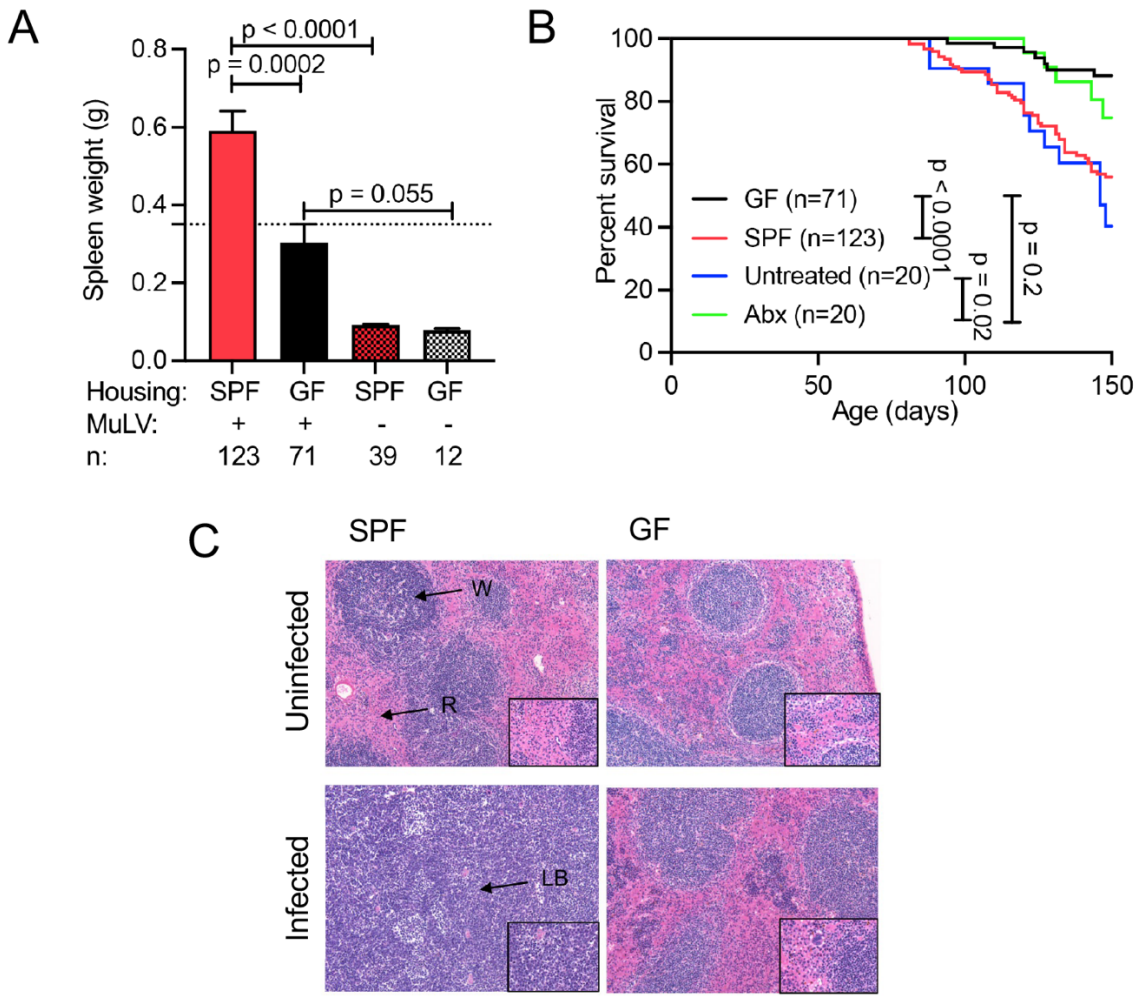

Figure 1.3. Dependence of MuLV-induced leukemia development on commensal microbiota.
Adult BALB/cJ females from different experimental groups were injected with MuLV and bred (G0 mice). Their offspring (G1 mice) were monitored for leukemia. Diseased mice removed from the cohorts and mice surviving up to 150 days were examined according to a leukemia scoring system based on histological analysis of the spleen (Figure 1.2A). **(A)** Spleen weights of infected and uninfected SPF and GF mice at 4-5 months of age. Dotted horizontal line indicates 0.35g. **(B)** Survival curves of G1 SPF, GF, and Abx-treated mice. **(C)** Example hematoxylin-and eosin stained-splenic sections from uninfected or infected SPF and GF mice at 4 months of age. Black arrows indicate red and white pulp. W, white pulp; R, red pulp; LB, leukemic blasts Magnification - 10X, 40X magnification is shown in lower right corners. Abx, antibiotic. n, number of mice used per group. *p* values were calculated using an unpaired *t* test **(A)** and Mantel-Cox test **(B)**. Error bars indicate standard error of the mean.

comparable to that observed in SPF mice (Figure 1.4E). Non-members of ASF, gram-positive *Enterococcus faecalis* (*E. faecalis*), and, interestingly, a gram-negative commensal *Bacteroides thetaiotaomicron* (*B. theta*) also conferred leukemia susceptibility to GF infected mice (Figures 1.4C and 1.4D). These data provide evidence that leukemia promoting factors are not inherent to all bacteria but are unique to certain bacteria across different bacterial phyla.

Based on the observed resistance of *P. goldsteinii* colonized mice to MuLV induced leukemia, we wondered if this resistance phenomenon is specifc to *P. goldsteinii* species or to all *Parabacteroides* strains. To address this question, we colonized one cohort of GF BALB/cJ mice with a non-ASF derived strain of *P. goldsteinii* (strain CL02) and a separate cohort of GF BALB/cJ mice with *P. distasonis* (strain ATCC 8503). One month post colonization, females were injected with 1 x 10^3 PFU of MuLV and put into mating. G1 progeny mice are currently being monitored for leukemia development. If both *P. goldsteinii* colonized and *P. distasonis* colonized mice are resistance to MuLV induced leukemia, then the resistance phenomenon may be general to *Parabacteroides* species. Conversely, if only *P. goldsteinii* colonized mice confer leukemia resistance while *P. distasonis* colonized mice promote leukemia development, then the resistance phenotype is specific to this species. In this instance, a comparison between *P. goldsteinii* and *P. distasonis* may yield structural or genetic differences that may influence the disparity in the bacterium's ability to support leukemia development.

Tumor promotion is often linked to chronic inflammation, which is defined as a prolonged, aberrant protective response to a loss of tissue homeostasis (Medzhitov, 2008). Inflammation-driven tumor promotion activates transcription factors in premalignant cells, which induce genes stimulating cell proliferation and survival (Grivennikov et al., 2010) . One candidate factor that contributes to inflammation and tumorigenesis, is the proinflammatory cytokine IL-6. IL-6 has been shown to be overexpressed by host cells within the tumor microenvironment and by tumors of various etiologies (Lippitz, 2013), and also shown to be microbially induced and necessary for pre-leukemic myeloproliferation in genetically susceptible mice (Meisel et al., 2018). To determine the

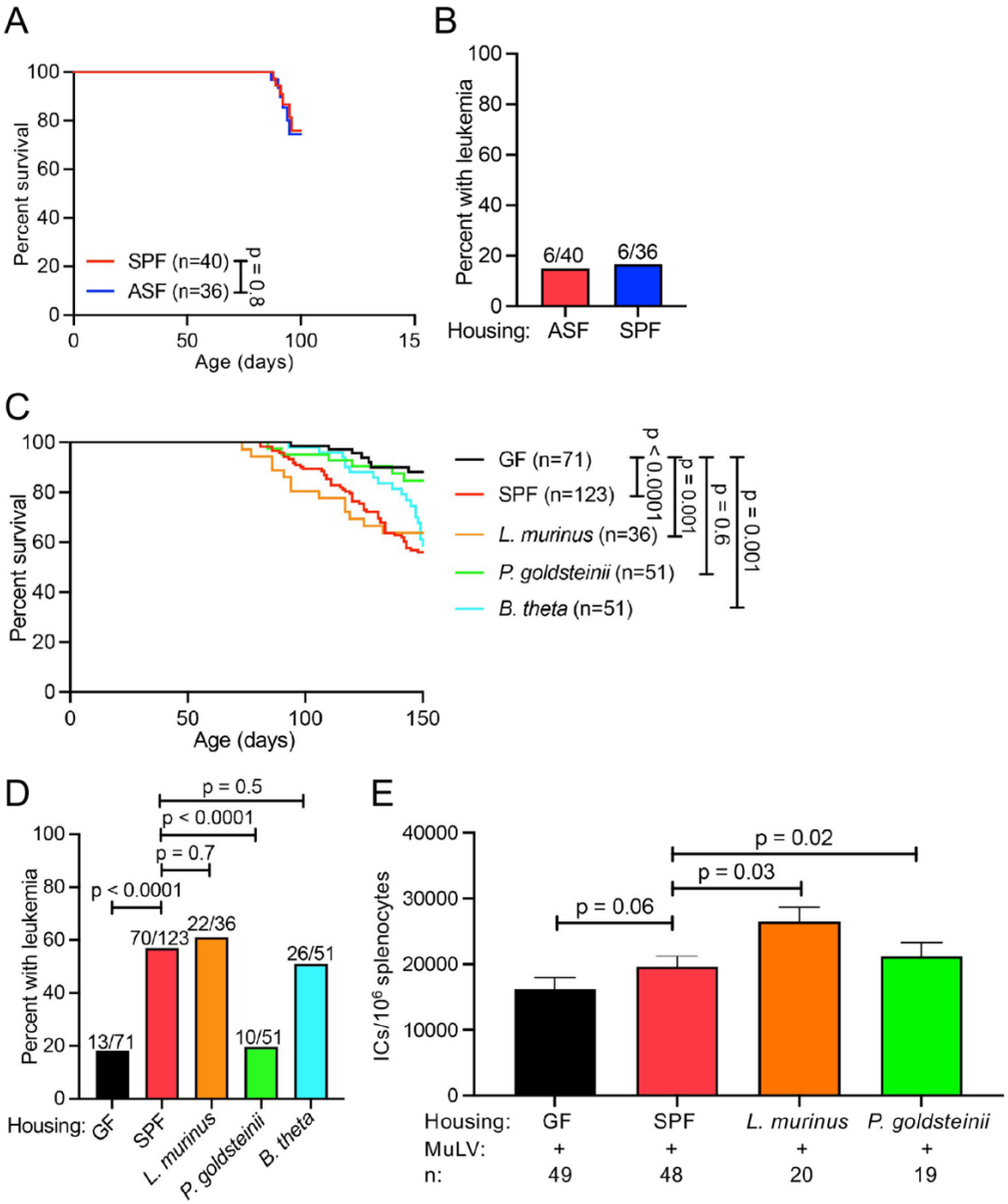

Figure 1.4. Certain bacteria are sufficient to confer MuLV-induced leukemia development. Adult BALB/cJ females from different experimental groups were injected with MuLV and bred (G0 mice). Their offspring (G1 mice) were monitored for leukemia. Diseased mice removed from the cohorts and mice surviving up to 150 days were examined according to a leukemia scoring system based on histological analysis of the spleen (Figure 1.2A). **(A)** Survival curves of MuLV-infected SPF and ASF- colonized BALB/cJ mice observed for 97 days. **(B)** Total leukemic incidence in infected ASF-colonized and infected SPF mice monitored for 97 days. **(C)** Survival of GF, SPF and gnotobiotic BALB/cJ mice colonized with single bacterial lineages monitored for 150 days. **(D)** Final assessment of leukemia development in mice from these groups at day 150. **(E)** Frequency of infected splenocytes (infectious centers, ICs) per 10^6 splenocytes in SPF and gnotobiotic mice. n, number of mice used per group. *p* values were calculated using Mantel-Cox test **(A, C)**, Fisher's exact test **(B, D)**, and unpaired *t* test **(E)**. Error bars indicate standard error of the mean.

role of IL-6 in virally- induced leukemia, IL-6-sufficient and -deficient female mice were infected with RL-MuLV and their progeny were monitored for leukemia. IL-6-sufficient and -deficient mice both developed leukemia at the same latency and with similar incidence (Figure 1.5A). Interestingly, while about 50% of infected SPF BALB/cJ WT mice develop leukemia by 150days (Figure 1.3B), we noticed that nearly 80% of SPF BALB/c IL-$6^{-/-}$ mice exhibit leukemia by 150 days (Figure 1.5A). This could be attributed among other possibilities to the difference in strain background between BALB/cJ (the background strain used for all mice in the studies) and BALB/cByJ mice (the background strain of the IL-$6^{-/-}$ mice) that could influence the microbiota altering the rate of leukemia development. In addition, other cytokines have been shown to support tumor immune evasion by inhibiting immune effector functions. IL-4 and IL-10 have been reported to facilitate monocyte differentiation in tumors towards an M2 phenotype which support tumor growth and invasion (Mantovani et al., 2002). Furthermore, IL-10 enhances T cell suppression and inhibits dendritic cell function, and elevated serum IL-10 has been described as a negative clinical outcome for a variety of tumors (Moore et al., 2001). To determine whether other cytokines are associated with leukemia development in MuLV infected mice, we measured protein levels of IL-6, IL-2, IL-4, IFN- γ, TNF-α, IL-17A, and IL-10 in the sera of uninfected, infected, and leukemic mice only to find that levels of these cytokines were unchanged (Figures 1.5B, 1.5C, 1.5D, 1.5E, 1.5F, 1.5G, and 1.5H). It is important to note that while we did not observe altered levels of these cytokines in the sera, that cytokine levels may be different at the level of tumor microenvironment. Furthermore, other cytokines omitted in our investigation could influence leukemia development. Thus, while we were unable to detect elevated or reduced levels of these cytokines in the sera of infected mice compared to uninfected mice, cytokines or other signaling molecules involved in MuLV induced leukemia development are yet to be established.

Maintenance of pre-cancerous and cancerous cells within the host requires the evasion or suppression of the immune response (Kim et al., 2007; Shankaran et al., 2001). To test the role of the adaptive immune response in resistance of GF mice to RL-MuLV-induced leukemia, we

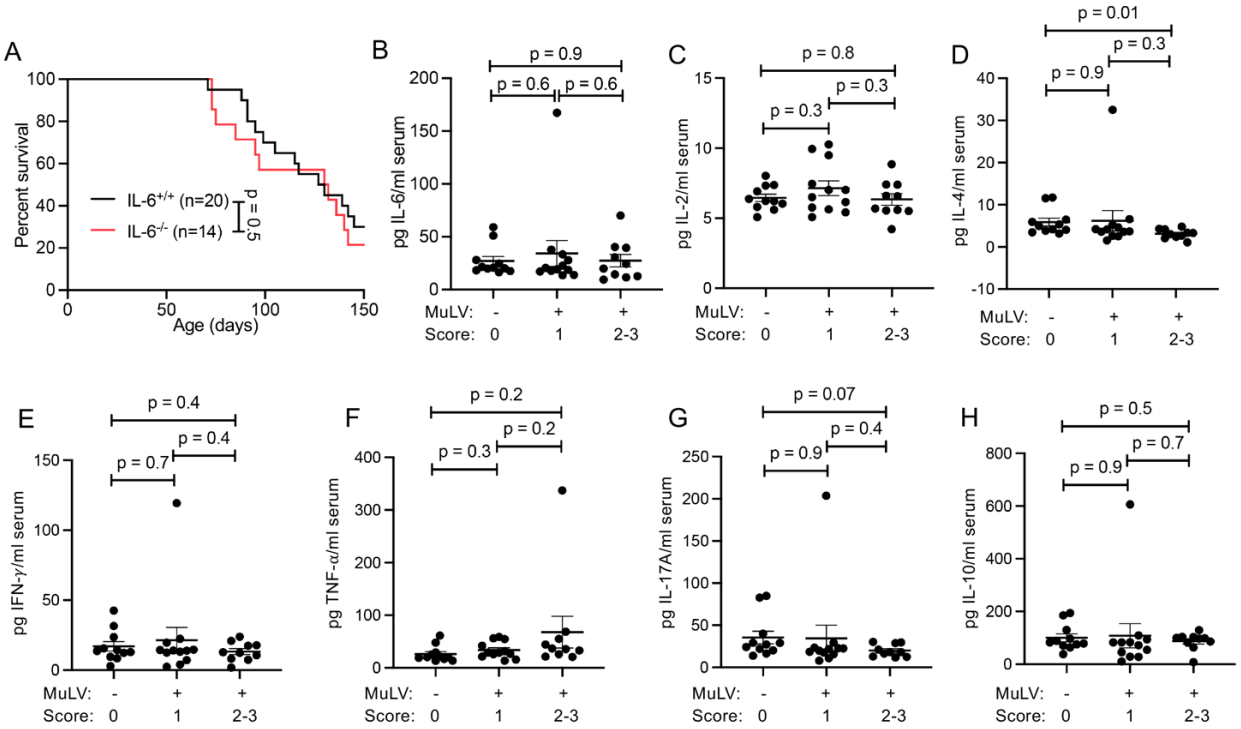

Figure 1.5. Expression of certain cytokines does not correlate with MuLV induced leukemia development.
(A) Survival of IL-6 sufficient and IL-6 deficient MuLV-infected SPF BALB/cJ mice. **(B-H)** Serum cytokine concentration was measured in uninfected (score 0), infected preleukemic (score 1) and infected leukemic (scores 2-3) BALB/cJ mice using a flow cytometry bead-based assay. **(B)** IL-6 **(C)** IL-2 **(D)** IL-4 **(E)** IFN-γ **(F)** TNF-α **(G)** IL-17A **(H)** IL-10. n, number of mice used. *p* values calculated using Mantel-Cox test **(A)** or unpaired *t* test **(B, C, D, E, F, G, H)**. Error bars indicate standard error of the mean.

monitored leukemia development in immunodeficient RAG1 recombinase negative (lacking a functional adaptive immune system) GF BALB/cJ G1 mice born to injected RAG1-deficient G0 mice. RAG1 deficiency led to enhanced susceptibility of RL-MuLV infected GF mice to leukemia (Figures 1.6A and 1.6B). Importantly, both GF and SPF RAG1$^{-/-}$ mice displayed a similar frequency of infected splenocytes, excluding the possibility that the sensitivity of RAG1-deficient mice to MuLV-induced tumors could be simply explained by an increase in viral replication in these mice (Figure 1.6C).

These data implied that increased leukemia susceptibility in SPF mice was a consequence of commensal bacteria suppressing the anti-tumor adaptive immune response. And, conversely, the absence of commensal bacteria in GF mice allowed an unsuppressed adaptive immune response to counteract the development of leukemia. Even though MuLV induces immunosuppression in SPF mice (Dittmer et al., 2004; Robertson et al., 2006), the immune response still controls leukemia development to a certain degree as SPF RAG1$^{-/-}$ mice exhibited increased leukemia susceptibility compared with SPF RAG1-sufficient mice (Figures 1.6A and 1.6B). This response was unrelated to the virus-specific antibodies (Abs) as neither infected GF nor SPF mice mounted potent virus-specific Ab responses (Figure 1.6D). In addition, significant susceptibility of GF RAG1$^{-/-}$ mice to MuLV-induced leukemia ruled out the possibility that resistance of GF wild-type mice to leukemia is due to the lack of provirus integration in the vicinity of oncogenes.

Considering B cell mediate antibody responses do not appear to restrict leukemia development in GF mice, the other subsets of the adaptive immune response absent in RAG1$^{-/-}$ mice, T cells and NKT cells, must play a more prominent role. To delineate which subset of the adaptive immune response controls leukemia development in GF mice, we generated CD4$^{-/-}$, CD8$^{-/-}$, and CD4$^{-/-}$CD8$^{-/-}$ mice on the BALB/cJ background using CRISPR Cas9 (Figures 1.7A and 1.7B). CD4^{+} and CD8^{+} T cells have been shown to play a direct role in anti-tumor immunity (Toes et al., 1999). Therefore, we reasoned these cell types may play a critical role in MuLV induced

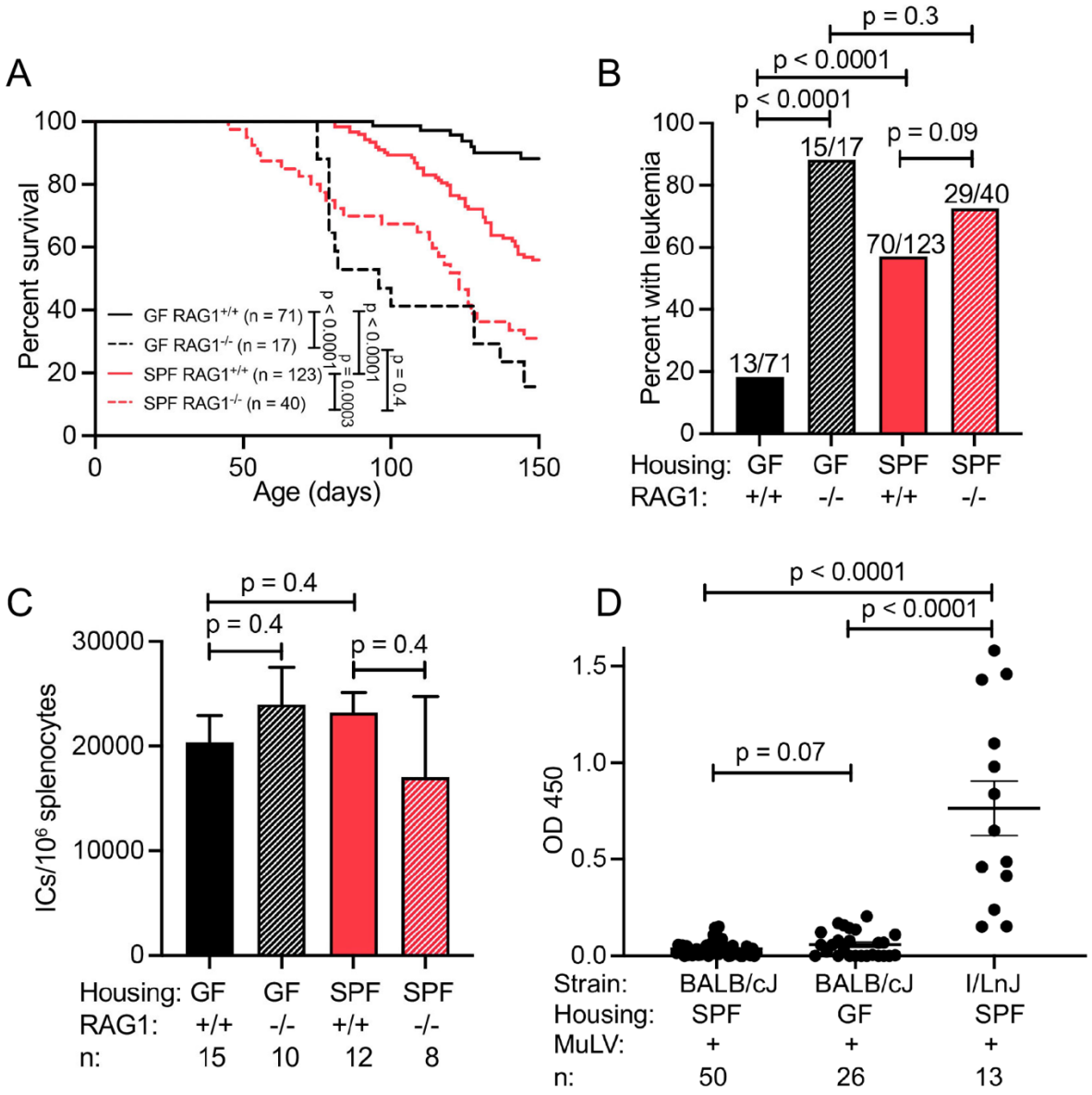

Figure 1.6. Comparison of leukemia susceptibility of immunosufficient and immunodeficient infected GF and SPF BALB/cJ mice.
(A) Survival of infected RAG1-sufficient SPF, RAG1-deficient SPF, RAG1-sufficient GF, and RAG1-deficient GF BALB/cJ miceover 150 days. **(B)** Total leukemia incidence of infected indicated mice at 150 days. **(C)** Comparison of the viral burden (frequency of infected cells per 10^6 splenocytes) in indicated preleukemic mice (score 1). **(D)** MuLV-specific ELISA to detect anti-virus antibodies. I/LnJ mice fostered on MuLV-infected BALB/cJ females are included as a positive control as they produce virus-neutralizing antibodies (Case *et al.*, 2008). n, number of mice used. *p* values calculated using Mantel-Cox test **(A)**, Fisher's exact test **(B)**, or unpaired *t* test **(C, D)**. Error bars indicate standard error of the mean.

leukemia development. CD4-, CD8-, and CD4/CD8-deficient mice were rederived as GF and bred to produce a sizeable colony. Females were injected with 1 x 10^3 PFU MuLV and bred to produce the subsequent generation. G1 mice are currently being monitored for leukemia. We hypothesize deficiency in the cell subset which enables protection from leukemia in the GF setting would render infected GF mice as susceptible to leukemia as GF RAG1$^{-/-}$ mice. We additionally generated similar colonies of CD4$^{-/-}$, CD8$^{-/-}$, and CD4$^{-/-}$CD8$^{-/-}$ mice in the SPF environment, infected females with MuLV, and are currently monitoring the G1 progeny. We expect mice deficient in the subset of cells which provide minor control of leukemia development in infected SPF mice will render mice as susceptible to leukemia as SPF RAG1$^{-/-}$ mice.

Among the factors influencing tumor development, the host's microbiota has been found to play a significant role. The intestinal microbiota has been implicated in progression of cancers of the gut or organs connected with the gut such as the liver. That effect is achieved by signaling through pattern recognition receptors or producing metabolites that lead to the induction of inflammatory cytokines and chemokines, as well as through production of DNA-damaging reactive oxygen and nitrogen species (Arthur et al., 2012; Hope et al., 2005; Rakoff-Nahoum & Medzhitov, 2007; Reddy et al., 1975; Yoshimoto et al., 2013). At the same time, the gut microbiota can be tumor suppressive (Donohoe et al., 2014) or enhance the effect of anti-cancer immunotherapy by modifying dendritic cell maturation and promoting tumor specific T cell responses (Sivan et al., 2015; Vetizou et al., 2015).

Using a model of retrovirally-induced leukemogenesis, we found the gut commensal bacteria constitute an additional factor, which is utilized by tumors to counteract the immune response. Importantly, this happens in an organ distant from the intestinal tract. The host microbiome has been already shown to support the pathogenic effects of various viruses (Baldridge et al., 2015; Kuss et al., 2011; Uchiyama et al., 2014). However, in these studies, decreased pathogenesis due to the microbiota ablation was clearly coupled with reduction of virus replication. In contrast to these experiments, we show that the decreased leukemogenesis

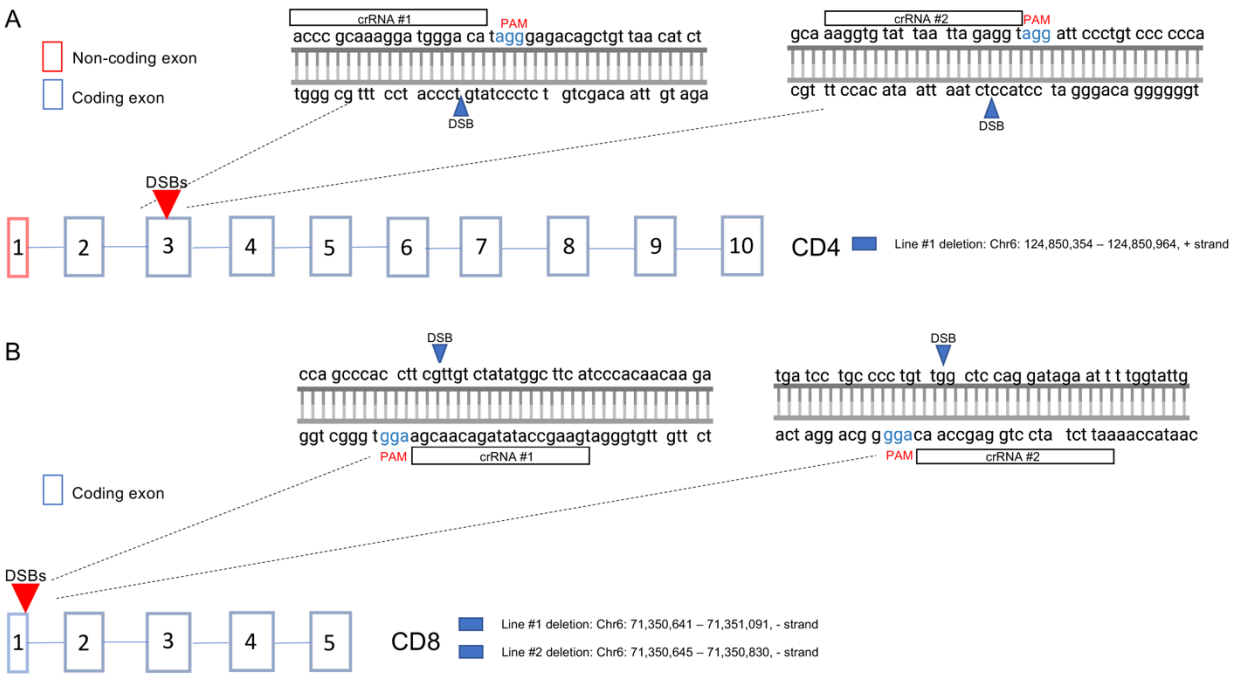

Figure 1.7. CRISPR-Cas9 targeting strategy for generation of CD4-, CD8-, and CD4/CD8-deficient mice.
CRISPR-Cas9 targeting strategy for **(A)** CD4 and **(B)** CD8. Red arrow indicates location of double-stranded breaks within the targeted gene. Targeted sequences are shown on the right. All lines generated and the regions of the chromosome deleted are listed in blue boxes. Guides for CD4 and CD8 were used in conjunction to generate double deficient mice.

observed in MuLV infected microbiota-free mice is not linked to a decrease in the virus burden. Thus, another tumor-promoting mechanism had to be found, which was subsequently identified as a negative regulation of adaptive immunity.

First, we discovered that adaptive immunity indeed controlled leukemogenesis in infected GF mice. The high susceptibility and rapidity with which MuLV infected GF RAG1$^{-/-}$ mice develop leukemia supports a role for cells expressing somatically rearranged immune receptors in controlling tumor development in GF mice. As neither SPF nor GF infected mice produce neutralizing antibodies against viral antigens (Figure 1.6D), any prominent role for B cells in a protective anti-tumor immune response seems unlikely. The absence of virus-neutralizing antibodies also explains the lack of control of the extracellular virus resulting in similar viral replication levels in GF and SPF mice. Therefore, the adaptive immune response against MuLV pathogenesis is likely controlled by T cells and/or NKT cells. Anti-tumor immunity response by NKT cells is thought to be primarily through their support of other effector cells like CD8$^+$ T cells and NK cells via production of Th1 cytokine IFN-γ (Crowe et al., 2002) or IL-2 (Metelitsa et al., 2001). Both CD4$^+$ T cells and CD8$^+$ T cells play decisive roles in suppressing tumor development and growth (Toes et al., 1999). CD4$^+$ T cells contribute to anti-tumor immunity by secretion of proinflammatory cytokines such as IL-2, IFN-γ, and TNF-α (Quezada et al., 2010). CD4$^+$ T cells have also been reported to adopt cytotoxic activity by means of Fas-mediated cell death or perforin and granzyme induced apoptosis (Nagata & Golstein, 1995; Raskov et al., 2021; Xie et al., 2010). However, the exact subset of the adaptive immune system that controls leukemia development in GF mice remains an area of investigation.

CHAPTER 2: TWO NEGATIVE IMMUNE REGULATORS CONTRIBUTE TO BACTERIA DEPENDENT MULV INDUCED LEUKEMIA DEVELOPMENT

Preface

The contents of this chapter are modified and adapted from J. Spring, S. Lara, A. Khan, K. O'Grady, J. Wilks, S. Gurbuxani, et al. bioRxiv 2022 Pages 2022.02.02478820. I performed most of the experiments described in this section. A.K. carried out computational analysis of the RNA-seq data. S.L. performed real time PCRs and IC assays for Serpinb9b$^{-/-}$ and Rnf128$^{-/-}$ mice. S.E. helped design CRISPR/Cas9 approaches to target Serpinb9b and Rnf128.

Abstract

Various methods by which the microbiota supports or suppresses tumor development and progression have been well documented (Arthur et al., 2012; Donohoe et al., 2014; Hope et al., 2005; Rakoff-Nahoum & Medzhitov, 2007; Reddy et al., 1975; Yoshimoto et al., 2013). Using MuLV as a model of retrovirally-induced leukemia, we identified a novel mechanism whereby negative immune regulators suppress the anti-tumor immune response in a microbiota dependent manner. These negative regulators, Rnf128 and Serpinb9b, which are associated with a poor prognosis of some spontaneous human cancers, were found to be crucial for MuLV induced leukemia development in the SPF setting.

Introduction

The immune system plays a critical role in controlling tumors of various etiology at each of the steps of tumor development mentioned above (Vinay et al., 2015). Immunosurveillance forces tumor cells to exploit multiple mechanisms of avoidance of the immune responses: induction of regulatory T cells (Jacobs et al., 2012), defective antigen presentation due to down-modulation of antigen processing machinery (Hicklin et al., 1999; Johnsen et al., 1999), production of immunosuppressive mediators (Lind et al., 2004; Pasche, 2001), and induction of tolerance (Staveley-O'Carroll et al., 1998), to name a few. As we have shown, the microbiota is an additional

factor that plays a role in tumor development. To further understand this phenomenon, we needed to discern the molecular mechanisms by which the microbiota promotes leukemia development in MuLV infected mice.

Results and discussion

To identify microbiota-mediated signaling pathway(s) essential for counteracting the immune response controlling leukemia progression, RNAseq was performed using spleens from infected and uninfected age-matched GF and SPF mice (GF, GF MuLV, SPF, SPF MuLV) at the pre-leukemic stage (score 1) (Figure 2.1A). Given the distinct phenotype of MuLV infected SPF mice, we sought to identify robust gene expression changes associated with both the presence of the microbiota and viral infection. We subjected the set of all genes quantified across all mice to a series of heuristic gene set filters. First, we identified gene expression changes common between SPF MuLV mice and GF, GF MuLV, and SPF mice (log-fold change > 0.5 and $p < 0.05$ Wilcoxon rank sum test): (a) SPF MuLV vs GF MuLV, (b) SPF MuLV vs SPF, and (c) SPF MuLV vs GF (Figure 2.1A, positive gene set). Second, we identified genes expression changes specific for GF, GF MuLV, and SPF mice that were different from SPF MuLV mice: (d) GF vs GF MuLV, (e) SPF vs GF, and (f) SPF vs GF MuLV (Figure 2.1A, negative gene set). Finally, we subtracted the negative gene set from the SPF MuLV specific positive gene set, resulting in candidate genes specifically impacted by the presence of both the virus and the microbiota. Knowing that leukemogenesis depends on the negative regulation of the immune response, we focused on genes that were known to have properties of negative immune regulation (Figure 2.1B, red arrows). Three genes - V-set immunoglobulin-domain-containing 4 (VSig4), serine (or cysteine) peptidase inhibitor, clade B, member 9b (Serpinb9b), and Ring finger protein 128 (Rnf128, also known as gene related to anergy in lymphocytes, or GRAIL) were selected for further *in vivo* analysis.

VSig4 was discovered as a complement receptor and then subsequently shown to inhibit T

cells (Vogt et al., 2006; Zeng et al., 2016). Serpinb9b is a serine protease inhibitor that acts on and suppresses granzyme M (Bots et al., 2005). Rnf128 is a ubiquitin ligase that among many functions has been shown to ubiquitinate CD3 and CD40L on T cells, leading to their degradation (Lineberry et al., 2008; Nurieva et al., 2010). To confirm the upregulation of these genes by MuLV and the microbiota, real time quantitative PCR (RT-qPCR) was performed using RNA isolated from the spleens of pre-leukemic mice. Whereas SPF pre-leukemic mice showed significant upregulation of these genes compared to uninfected SPF mice (Figure 2.2A), GF pre-leukemic mice did not (Figure 2.2B) confirming the RNAseq data (shown in Figure 2.1B). Notably, the expression of VSig4, Serpinb9b, and Rnf128 was also upregulated in the spleens of *L. murinus*-colonized mice but not *P. goldsteinii* colonized mice (Figure 2.2C) indicating that their induction correlated with the presence of bacteria with leukemia-promoting properties. Interestingly, Rnf128 was the only factor upregulated in the spleens of *B. theta* and *E. faecalis* colonized mice (Figure 2.2C), which exhibited high leukemia susceptibility. Together, these data suggest that one or a combination of these negative immune regulators function in a microbiota dependent fashion to suppress the anti-tumor immune response.

To provide definitive proof that all or some of these genes (VSig4, Serpinb9b, and Rnf128) function to promote leukemia, a CRISPR-Cas9 approach was taken to generate BALB/cJ mice lacking these genes with the expectation that elimination of the critical factor(s) would result in leukemia resistance even in the presence of commensal bacteria. Guides were designed to target exon 1 of VSig4 (Figure 2.3A), exon 2 of Serpinb9b (Figure 2.3B), and the ring finger domain within exon 4 of Rnf128 (Figure 2.3C) resulting in frameshifting indels (VSig4 and Serpinb9b) (Figure 2.3D) and disruption of a functionally important domain of Rnf128 (Anandasabapathy et al., 2003). Mice with targeted mutations, their wild-type littermates, and BALB/cJ mice bred in the same colony were injected with the virus and further bred to produce infected offspring to be monitored for leukemia. VSig4-deficient mice developed leukemia at a similar latency and incidence as VSig4-sufficient mice (Figures 2.4A, 2.4B, and 2.4D), indicating VSig4 by itself

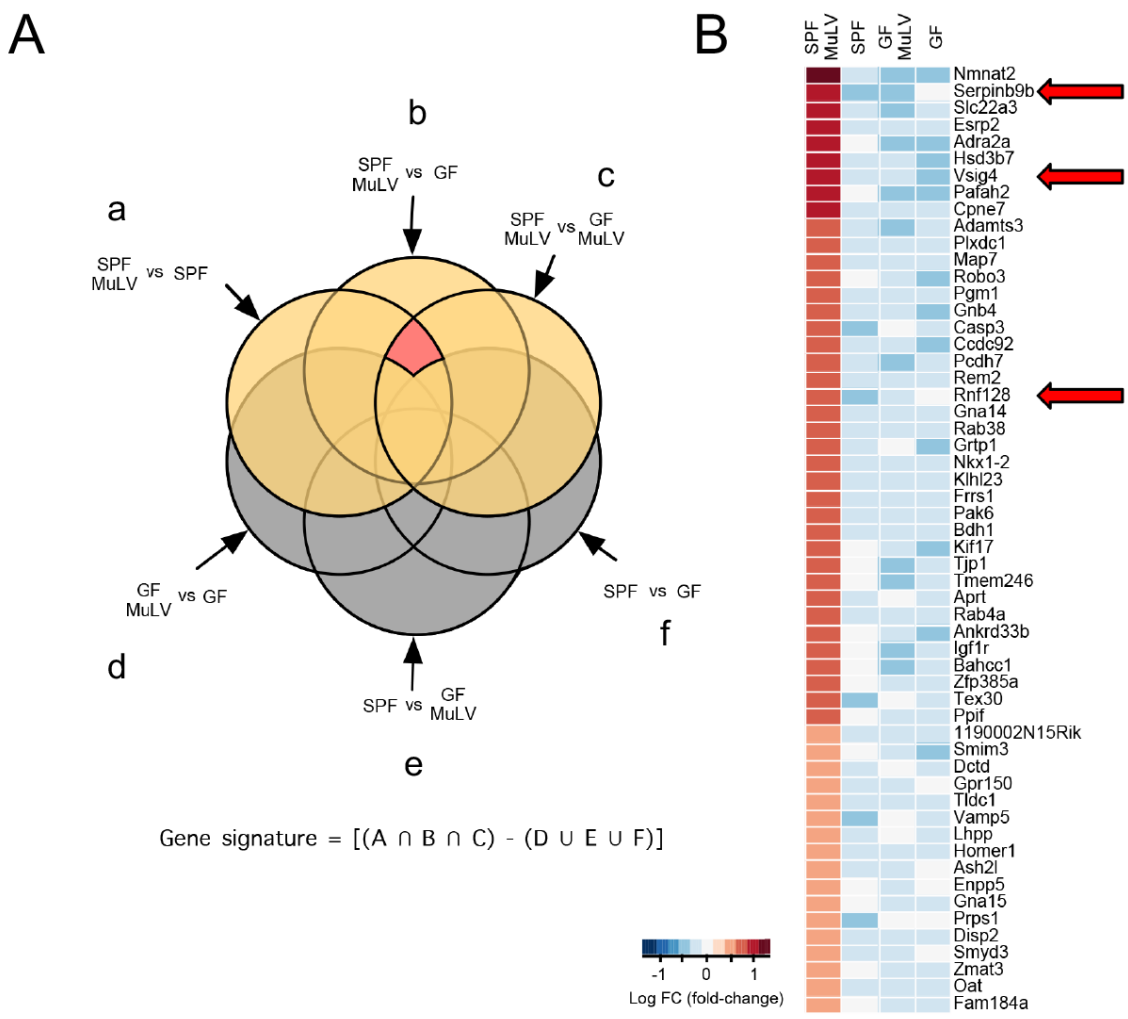

Figure 2.1. Gene expression mediated by commensal bacteria and the virus.
RNA isolated from spleens of preleukemic mice (score 1) of 4 groups (SPF +/- MuLV infection and GF +/- MuLV infection) was subjected to high throughput sequencing. **(A)** Diagram detailing the series of operations taken to identify genes differentially expressed in spleens of mice from four groups. See explanation in the text. **(B)** Heat map of gene expression found to be significantly upregulated in SPF MuLV-infected mice compared to mice from all other groups. Red arrows indicate established negative regulators of adaptive immunity. Two-way ANOVA was used to identify genes upregulated in infected SPF mice compared to uninfected SPF, uninfected GF, and infected GF mice.

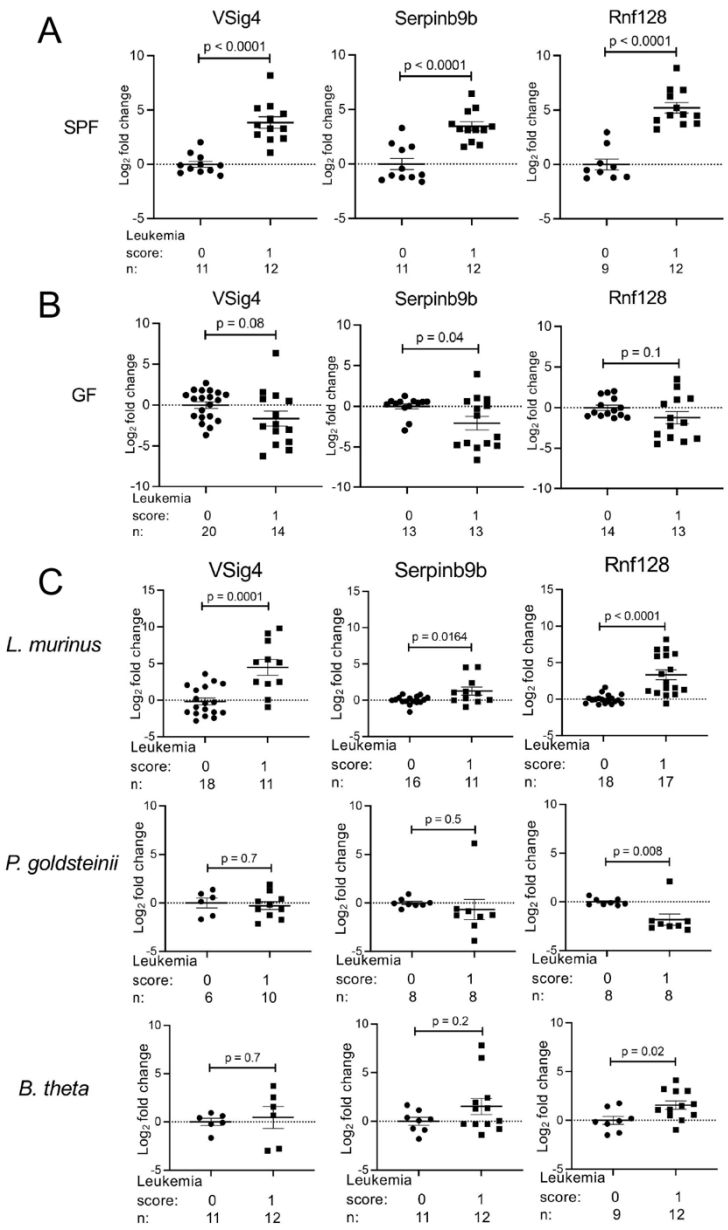

Figure 2.2. Induction of negative regulators of the immune response by commensal bacteria and the virus.

(A, B) Real time quantitative PCR (qPCR) measurement of expression of the negative regulators of immune response in SPF and **(B)** GF mice. Mice were either uninfected (score 0) or infected pre-leukemic (score 1). **(C)** qPCR with RNA isolated from spleens of uninfected (score 0) and infected pre-leukemic (score 1) mice colonized with *L. murinus*, *P. goldsteinii,* or *B. theta*. Data are represented as $\log_2$ fold change compared to uninfected controls, normalized to the endogenous control (beta-actin). n, number of mice used. *p* values calculated using unpaired *t* test **(A, B, C)**. Error bars indicate standard error of the mean.

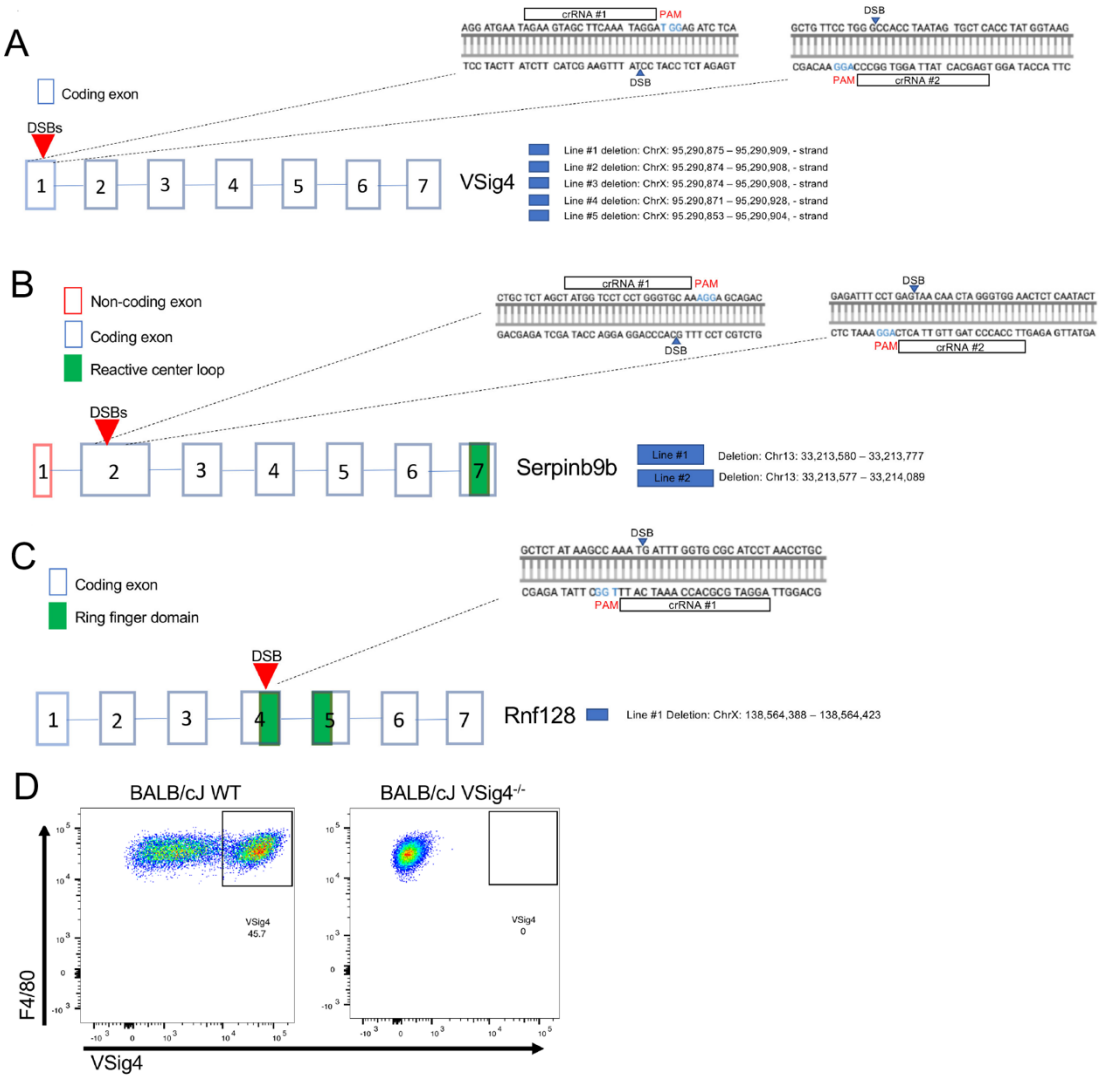

Figure 2.3. CRISPR-Cas9 targeting strategy for generation of VSig4-, Serpinb9b-, and Rnf128-deficient mice.
CRISPR-Cas9 targeting strategy for **(A)** VSig4, **(B)** Serpinb9b, and **(C)** Rnf128. Red arrow indicates location of double-stranded breaks within the targeted gene. Targeted sequences are shown on the right. All lines generated and the regions of the chromosome deleted are listed in blue boxes. **(D)** Peritoneal macrophages isolated from wild-type mice and VSig4$^{-/-}$ mice were stained with anti-VSig4 and anti-F4/80 antibodies. Representative FACS plot depicting staining in a wild-type mouse (plot on the left) and VSig4$^{-/-}$ mouse from line #2 (plot on the right). Deletion of VSig4 in the other lines was confirmed by FACS (data not shown).

does not contribute to MuLV-induced leukemia development. Serpinb9b-deficient mice showed a significant delay in leukemia development (Figures 2.4A and 2.4E) and reduced incidence of leukemia (Figure 2.4B) compared to wild-type and littermate mice (Figures 2.4A, 2.4B, and 2.4E). Interestingly, latency and incidence of leukemia development in Rnf128-deficient SPF mice were both significantly delayed and reduced compared to wild type mice (Figures 2.4A and 2.4B). Thus, Serpinb9b-deficiency and Rnf128-deficiency reverted leukemia susceptibility in SPF conditions to that of GF WT mice without affecting viral replication (Figure 2.4C).

Rnf128 was upregulated in $CD3^+$ cells, specifically $CD4^+$ T cells (Figures 2.5A), supporting a role for Rnf128 in mediating $CD4^+$ T cell unresponsiveness as previously reported (Kriegel et al., 2009; Nurieva et al., 2010). Serpinb9b was not upregulated in B cells, T cells, macrophages, or NK cells upon viral infection (Figure 2.5B). Overall, these data suggesting a pivotal role for T cells lacking Rnf128 and non-B, T, macrophage, or NK cells lacking Serpinb9b in blocking leukemia progression.

Although VSig4 does not contribute to MuLV induced leukemia development, VSig4 expression correlated very well with progression of leukemia in infected mice (Figures 2.6A and 2.6B). Importantly, the observed increase in VSig4 expression was not due to an influx of $F4/80^+$ macrophages into the spleen. Suggesting the increase in VSig4 expression is due to an altered transcriptional state in splenic resident macrophages rather than an influx of monocyte derived macrophages from the bone marrow. Therefore, we entertained the possibility that VSig4 expressing splenic resident macrophages contribute to leukemia development rather than VSig4 itself. There is precedence supporting macrophages contributing to tumor development. Tumor associated macrophages (TAMs) have been shown to support an inflammatory state in the tumor microenvironment (Mantovani et al., 2002). Specifically, TAMs exhibit reduced antigen presenting capacity and suppress T cell activation via release of inhibitory IL-10 and TGF-β. Additionally, TAMs secrete growth factors such as epidermal growth factor and vascular

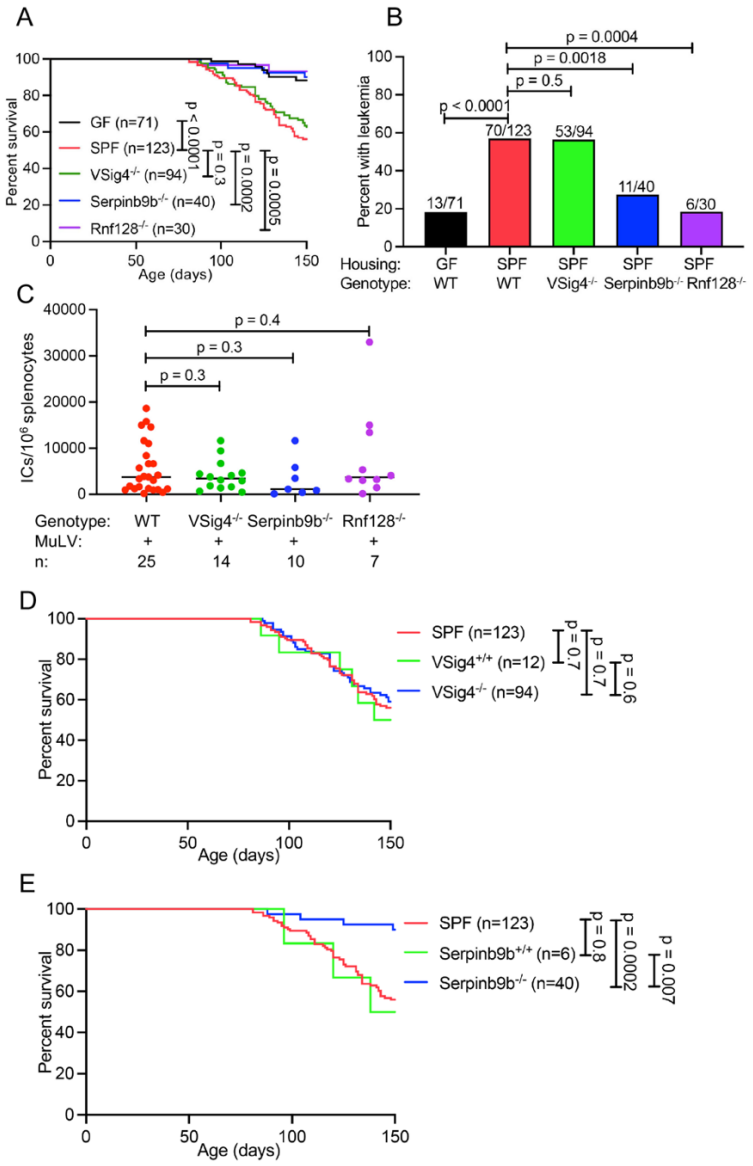

Figure 2.4. Resistance of Rnf128-deficient and Serpinb9b-deficient SPF mice to MuLV-induced leukemia.
MuLV-infected BALB/cJ mice deficient in either VSig4, Serpinb9b, or Rnf128 were monitored for leukemia development. **(A)** Survival curves for up to 150 days are shown. **(B)** Final leukemia assessment at 150 days. **(C)** Infectious centers per 10^6 splenocytes from pre-leukemic (score 1) SPF WT, VSig4$^{-/-}$, Serpinb9b$^{-/-}$, and Rnf128$^{-/-}$ mice. **(D)** Survival curve of SPF MuLV-infected VSig4$^{-/-}$, VSig4$^{+/+}$ littermates, and wild-type non-littermate BALB/cJ mice bred in the colony. **(E)** Survival curve of SPF MuLV- infected SPF Serpinb9b$^{-/-}$, Serpinb9b$^{+/+}$ littermates, and wild-type non-littermate BALB/cJ mice bred in the colony. As Rnf128 is mapped to X chromosome we had limited Rnf128+/+ mice as littermate controls and thus, used non-littermate BALB/cJ mice bred in the colony as experimental controls. n, number of mice used. *p* values calculated using Mantel-Cox test **(A, D, E)**, Fisher's exact test **(B)**, and unpaired *t* test **(C)**. Error bars indicate standard error of the mean.

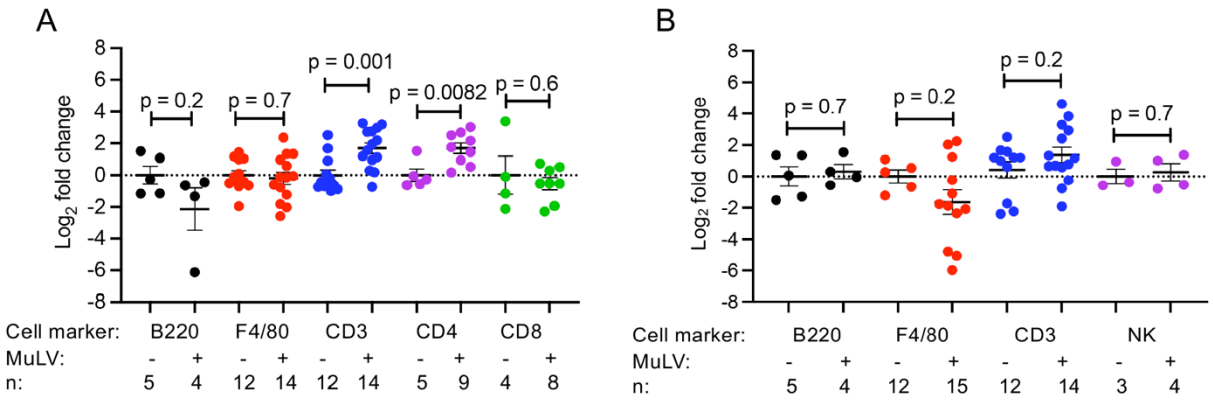

Figure 2.5. Cell expression of Rnf128 and Serpinb9b.
Expression of Rnf128 and Serpinb9b in sorted splenic cell RNA from uninfected and infected SPF WT mice analyzed by qPCR. Data are represented as log_2 fold change compared to uninfected controls, normalized to the endogenous control (beta-actin). **(A)** Expression of Rnf128 in $B220^+$, $F4/80^+$, $CD3^+$, $CD4^+$, and $CD8^+$ sorted cells. **(B)** Expression of Serpinb9b in $B220^+$, $CD3^+$, and $F4/80^+$ sorted cells. n, number of mice used. *p* values calculated using unpaired *t* test **(A, B)**.

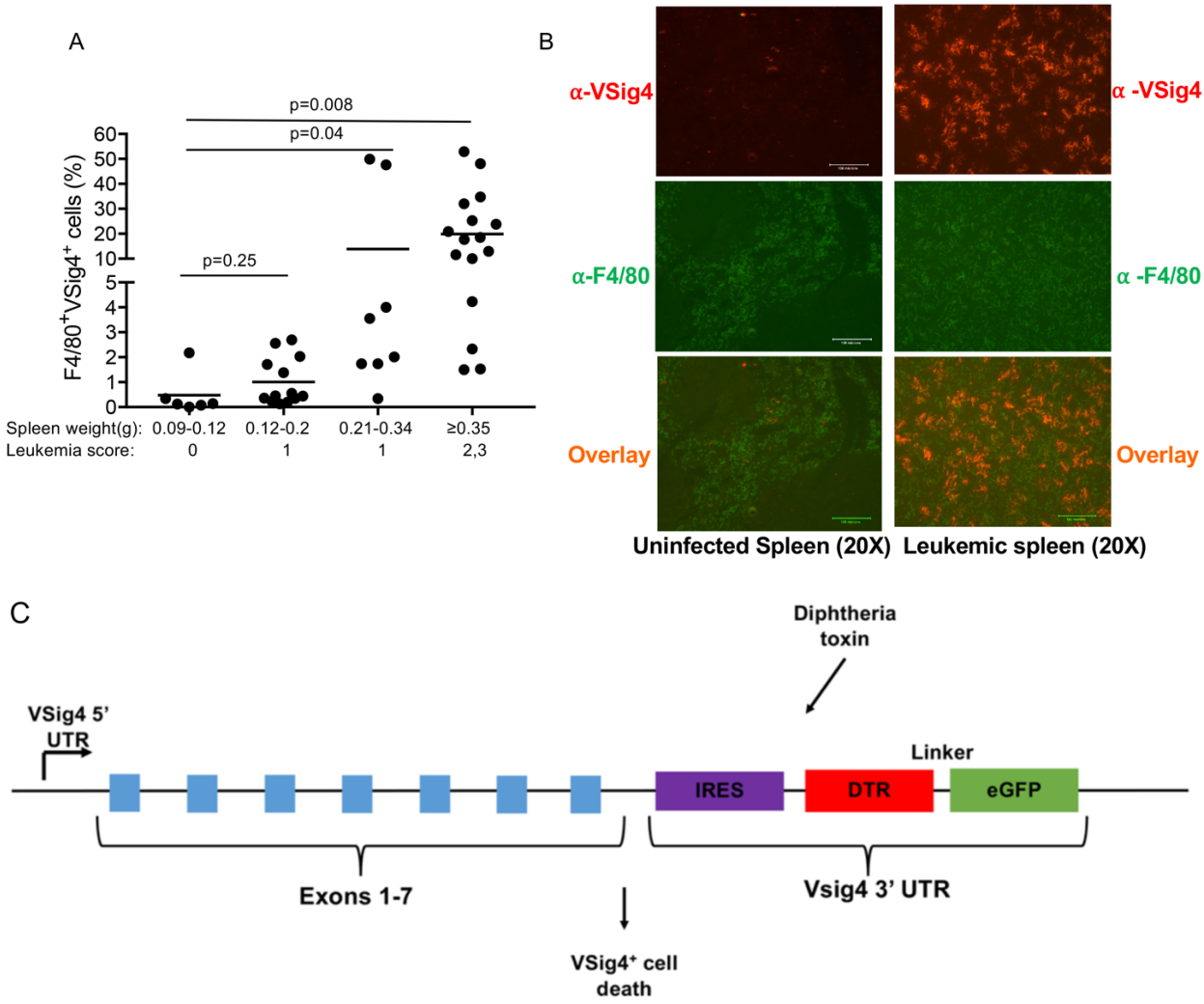

Figure 2.6. Analysis of the role of VSig4 in MuLV-induced leukemia development. **(A)** Percentage of F4/80^{+}VSig4^{+} splenocytes in uninfected and infected WT SPF mice analyzed by FACS. **(B)** Expression of F4/80^{+}VSig4^{+} splenocytes in uninfected (left) and leukemic (right) spleen analyzed by immunohistochemistry. The top panel shows staining for VSig4 in red. The middle panel reflects F4/80 staining in green. The bottom panel is an overlay of the top two panels. Orange color results from overlapping VSig4 (red) and F4/80 (green) fluorescence. **(C)** CRISPR-Cas9 targeting strategy for VSig4 IRES-DTR-GFP knock-in. *p* values calculated using unpaired *t* test **(A)**.

endothelial growth factor that influence tumor cell proliferation and angiogenesis (Mantovani et al., 2002). To test our hypothesis that VSig4 expressing splenic resident macrophages support leukemia development, we will be generating a mouse in which we can specifically delete VSig4 expressing macrophages. Using CRISPR/Cas9, an IRES-DTR-GFP fusion protein was inserted in the 3' UTR region of the VSig4 gene (Figure 2.6C). As the diphtheria toxin receptor (DTR) is not native to mice, only cells expressing the receptor will be susceptible to killing by the diphtheria toxin (Dtx). Upon exposure to Dtx, the catalytic A subunit will ADP-ribosylate elongation factor 2 (EF-2). ADP-ribosylation inactivates EF-2 and therefore prevents protein synthesis, leading to apoptosis mediated cell death (Ruedl & Jung, 2018). As $F4/80^{+}$ VSig4 expressing macrophages in the spleen are resident macrophages derived from the fetal liver, they will not be replenished by bone marrow derived monocytes after Dtx treatment (Perdiguero & Geissmann, 2016). Therefore, this is an effective mechanism by which to eliminate resident splenic macrophages expressing VSig4. Expression of this fusion protein will be confirmed by FACS and founder mice bred to establish a colony. To test whether VSig4 expressing macrophages contribute to leukemia development, the following study will be conducted. Female knock-in (KI) mice will be infected, and their progeny will be injected with a few doses of Dtx post weaning. Absence of VSig4 expressing macrophages will be confirmed by FACS. G1 treated KI mice will be monitored for leukemia along with G1 untreated KI mice. If Dtx treated KI mice develop leukemia at a slower rate than untreated KI mice, we can conclude that VSig4 expressing resident splenic macrophages support MuLV induced leukemia development.

In conclusion, RNA-seq analysis revealed three negative immune regulators whose expression was significantly increased in the presence of both the virus and the microbiota. Rnf128 and Serpinb9b proved to be critical for leukemia development in MuLV-infected SPF mice. In line with our results, overexpression of members of the ovalbumin family of serpins, to which Serpinb9b belongs, and Rnf128, are markers for poor prognosis in some human cancers (Bai et al., 2020; ten Berge et al., 2002; Uhlen et al., 2017) and our own analysis of previously

published data (Bolouri et al., 2018). A homolog for Serpinb9b has not been identified in humans, but related family member, human proteinase inhibitor 9 (SerpinB9) inhibits perforin-mediated cytotoxic T lymphocyte (CTL) cytotoxicity (Medema et al., 2001). Additionally, murine Serpinb9 was shown to protect mouse melanoma tumors from granzyme B mediated killing (Jiang et al., 2020). Published data support the idea that Serpinb9b functions in a similar manner by inhibiting the action of granzymes toward tumors (Bots et al., 2005). Rnf128 is highly expressed in T cells undergoing anergy and subsequently found to regulate T cell function by ubiquitinating key activation signaling molecules, such as CD3 and CD40L, resulting in their degradation (Lineberry et al., 2008; Nurieva et al., 2010). Rnf128 deficient primary $CD4^+$ T cells did not develop anergic phenotype in various models and also exhibited hyperactivation upon TCR stimulation (Kriegel et al., 2009). Rnf128 deficiency in $CD8^+$ T cells enhances their anti-tumor effector function by increasing expression of IFN-γ, granzyme B, perforin 1, and TNF-α (Haymaker et al., 2017). Precisely how Serpinb9b and Rnf128 function in the context of MuLV infection is unknown, but it is likely that they mediate immune suppression via these described pathways.

Interestingly, $VSig4^{-/-}$ mice were as susceptible as wild-type littermates to MuLV-induced leukemia (Figures 2.4A and 2.4B). Although VSig4 is a *bona fide* negative regulator, in this case it may have been a marker of cells that upregulate VSig4 but have immunosuppressive function that is independent of it. For example, resident macrophages, in which VSig4 is expressed, are known to have immunosuppressive function (Chen et al., 2011; Chen et al., 2010; Fu et al., 2012; Vogt et al., 2006; Xu et al., 2010).

CHAPTER 3: INNATE IMMUNE SENSORS OF BACTERIA MODULATE LEUKEMIA DEVELOPMENT BY UPREGULATION OF NEGATIVE IMMUNE REGULATORS

Preface

The contents of this chapter are modified and adapted from J. Spring, S. Lara, A. Khan, K. O'Grady, J. Wilks, S. Gurbuxani, et al. bioRxiv 2022 Pages 2022.02.02478820. I performed most of the experiments described in this section. J.W. monitored TLR2$^{-/-}$, TLR4$^{-/-}$, and TLR2$^{-/-}$ TLR4$^{-/-}$ mice for leukemia and conducted infectious center assays on these mice. S.L. assisted with qPCR analysis of negative immune regulators in Caspase1/11$^{-/-}$ and RIPK2$^{-/-}$ mice. S.L. analyzed 16S rRNA sequencing.

Abstract

Presence and detection of the commensal microbiota plays a crucial role in establishing and maintaining the host's health. However, certain pathogens have made use of the host's detection of commensal microbes for their own advantage, enabling evasion and suppression of the immune system (Baldridge et al., 2015; Ichinohe et al., 2010; Kane et al., 2011; Kuss et al., 2011; Uchiyama et al., 2014). While the influence of commensal microbes on viral infection is well established, in many studies the nature of the microbial derived factor(s) and the host sensor(s) that detects this factor to manipulate the host response to the pathogen is not well understood. In this chapter, we describe how in the context of MuLV infection, detection of bacteria derived factors via innate immune sensors Caspase1/11 and RIPK2 upregulates negative immune regulator Serpinb9b, promoting leukemia development likely via suppression of the anti-tumor immune response. A novel mechanism utilized by a pathogen to suppress the immune response.

Introduction

Known mechanisms by which the microbiota influences cancer development requires detection of the microbe(s) through host pattern recognition receptors or microbial mediated production of metabolites which in turn induces production of signaling molecules or inflammation to promote tumor growth (Arthur et al., 2012; Hope et al., 2005; Rakoff-Nahoum & Medzhitov, 2007; Reddy et al., 1975; Yoshimoto et al., 2013). As we have shown, the host microbiota supports MuLV induced leukemia development through upregulation of negative immune regulators that suppress the immune response against MuLV pathogenesis. Our next goal was to identify how the host detects tumor promoting bacteria and whether this sensing directly mediates expression of the negative immune regulators.

Results and discussion

To ascertain how the host detects microbial derived factors which subsequently leads to upregulation of negative immune regulators, we investigated the role of host innate immune receptors in RL-MuLV- induced leukemia. Given that bacteria are sufficient to promote RL-MuLV induced leukemia, we investigated pattern recognition receptors that specifically detect bacterial moieties. We hypothesized that removal of the host sensor detecting leukemia-promoting bacteria would result in resistance to leukemia even in the presence of the microbiota. Mice lacking innate immune receptors TLR2, TLR4, Caspase1/11, and mice unable to signal through NOD1/2 via deficiency in adaptor RIPK2 were bred on the BALB/cJ background, infected with RL-MuLV and their offspring were monitored for leukemia. Mice deficient in TLR2, a receptor for bacterial products including lipoteichoic acid and capsular polysaccharide (de Oliviera Nascimento et al., 2012; Graveline et al., 2007; Han et al., 2003), displayed latency and incidence of leukemia similar to WT SPF mice (Figures 3.1A and 3.1B). Similarly, TLR4-deficient mice, which are unable to detect LPS (Poltorak et al., 1998), exhibited leukemia latency and incidence similar to WT SPF mice (Figures 3.1A and 3.1B). However, it

was possible that signaling through either TLR2 or TLR4 could be redundant and promote leukemia development. To address this possibility, we infected TLR2$^{-/-}$TLR4$^{-/-}$ mice and monitored their offspring for leukemia to find that they were as susceptible as mice deficient in either single receptor (Figures 3.1A and 3.1B).

Caspase1/11 deficient mice, which lack the ability to detect intracellular LPS (Huang et al., 2019), had a leukemia latency comparable to WT GF mice (Figure 3.2A). However, upon closing Caspase1/11 deficient mice at the end of the experiment, it was discovered that despite a lack in overt symptoms of leukemia, many mice had spleens weighing ≥ 0.35g and were thus considered leukemic. Therefore, total leukemia incidence in Caspase1/11 deficient mice is comparable to WT SPF mice (Figure 3.2B). Overall, Caspase1/11 deficiency delays leukemia development, but does not decrease the incidence of leukemia.

At the same time, mice deficient in RIPK2, the downstream adaptor of intracellular peptidoglycan receptors NOD1 and NOD2 (which detect γ-D-Glu-mDAP and MurNAc-L-Ala-D-isoGln, respectively) (Caruso et al., 2014), had significantly increased latency and decreased total leukemia incidence compared to WT SPF mice (Figures 3.1A and 3.2B). These data suggest that detection of microbial products, likely intracellular peptidoglycan, and signaling through the NOD1/2 RIPK2 pathway promoted RL-MuLV induced leukemia development. Importantly, viral burden was not decreased in Caspase1/11- or RIPK2- deficient mice compared to littermate controls, ruling this out as a possibility for the increased resistance to leukemia (Figures 3.2C and 3.2D). Although RIPK2 deficient mice were significantly more resistant to leukemia development compared to WT SPF mice, RIPK2 deficiency did not confer the level of leukemia resistance as observed in WT GF mice (Figures 3.2A and 3.2B). Suggesting that other innate immune sensors also play a role in RL-MuLV induced leukemia development.

We next contemplated how signaling through Caspase1/11 and RIPK2 could impact leukemia development. Considering upregulation of the negative immune regulators Rnf128,

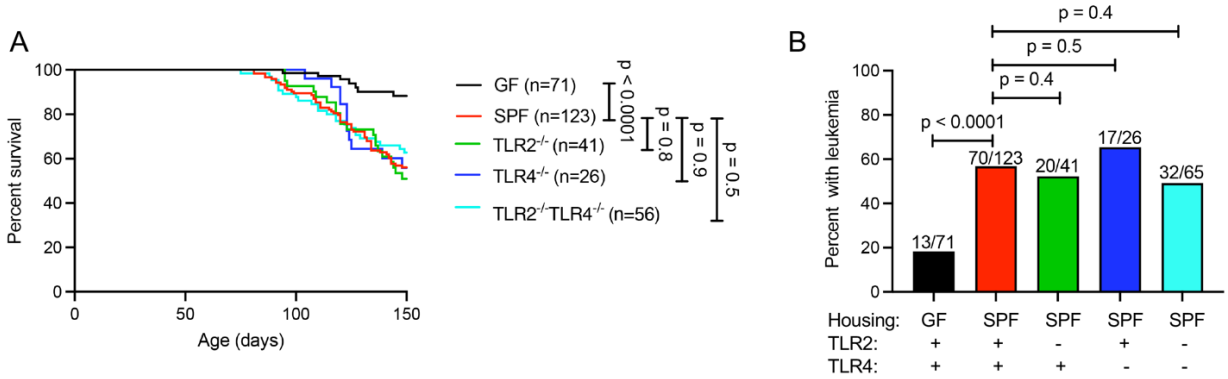

Figure 3.1. Innate immune receptors TLR2 and TLR4 do not contribute to MuLV-induced leukemia development.
MuLV-infected BALB/cJ mice deficient in either TLR2, TLR4, or both were monitored for leukemia development. **(A)** Survival curves for up to 150 days are shown. **(B)** Final leukemia assessment at 150 days. n, number of mice used in the study. *p* values calculated using Mantel-Cox test **(A)** and Fisher's exact test **(B)**.

VSig4, and Serpinb9b is dependent upon the microbiota, we wondered if detection of the microbiota through Caspase1/11 and/or RIPK2 would directly induce expression of these genes. To address this, we analyzed RNA expression of the negative immune regulators in infected Caspase1/11 and RIPK2 deficient mice. RNA from the spleens of infected and uninfected Caspase1/11 and RIPK2 deficient mice as well as their WT littermate counterparts was isolated. Expression of the negative immune regulators was assayed using SYBR green RT-qPCR. Neither Caspase1/11 nor RIPK2 deficiency influenced VSig4 expression upon infected (Figures 3.3A and 3.3B). Similarly, Rnf128 expression was upregulated in infected Caspase1/11 and RIPK2 deficient mice compared to uninfected deficient mice (Figures 3.3C and 3.3D). In contrast, Serpinb9b was not upregulated in either infected Caspase1/11 or RIPK2 deficient mice (Figures 3.3E and 3.3F). Importantly, Serpinb9b was upregulated in infected Caspase1/11-sufficient and RIPK2-sufficient control mice (Figures 3.3E and 3.3F). Together, these data demonstrate that activation of RIPK2 and Caspase1/11 contributes to the upregulation of Serpinb9b in the presence of both the virus and commensal bacteria. Therefore, a lack of Serpinb9b upregulation in Caspase1/11 and RIPK2 deficient mice is likely the basis for the observed increase in leukemia resistance.

If signaling through Caspase1/11 and RIPK2 induces Serpinb9b expression, why is there no upregulation of Serpinb9b in mice deficient in only one receptor? We hypothesize signaling through these receptors has an additive effect which leads to a detectable increase in Serpinb9b expression. This could explain why neither Caspase1/11 or RIPK2 deficient mice are as resistant to leukemia development as Serpinb9b deficient mice (Figures 3.2A, 3.2B, 2.4A, and 2.4B). Further delving into this hypothesis requires Caspase1/11/RIPK2 double deficient mice, which are currently being generated. If Serpinb9b expression upon MuLV infection is dependent upon signaling through Caspase1/11 and RIPK2, we would expect double deficient mice to have even lower levels of Serpinb9b expression compared to single deficient mice and similar leukemia resistance as mice lacking Serpinb9b. Finally, while signaling through

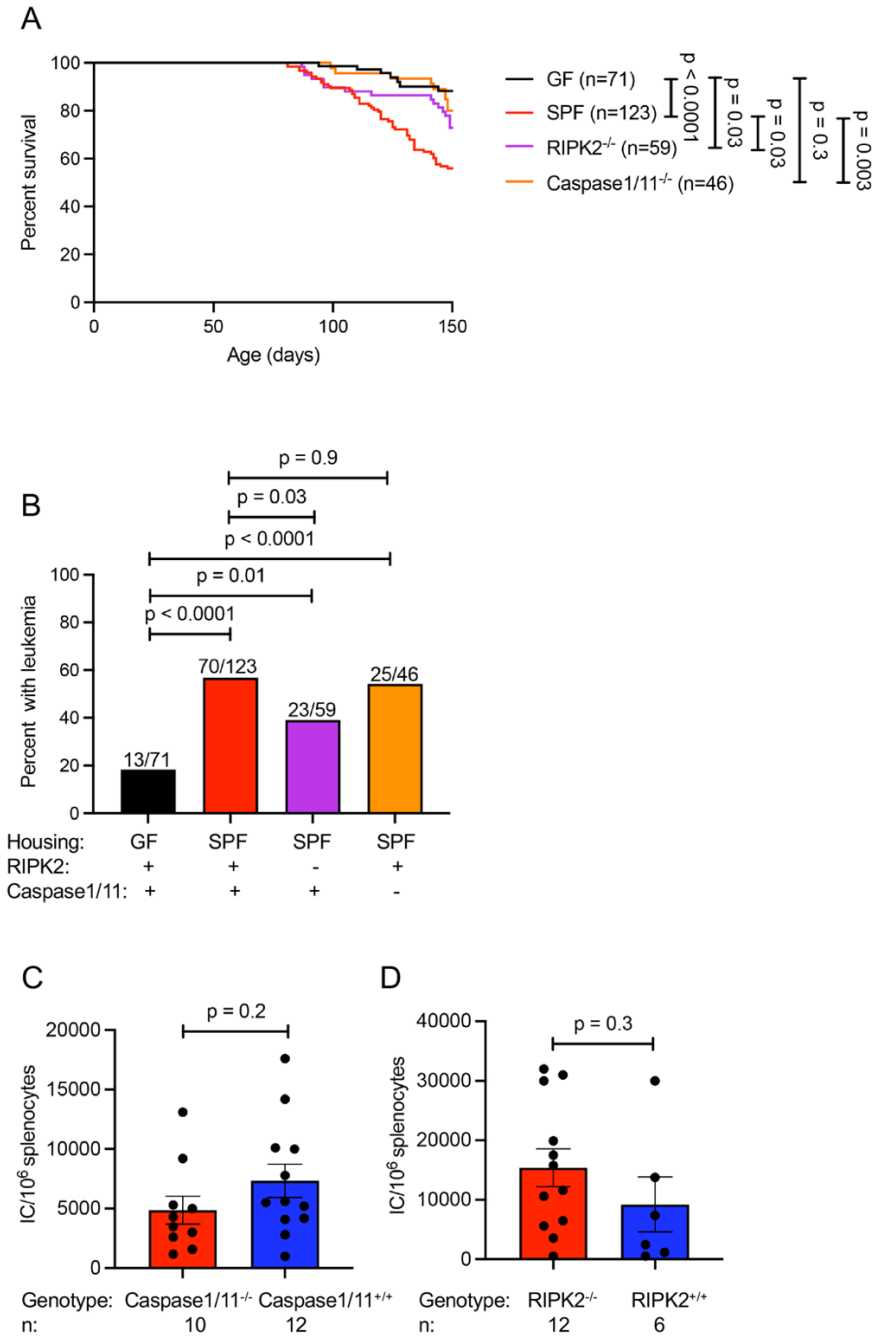

Figure 3.2. NOD1/2 adaptor RIPK2 and Caspase1/11 contribute to MuLV-induced leukemia.
Leukemia development was monitored in RL-MuLV-infected SPF BALB/cJ mice deficient in either RIPK2 or Caspase1/11. **(A)** Survival curves up to 150 days. **(B)** Total leukemia incidence at 150 days. **(C, D)** Comparison of viral load [number of infectious centers (ICs) per 10^6 splenocytes] in Caspase1/11-deficient and sufficient **(C)** or RIPK2-deficient and sufficient **(D)** animals. IC assay was done on preleukemic mice with score 1. n, number of mice used. *p* values were calculated using Mantel-Cox test **(A)**, Fisher's exact test **(B)**, and unpaired *t* test **(C)**. Error bars indicate standard error of the mean.

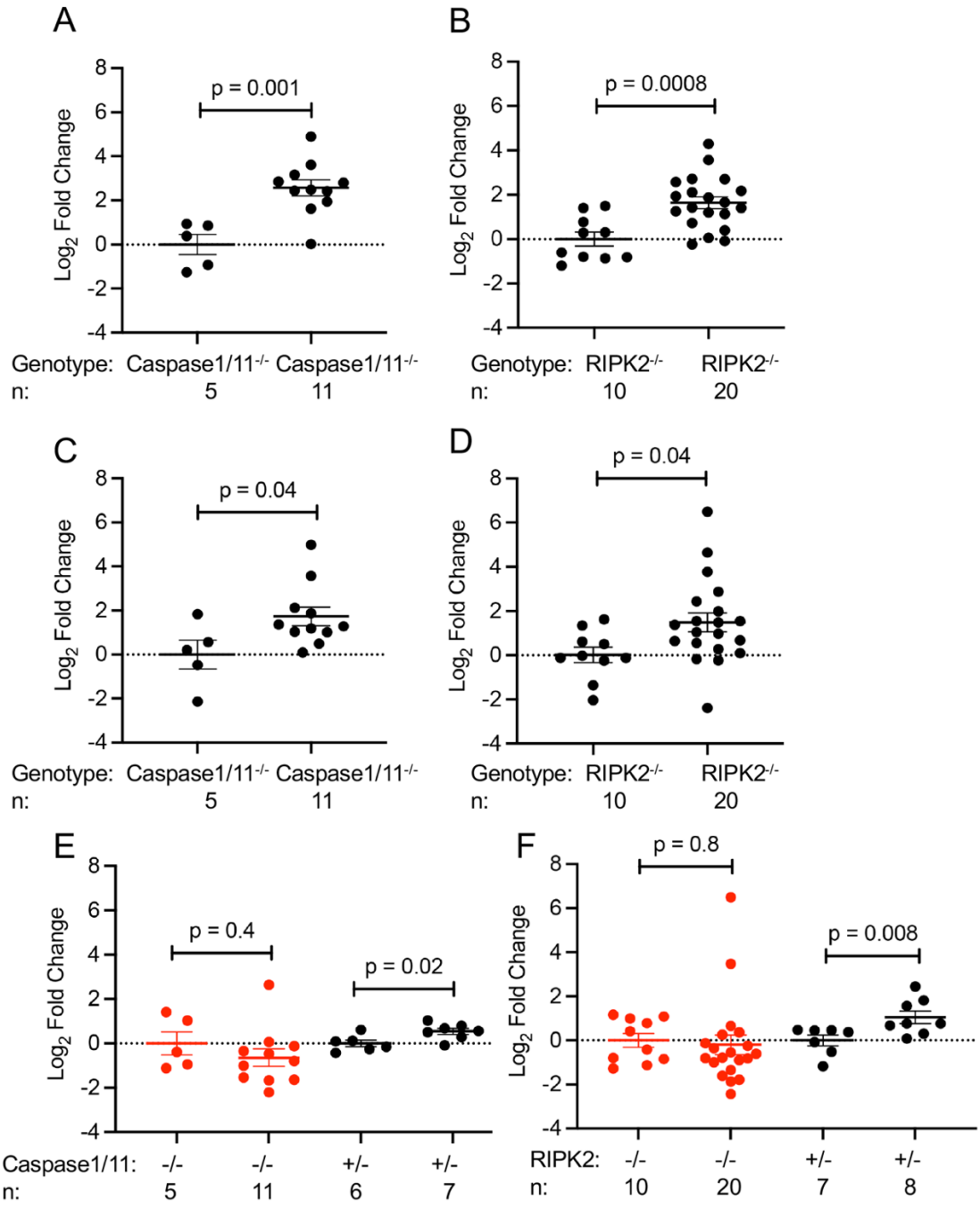

Figure 3.3. Caspase1/11 and NOD1/2 adaptor RIPK2 mediate MuLV-induced leukemia via upregulation of Serpinb9b.
(A-D) Expression of VSig4 **(A, B)** and Rnf128 **(C, D)** in splenic RNA from Caspase1/11$^{-/-}$ and RIPK2$^{-/-}$ uninfected and infected mice analyzed by qPCR. **(E, F)** Expression of Serpinb9b in splenic RNA from Caspase1/11$^{-/-}$ and control Caspase1/11$^{+/-}$ **(E)** or RIPK2$^{-/-}$ and control RIPK2$^{+/-}$ **(F)** uninfected and infected mice analyzed by qPCR. Data are represented as $\log_2$ fold change compared to uninfected controls, normalized to the endogenous control (beta-actin). n, number of mice used. *p* values calculated using unpaired *t* test **(A, B, C, D, E, F)**.

Caspase1/11 and RIPK2 leads to Serpinb9b upregulation, the signaling pathway that upregulates Rnf128 is currently unknown.

Previous research from our lab has described the influence of host genetics on the microbiota composition (Khan et al., 2019). Furthermore, NOD2 and Caspase1, and Caspase11 deficiency in mice has been shown to alter the microbiota (Brinkman et al., 2011; Demon et al., 2014; Petnicki-Ocwieja et al., 2009; Rehman et al., 2011). NOD2 deficient mice display outgrowth of bacteria in the terminal ileum compared to WT mice (Petnicki-Ocwieja et al., 2009). This may be due to reduced expression of certain cryptdins (α-defensins in humans) and reduced killing of bacteria by Paneth cells in the terminal ileum crypts of NOD2 deficient mice (Kobayashi et al., 2005; Petnicki-Ocwieja et al., 2009). Therefore, while investigating the induction of the negative immune regulators via signaling through innate immune receptors, we also investigated the influence of RIPK2 and Casapse1/11 deficiency on microbial composition.

As we have shown, certain bacteria support leukemia development while others do not (Figures 1.4C and 1.4D). Therefore, it is possible that in RIPK2 or Caspase1/11 deficient mice the microbiota is altered toward a tumor suppressing phenotype. To determine whether deficiencies in these receptors alters the microbiota we took the following approach. RIPK2 and Caspase1/11 deficient mice were rederived as GF, bred to produce a sizeable colony, and then housed in individual isolator cages based on genotype. Age matched mice of both genders from each genotype were used. GF RIPK2 deficient, Caspase1/11 deficient, and WT BALB/cJ mice were gavaged with 200μl of suspended cecal content from three C57/BL6 taconic mice. Two weeks post association, mice were sacrificed and cecal contents were collected. Cecal contents from associated mice along with the input cecal content was sent for 16S rRNA sequencing.

There was no significant difference in Alpha diversity between the cecal content of each genotype as analyzed by Shannon and Simpson diversity indexes (Figure 3.4). To analyze the overall similarity or dissimilarity in cecal content between WT, RIPK2 KO, and Caspase1/11 KO

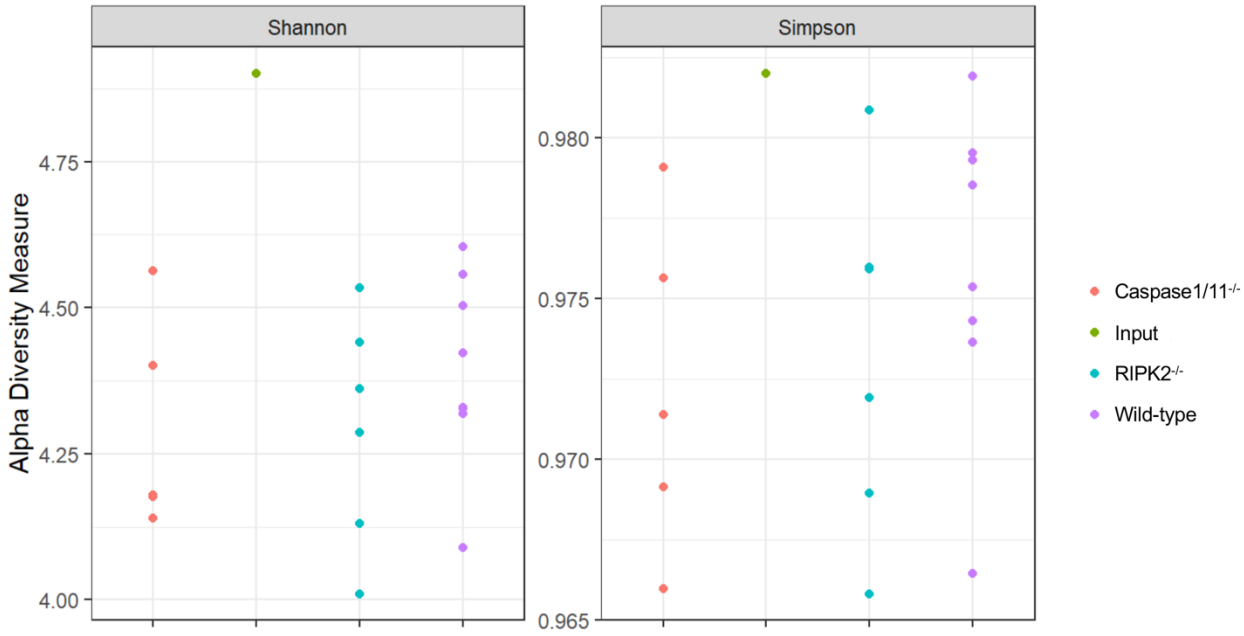

Figure 3.4. Alpha diversity is not altered in Caspase1/11- or RIPK2-deficient mice compared to WT mice when colonized with C57BL/6 cecal content.
Alpha diversity in WT, Caspase1/11$^{-/-}$, and RIPK2$^{-/-}$ mice as measured by Shannon (left) and Simpson (right) diversity indices. Each dot is a single mouse.

mice, principal coordinates analysis (PCoA) plots were constructed using Bray-Curtis distance. Each data point represents an individual mouse whose cecal contents were sequenced. When mice of all three genotypes are compared together, there is no significant clustering between mice of the same genotype, suggesting minor differences in cecal content between all of the mice regardless of genotype (Figure 3.5A). A comparison between Caspase1/11 deficient mice and WT mice does not yield significant differences in cecal content between the two groups as data points for Caspase1/11 deficient mice do not cluster separately from data points for WT mice (Figure 3.5B). Likewise, RIPK2 deficient associated mice have cecal contents similar to WT associated mice (Figure 3.5C). Overall, these data indicate minimal differences in the bacterial composition of the cecum between WT, Caspase1/11$^{-/-}$, and RIPK2$^{-/-}$ mice when colonized with the same input microbiota.

While PCoA plots are useful for observing large overall differences between different groups, small differences are likely to be missed. Additionally, PCoA plots are unable to tell us what is specifically different in the cecal contents between mice of different genotypes. To achieve this, we analyzed the abundance of amplicon sequence variants (ASVs) at the level of family and genus between mice of each genotype (Figures 3.6A and 3.6B). Heat maps were constructed to illustrate the few ASVs which were significantly altered in abundance between the three genotypes (Figures 3.7A and 3.7B). As it is difficult to visualize the differences in abundance between mice of different genotypes when *Lachnospiraceae* NK4A136 group is included in the heat map (Figure 3.7A), an identical heatmap minus this genus is included (Figure 3.7B). Members of the *Prevotellaceae* and *Ligilactobacillus* genus were higher in abundance in RIPK2 deficient cecal contents compared to WT cecal contents. Conversely, WT cecal contents contained greater abundance of bacteria from the Erysipelotrichaceae family and *Mucispirillum*, *Roseburia*, and *Harryflintia* genera. Representatives of the *Lachnospiraceae* NK4A136 group were in greater abundance in Caspase1/11 deficient mice compared to WT mice. However, constituents of the *Parabacteroides*, *Peptococcus*, and *Mucispirillum* genera

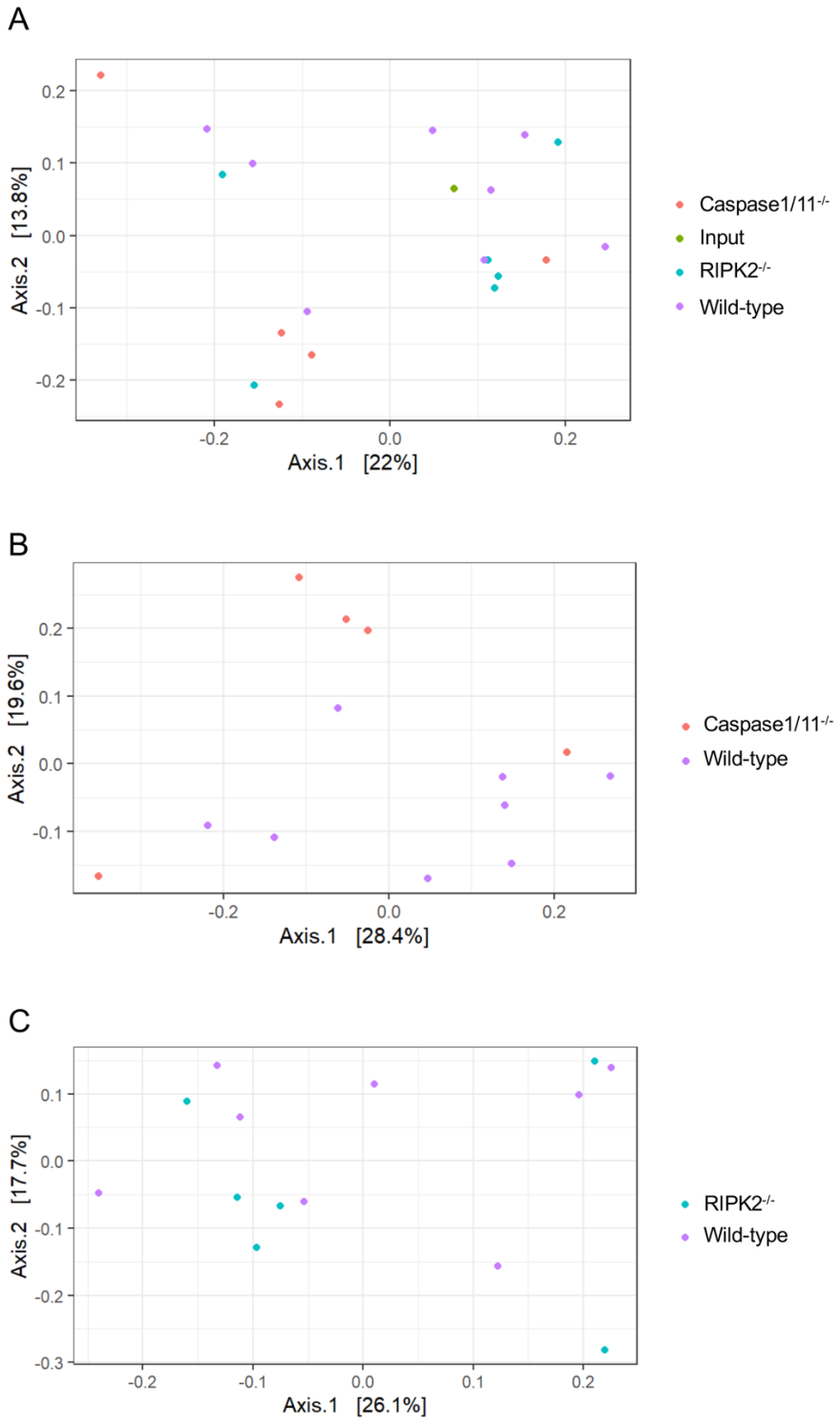

Figure 3.5. PCoA plots of cecal derived bacterial content from WT, Caspase1/11$^{-/-}$, and RIPK2$^{-/-}$ mice colonized with C57BL/6 cecal contents.
(A) Comparison of overall bacterial similarity between cecal contents of WT, Caspase1/11$^{-/-}$, and RIPK2$^{-/-}$ mice. **(B, C)** Analysis of similarity between WT and Caspase1/11$^{-/-}$ **(B)** or WT and RIPK2$^{-/-}$ **(C)** bacterial cecal content. Each dot is an individual mouse.

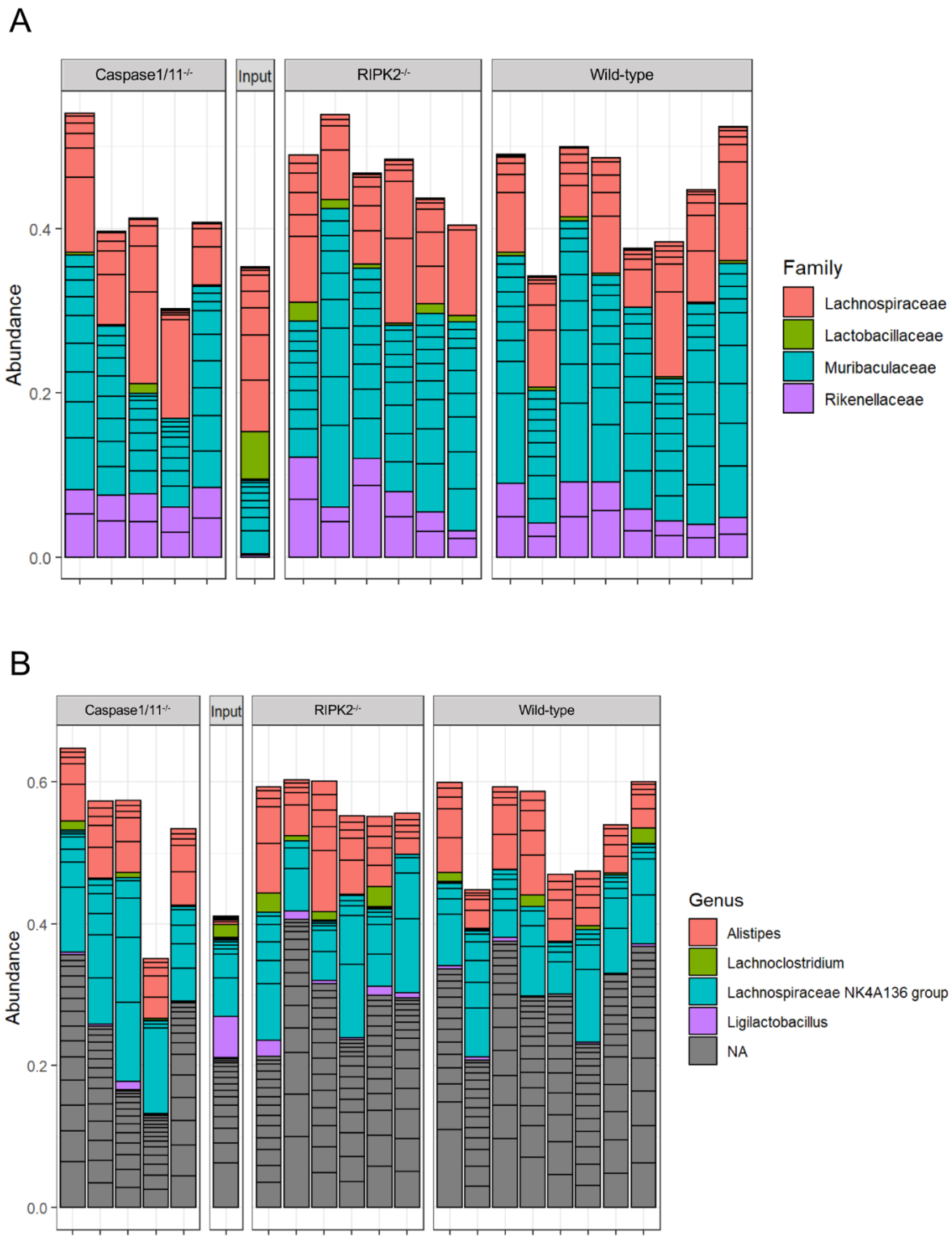

Figure 3.6. Bacterial abundance in cecal content of WT, Caspase1/11$^{-/-}$, and RIPK2$^{-/-}$ mice colonized with C57BL/6 cecal microbiota.
(A, B) Bacterial abundance at the level of family **(A)** and genera **(B)**.

were of higher abundance in WT cecal contents compared to cecal contents from Caspase1/11 deficient mice. Finally, only members of two genera, *Prevotellaceae* and *Eubacterium* nodatum group, were in greater abundance in RIPK2 deficient mice compared to Caspase1/11 deficient mice.

It is important to note that these differences we observe are specific to the input from C57BL/6 Taconic mice. We wondered if the microbiota specific to our facility would be influenced by the absence of Caspase1/11 or RIPK2. Based on previous literature illustrating the influence of NOD2, Caspase1, and Caspase11 on the commensal microbial composition, we entertained the possibility that RIPK2 and Caspase1/11 apply pressure to the microbiota influencing diversity and abundance, which may in turn effect microbiota dependent MuLV induced leukemia development. To determine which bacterial species are suppressed in WT mice and therefore gained in RIPK2 or Caspse1/11 deficient mice the following experiment was conducted. Cecal content from three RIPK2 deficient mice within our SPF colony was collected, combined, and snap frozen. GF WT, RIPK2$^{-/-}$, and Caspse1/11$^{-/-}$ mice housed in isolator cages based on genotype were gavaged with cecal content from RIPK2$^{-/-}$ mice. Two weeks post association, mice were euthanized and cecal content was collected for 16S rRNA sequencing.

Bacterial diversity within the cecal content of WT, Caspase1/11-, and RIPK2-deficient mice was not significantly different (Figure 3.8). Further analysis shows high similarity between the cecal composition of mice regardless of Caspase1/11 or RIPK2 expression (Figures 3.9A-C). The top 30 ASVs by abundance at the family and genus level were comparable between mice of all genotypes (Figures 3.10A and 3.10B). Overall, 14 ASVs at the level of genus were significantly different between WT, Caspase1/11-, and RIPK2-deficient mice (Figures 3.11A and 3.11B). However, only two ASVs, genus *Tuzzerella* and member of the family Erysipelotrichaceae were significantly more abundant in RIPK2$^{-/-}$ mice compared to WT mice. Furthermore, these ASVs made up around 0.2% and 0.4%, respectively, of total bacterial abundance. As these are at very low abundance, it is unlikely they play a significant role in

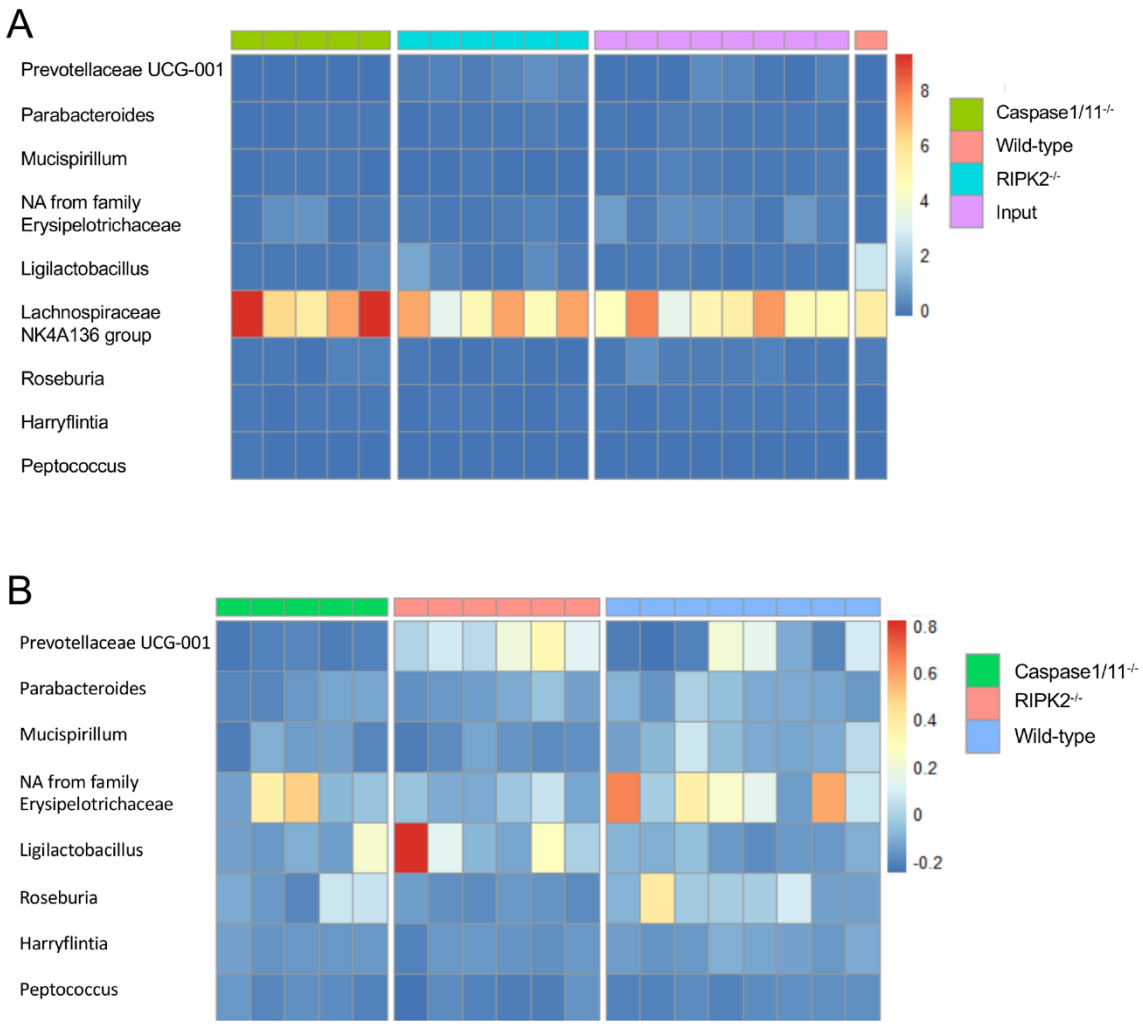

Figure 3.7. Heat maps of ASVs at the genus level with significantly different abundances between WT, Caspase1/11$^{-/-}$, and RIPK2$^{-/-}$ mice colonized with C57BL/6 cecal content. **(A)** Heat map of nine ASVs that exhibit significantly different abundances between mice of indicated genotypes. **(B)** Heat map in (A) minus *Lachnospiraceae* NK4A136 group. Each column is an individual mouse. Each row is a specific ASV.

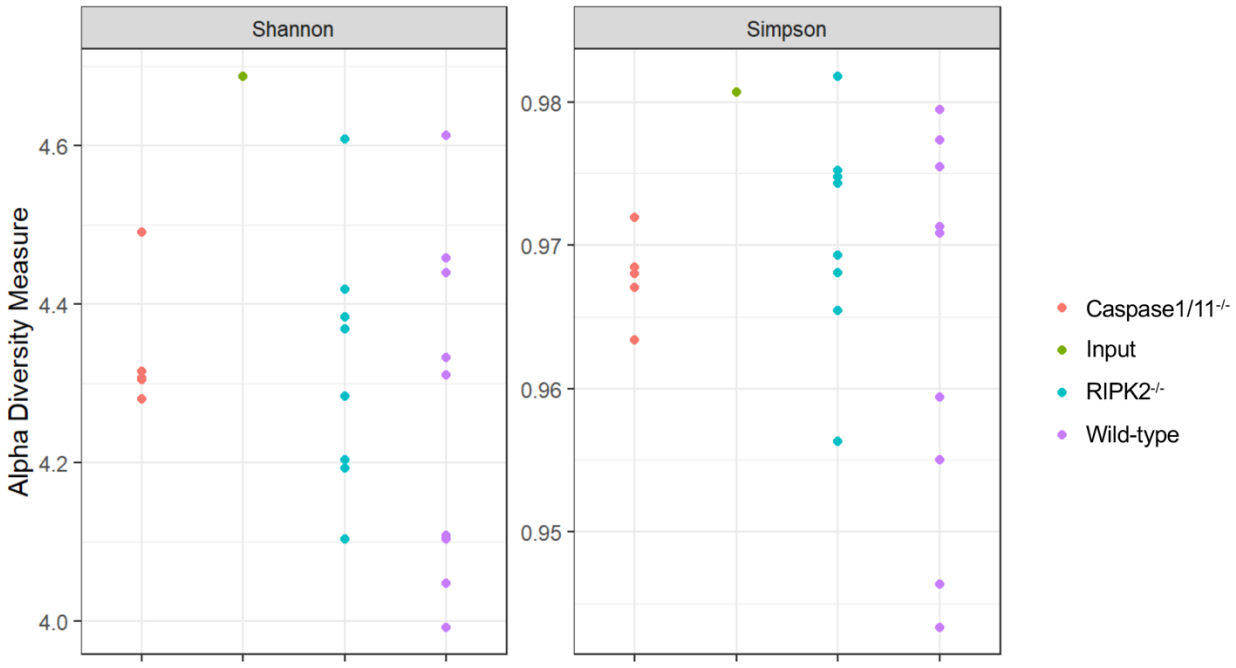

Figure 3.8. Alpha diversity in WT, Caspase1/11$^{-/-}$, RIPK2$^{-/-}$ mice colonized with cecal content from SPF RIPK2$^{-/-}$ mice.
Diversity as measured by Shannon (left) and Simpson (right) index is not significantly different between mice of different genotypes analyzed. Each point is an individual mouse.

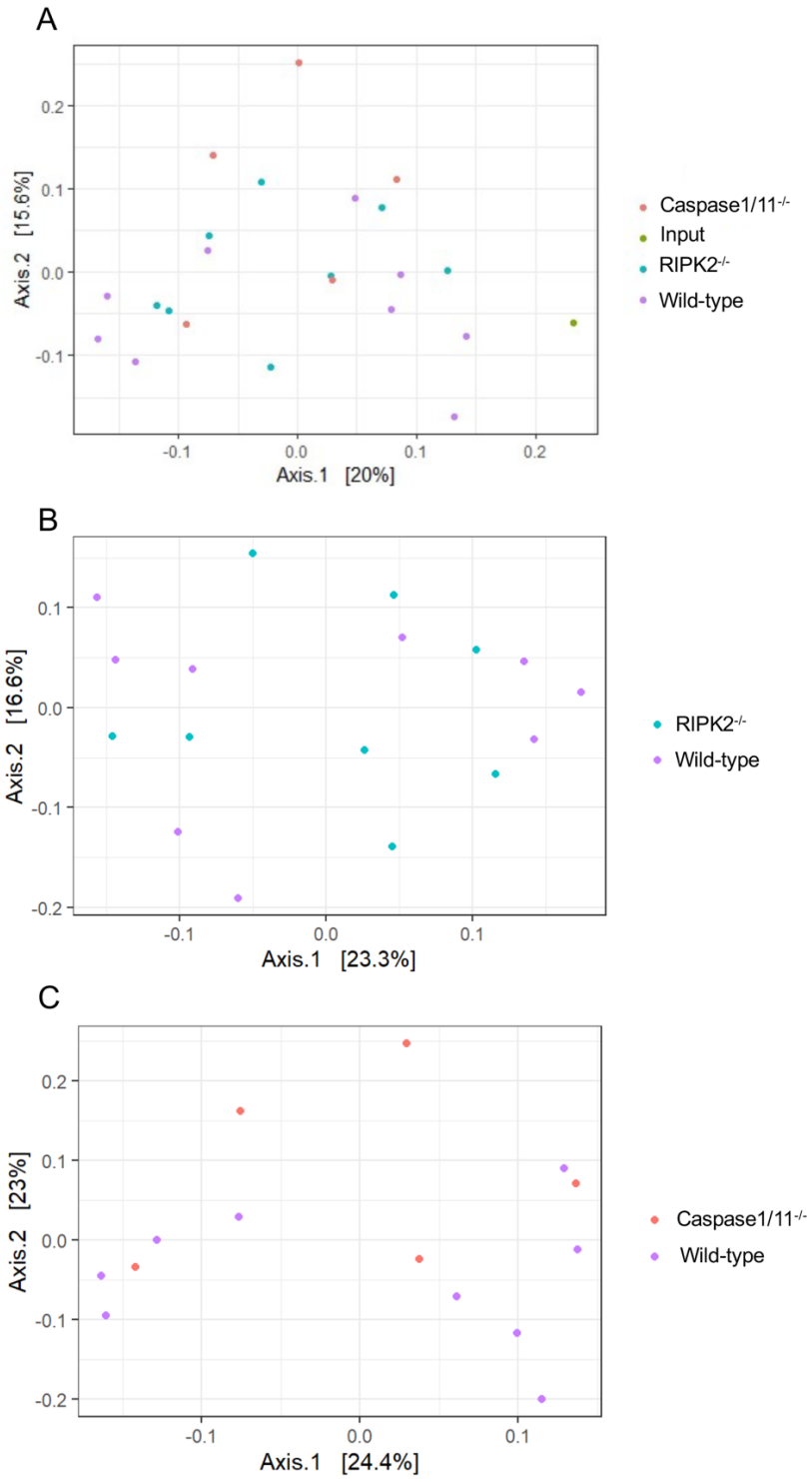

Figure 3.9. Cecal bacterial composition is highly similar between WT, Caspase1/11$^{-/-}$, and RIPK2$^{-/-}$ mice colonized with SPF RIPK2$^{-/-}$ cecal content.
(A) PCoA plot comparing WT, Caspase1/11$^{-/-}$, RIPK2$^{-/-}$, and input bacterial composition. **(B, C)** PCoA plots assessing similarity of bacterial composition between WT and RIPK2$^{-/-}$ mice **(B)** or WT and Caspase1/11$^{-/-}$ mice **(C).** Each dot is an individual mouse.

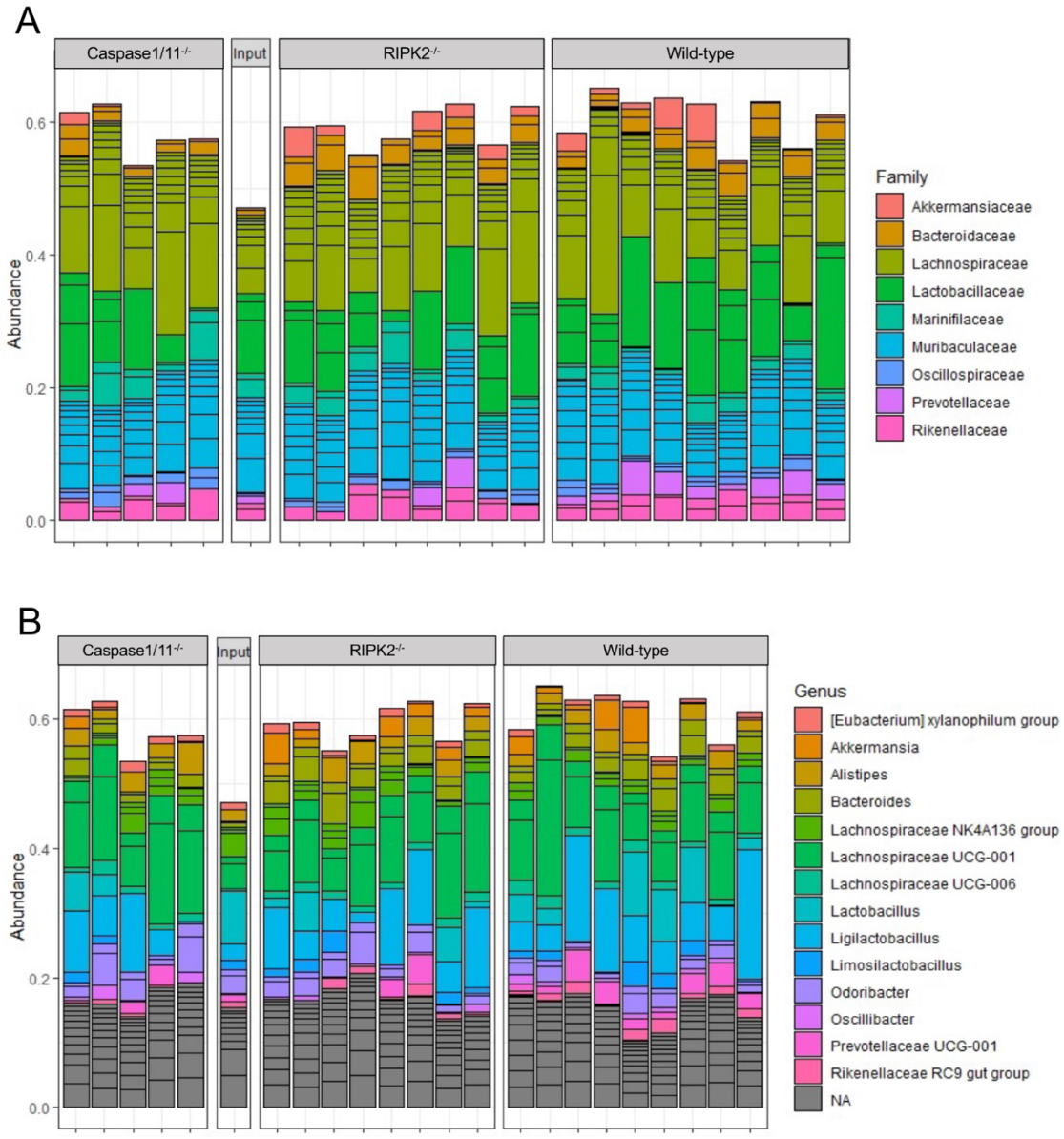

Figure 3.10. Abundance of top 30 ASVs from WT, Caspase1/11$^{-/-}$, RIPK2$^{-/-}$, and input cecal content.
(A, B) Abundance of the top 30 ASVs at the family **(A)** or genus level **(B).** Each column is an individual mouse.

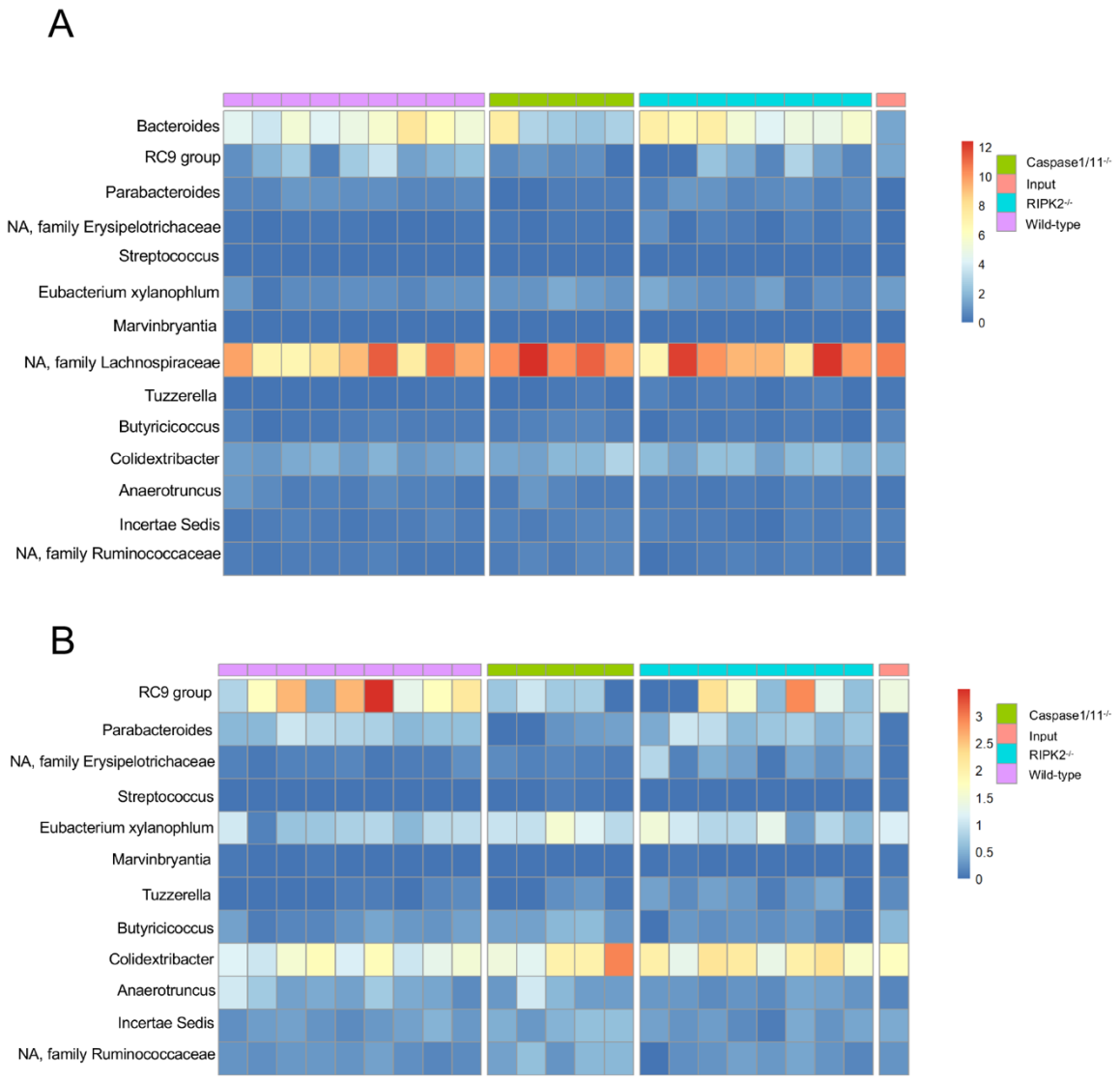

Figure 3.11. Heatmap of ASVs at the genus level whose abundances are significantly different between WT, Caspase1/11$^{-/-}$, and RIPK2$^{-/-}$ mice associated with cecal content from SPF RIPK2$^{-/-}$ mice.
(A) 14 ASVs with significantly different abundances. **(B)** Heatmap shown in (A) minus *Bacteroides* and NA from the Lachnospiraceae family. Each row is an ASV, and each column is an individual mouse.

conferring MuLV-induced leukemia resistance. Suggesting that direct signaling through RIPK2 promotes leukemia development.

To determine whether the microbiota is significantly altered in Caspase1/11-deficient mice and potentially contributing to increased leukemia resistance, deficient and sufficient GF mice will need to be colonized with cecal content from SPF Caspase1/11$^{-/-}$ mice and the diversity/abundance of bacteria analyzed. Finally, the gut microbiome also consists of viruses, fungi, archaea, and protists which may contribute to microbiota dependent MuLV induced leukemia. However, due to availability and accuracy in microbial sequencing techniques, we focused on the bacterial members of the gut microbiome.

CHAPTER 4: COMMENSAL BACTERIUM AND VIRUS DIFFERENTIALLY ALTER METABOLITE PROFILE

Preface

Colonization of GF mice with *L. murinus* and collection of plasma and spleens for analysis was done by me. Tandem liquid-chromatography/mass-spectrometry was conducted by Brain DeFelice of Chan Zuckerburg Biohub in partnership with our collaborator, Michael Fischbach of Stanford. Analysis of the metabolomics data was conducted by Vera Beilinson.

Abstract

Commensal bacteria, including numerous bacterial derived compounds, have been shown to modulate many diseases including infections with pathogens, autoimmunity, and cancer development (Chervonsky, 2013; Garrett, 2015; Wilks & Golovkina, 2012; Xu et al., 2019). Additionally, microbial dependent metabolites and secondary bile acids have recently been shown to modify disease states, including tumor development (Hezaveh et al., 2022; Mishra et al., 2021; Rossi et al., 2020). Therefore, we utilized metabolomics to further investigate bacterial dependent metabolites that may contribute to MuLV pathogenesis. Furthermore, while a few studies have examined alterations in metabolites after bacterial colonization (Han et al., 2021; Wikoff et al., 2009) or viral infection (Groves et al., 2020) it is unknown how bacteria plus viral infection alter the metabolomic landscape. Using tandem liquid-chromatography/mass-spectrometry we analyzed the effect of bacterial colonization and MuLV infection on metabolite abundances within the spleen and plasma.

Introduction

Investigations into leukemia susceptibility in SPF mice deficient in various innate immune receptors indicates activators of Caspase1/11 and RIPK2 contribute to MuLV induced leukemia. However, neither Caspase1/11 deficient nor RIPK2 deficient SPF mice display

leukemia resistance comparable to GF mice. Implying additional factors derived from bacteria and their cognate host sensors mediate MuLV induced leukemia. So far, our studies have focused on host receptors that detect structural features of bacteria. However, many studies have illustrated a role for bacterial derived metabolites in cancer development (Hezaveh et al., 2022; Mishra et al., 2021; Rossi et al., 2020). To begin investigating a role for metabolites in MuLV pathogenesis, the metabolites expressed in the periphery of infected colonized mice were determined using an unbiased metabolomics approach.

Results and discussion

To minimize the complexity and number of metabolites identified in the metabolomics screen, we made use of monocolonized mice. As previously shown, progeny of MuLV infected *L. murinus* colonized females developed leukemia at a similar rate as SPF mice. To identify metabolites influenced by the presence of bacteria and the virus, spleens and plasma were collected from uninfected and progeny of MuLV infected *L. murinus* colonized mice as well as uninfected and progeny of MuLV infected GF mice. Samples were subjected to tandem liquid chromatography/mass spectrometry at the Chan Zuckerburg Biohub in partnership with our collaborator, Michael Fischbach, at Stanford. Hydrophilic interaction liquid chromatography (HILIC) separated small polar compounds based on molecular size and affinity for the non-polar mobile and polar stationary phases of the column. Compounds were eluted at a gradient whereby non-polar compounds eluted faster followed by polar compounds. Spectra based on mass to charge ratios were collected on a mass spectrometer in both the positive and negative ionization mode. Metabolites were annotated using a local and global library. The local library was created through analysis of metabolite standards using the same protocol described for this study. The global library relies on the pattern produced from metabolite fragmentation to assign an identity to an unknown metabolite. From the spleens of mice from all four groups, a total of 2153 metabolites, of which 204 are known and 1949 unknown, were detected under the positive

ionization mode. Under the negative ionization mode, 1202 metabolites were detected of which 124 are known and 1078 unknown. Many of the detected metabolites are unknown because we can only identify metabolites which are included in the local or global libraries. Within each group of mice, the standard deviation of individual detected metabolites was compared. Those metabolites with a relative standard deviation greater than 30% from any one group were discarded from all groups. This normalizes the metabolites identified within each group and left us with 60 known and 852 unknown metabolites detected under positive ionization and 52 known and 739 unknown metabolites detected under negative ionization mode (Figure 4.1A and Supplemental Tables 4.1A, and 4.1B).

Metabolomics of the plasma was conducted in a similar manner. After discarding metabolites with a relative standard deviation greater than 30%, 73 known metabolites detected under positive ionization and 56 known metabolites detected under negative ionization were further analyzed (Figure 4.1B and Supplemental Tables 4.1C, and 4.1D).

By analyzing all metabolites detected within the spleen, we clearly see how presence of bacteria, MuLV, or both alters the metabolomic landscape within the spleen (Figures 4.2A and 4.2B). Next, two-way ANOVA was utilized to find metabolites whose expression is modified by the presence of both *L. murinus* and MuLV. While abundance of 306 metabolites and 103 metabolites were influenced by solely colonization or infection, respectively, a total of 428 metabolites detected within the spleen were found to be influenced by both bacterial colonization and viral infection (Figures 4.3A and 4.3B). However, the vast majority of these metabolites are not annotated, with only 21 being identified (Table 4.1).

Analogous to our analysis of metabolites within the spleen, we observed significant changes in the type and abundance of metabolites in the plasma of mice upon colonization, MuLV infection, or both (Figures 4.2C and 4.2D). Strikingly, and in contrast to what we observed in the spleen, colonization alone appeared to have the greatest effect upon metabolites within the plasma (Figure 4.2C). Colonization significantly altered the abundance of 53 metabolites

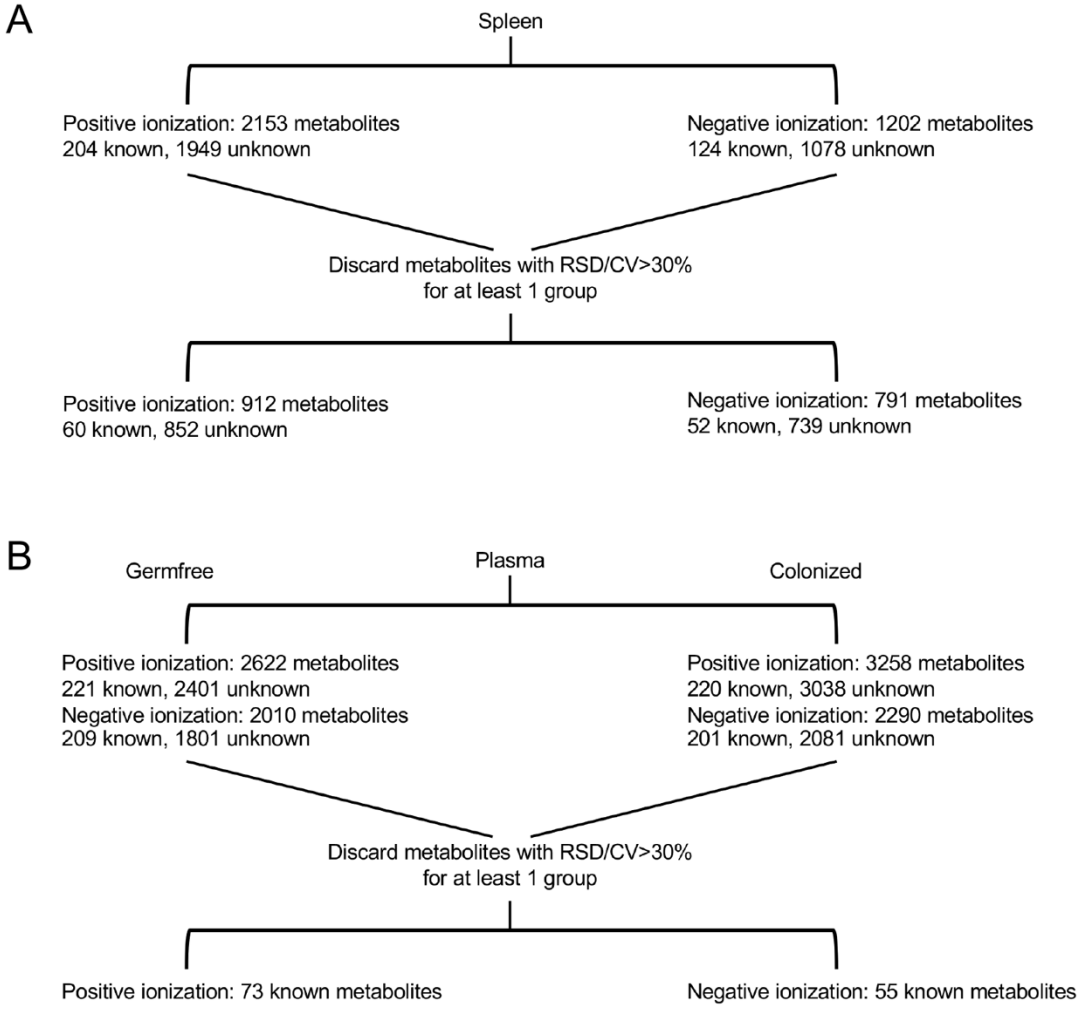

Figure 4.1. Flow chart illustrating the processing of spleen and plasma samples for metabolomics.
(A, B) Spleen **(A)** and plasma **(B)** samples were subjected to mass spectrometry under positive and negative ionization modes. Metabolites with an RSD > 30% were discarded leaving the indicated number of known and unknown metabolites.

Nicotinamide	Ethanolamine	Anserine	Tyrosine	Pyridoxal	Threonine	Valine	Carnitine
Hypoxanthine	Pyrazinamide	Taurine	Urea	Tryptophan	Cytidine	Arginine	Phenylalanine
Aspartic acid	Methionine	Uracil	Xanthine	Choline [M]+	Serine	Proline	Alanine
Glutamic acid	Asparagine	Histidine	Thiamine Cation	Argininosuccinic acid	Sphinganine	Glucose-6-phosphate	N-epsilon-Acetyllysine
2'-Deoxycytidine	N,N-Dimethylarginine	Ergothioneine	3'-O-Methylinosine	Epsilon.-Caprolactam	N-Acetyl-D-glucosamine	Palmitoyl sphingomyelin	Nicotinamide riboside cation
N.epsilon.-Methyl-L-lysine	Gamma.-Aminobutyric acid	Methioninesulfoxide [M+H]+	1,2-Cyclohexanedione	1,2-Dilinoleoyl-sn-glycero-3-phosphocholine	1-Myristoyl-2-stearoyl-sn-glycero-3-phosphocholine	(2R)-3-Hydroxyisovaleroylcarnitine	1,2-Diarachidonoyl-sn-glycero-3-phosphocholine
1-O-Hexadecyl-2-O-(4Z,7Z,10Z,13Z,16Z,19Z-docosahexaenoyl)-sn-glyceryl-3-phosphorylcholine	1-(1Z-Octadecenyl)-2-(5Z,8Z,11Z,14Z-eicosatetraenoyl)-sn-glycero-3-phosphoethanolamine	1-(1Z-Octadecenyl)-2-(4Z,7Z,10Z,13Z,16Z,19Z-docosahexaenoyl)-sn-glycero-3-phosphoethanolamine	2-Docosahexaenoyl-1-stearoyl-sn-glycero-3-phosphoethanolamine	1-Stearoyl-2-linoleoyl-sn-glycero-3-phospho-L-serine	1,2-Dipentadecanoyl-sn-glycero-3-phosphocholine	2-Arachidonoyl-1-palmitoyl-sn-glycero-3-phosphoethanolamine	1,2-dioleoyl-sn-glycero-3-phosphatidylcholine
1-Palmitoyl-2-docosahexaenoyl-sn-glycero-3-phosphocholine	1-Oleoyl-2-myristoyl-sn-glycero-3-phosphocholine	2-Oleoyl-1-palmitoyl-sn-glycero-3-phosphocholine	Nepsilon, Nepsilon-Trimethyllysine				

Table 4.1. Known metabolites found in spleens under positive ionization.
Metabolites identified in the spleens of GF, GF infected, *L. murinus* colonized, and *L. murinus* colonized and infected mice under positive ionization.

PE 38:4	Galactitol	Uracil	Xanthine	Arginine	Gly-Asp	Taurine	myo-Inositol
Threonine	Hypoxanthine	N-Acetylserine	2'-Deoxycytidine	Xylitol	N-Acetylalanine	2-Deoxyuridine	Allantoin
Aspartic acid	Glucose	PC 32:0	Serine	Threonic acid	PE 38:6	PC 32:1	Glutamine
D-Asparagine	Histidine	Gly-Gly	PS 36:2	PE 36:4	Valine	Orotic acid	Glutamic acid
Ribose-5-phosphate	Tyrosine	Cytidine	Pseudouridine	N-epsilon-Acetyllysine	Glucose-1-phosphate	Dihydroxyacetone phosphate	Glucose-6-phosphate
N,N-Dimethylarginine	Pyroglutamic acid	Palmitoyl sphingomyelin	Ribose-1-phosphate	Plasmenyl-PE 38:6	L-.gamma.-Glutamyl-L-glutamic acid	Plasmenyl-PE 36:4	Plasmenyl-PE 38:4
O-Phosphocolamine	2-Docosahexaenoyl-1-stearoyl-sn-glycero-3-phosphoserine	1-Stearoyl-2-arachidonoyl-sn-glycero-3-phosphoserine	1-Palmitoyl-2-docosahexaenoyl-sn-glycero-3-phosphocholine				

Table 4.2. Known metabolites found in spleens under negative ionization.
Known metabolites identified in the spleens of GF, GF+MuLV, *L. murinus* colonized, and *L. murinus* colonized+MuLV under negative ionization.

5-Methylcytidine	Creatine	Isoleucine	Creatinine	Leucine	Acetylcarnitine	Cystathionine	Linoleoylcarnitine	Alanine
Cytidine	Lysine	Methionine	Nicotinamide	Riboflavin	Betaine	Glu-Thr	2'-Deoxycytidine	Carnitine
3-Methylcytidine	Choline [M]+	homocitrulline	Taurine	Hypotaurine	Pipecolic acid	Phenylalanine	Urea	Arginine
Valine	Ornithine	Proline	Citrulline	Oleoyl-L-carnitine	Serine	N,N-Dimethylarginine	Guanidinoacetic acid	Palmitoylcarnitine
7,8-Dihydrobiopterin	gamma-Glutamylleucine	N6,N6-dimethyllysine	1-Methyladenosine	N-epsilon-Acetyllysine	N-.alpha.-Acetyl-L-arginine	Palmitoyl sphingomyelin	Myristoyl-L-carnitine	Methioninesulfoxide [M+H]+
2-Arachidonoylglycerol	Nalpha-acetyl-L-Lysine	SN-Glycero-3-Phosphocoline	1-Palmitoyl-sn-glycero-3-phosphocholine late	5-Methyl-2'-deoxycytidine	N-Oleoyl-D-erythro-sphingosylphosphorylcholine	Palmitoyleicosapentaenoyl phosphatidylcholine	1-Stearoyl-2-hydroxy-sn-glycero-3-phosphocholine	1-Heptadecanoyl-sn-glycero-3-phosphocholine late
1,2-Dilinoleoyl-sn-glycero-3-phosphocholine	1-(1Z-Octadecenyl)-2-(5Z,8Z,11Z,14Z-eicosatetraenoyl)-sn-glycero-3-phosphocholine	1-Oleoyl-sn-glycero-3-phosphoethanolamine	1-(1Z-Octadecenyl)-2-(4Z,7Z,10Z,13Z,16Z,19Z-docosahexaenoyl)-sn-glycero-3-phosphocholine	1-O-Hexadecyl-2-O-(5Z,8Z,11Z,14Z,17Z-eicosapentaenoyl)-sn-glyceryl-3-phosphorylcholine	1-(1Z-Hexadecenyl)-sn-glycero-3-phosphocholine late	1-O-Hexadecyl-2-O-(4Z,7Z,10Z,13Z,16Z,19Z-docosahexaenoyl)-sn-glyceryl-3-phosphorylcholine	1-Stearoyl-2-hydroxy-sn-glycero-3-phosphoethanolamine	1-Hexadecyl-2-(5Z,8Z,11Z,14Z-eicosatetraenoyl)-sn-glycero-3-phosphocholine
1,2-dioleoyl-sn-glycero-3-phosphatidylcholine	1-(1Z-Octadecenyl)-sn-glycero-3-phosphocholine early	1-Palmitoyl-2-docosahexaenoyl-sn-glycero-3-phosphocholine	1-(1Z-Hexadecenyl)-sn-glycero-3-phosphocholine early	1-Myristoyl-sn-glycero-3-phosphocholine	1-O-Octadecyl-sn-glyceryl-3-phosphorylcholine	1-O-Hexadecyl-2-O-acetyl-sn-glyceryl-3-phosphorylcholine	1-(1Z-Octadecenyl)-sn-glycero-3-phosphocholine late	1-Palmitoyl-sn-glycero-3-phosphocholine early
1,2-Dipalmitoleoyl-sn-glycero-3-phosphocholine								

Table 4.3. Known metabolites in the sera under positive ionization.
Metabolites identified in the sera of GF, GF infected, *L. murinus* colonized, and *L. murinus* colonized and infected mice under positive ionization.

Citrulline	4-Nitrophenol	Cytidine	Allantoin	Hypotaurine	Arabitol	Isoleucine	Adipic acid
Arginine	Leucine	Asparagine	lysoPC 14:0	Citric acid	Vanillin	Thymidine	Taurine
Serine	Pseudouridine	myo-Inositol	lysoPC 16:0 early	lysoPC 18:2 late	lysoPC 18:0 late	lysoPE 16:0 late	lysoPC 18:2 early
Delta-Hydroxylysine	lysoPC 18:0 early	lysoPE 16:0 early	lysoPC 17:0 late	lysoPC 20:4 late	lysoPC 16:0 late	lysoPC 20:4 early	N-Acetylalanine
lysoPC 18:1 late	lysoPE 18:0 late	lysoPC 18:1 early	lysoPE 18:0 early	Pantothenic acid	Methioninesulfoxide	N-epsilon-Acetyllysine	N-Acetylleucine
Palmitoyl sphingomyelin	N-Acetylhistidine	N,N-Dimethylarginine	N-Methylglutamic acid	N-.alpha.-Acetyl-L-ornithine	Methyl-beta-galactopyranoside	2-Deoxyuridine	2-Mercaptobenzothiazole
2-Hydroxypalmitic acid	Beta.-Glycerophosphate	3-Hydroxyoctanoic acid	1-Palmitoyl-2-linoleoyl-sn-glycero-3-phosphocholine	1-Palmitoyl-2-docosahexaenoyl-sn-glycero-3-phosphocholine	1-Palmitoyl-2-arachidonoyl-sn-glycero-3-phosphocholine	1-(1Z-Hexadecenyl)-sn-glycero-3-phosphocholine	

Table 4.4. Metabolites identified in the sera under negative ionization.
Known metabolites in the sera of GF, GF+MuLV, *L. murinus* colonized, and *L. murinus* colonized+MuLV mice under negative ionization.

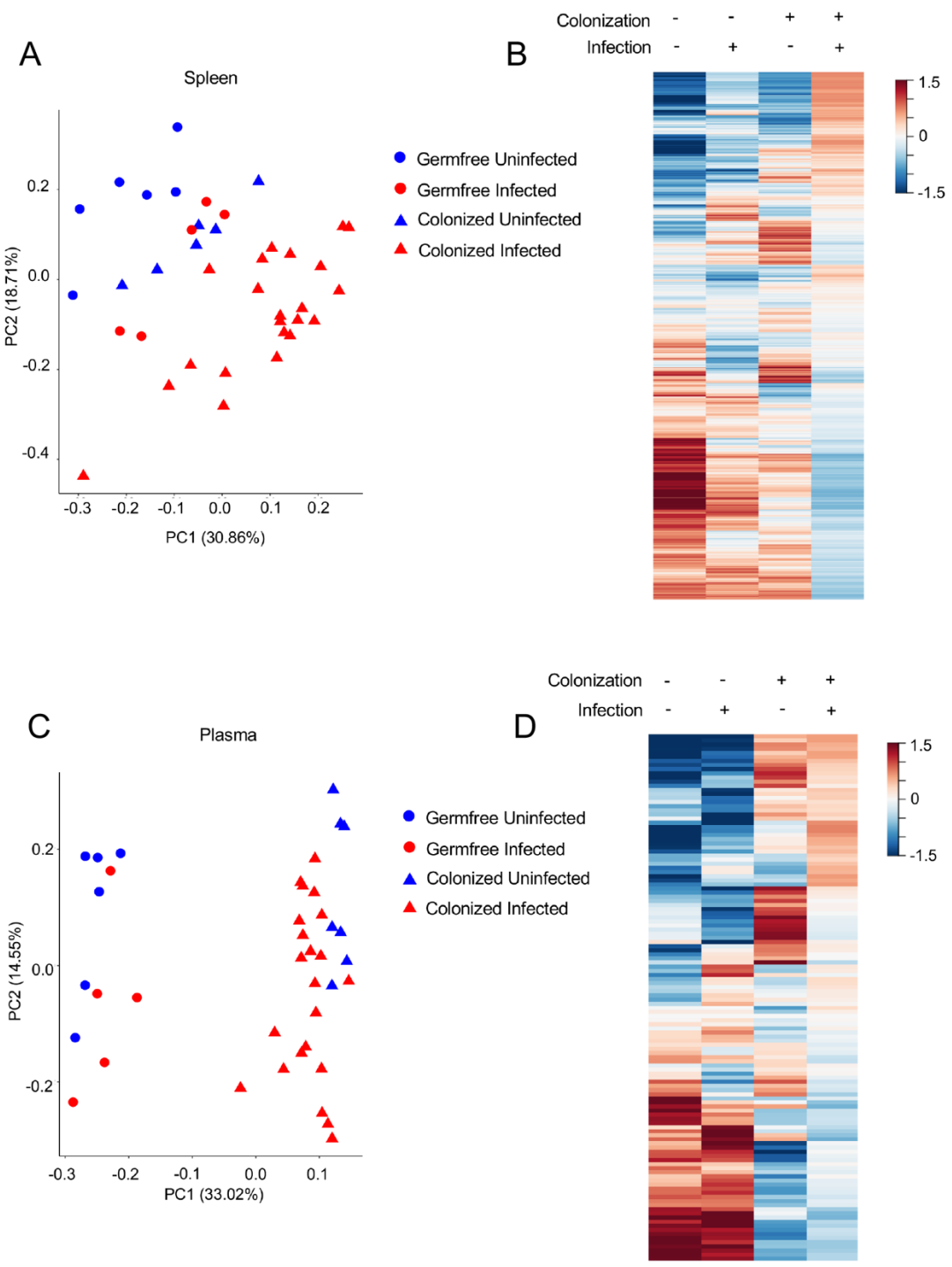

Figure 4.2. MuLV infection and bacteria colonization alter the metabolomics profile in the spleen and plasma.
(A, C) PCoA plot of metabolites within the spleen **(A)** or plasma **(C)** of the indicated mice. Each point is an individual mouse. **(B, D)** Heatmaps of metabolite abundances in the spleens **(B)** or plasma **(D)** of the four groups of mice. Each row is a metabolite.

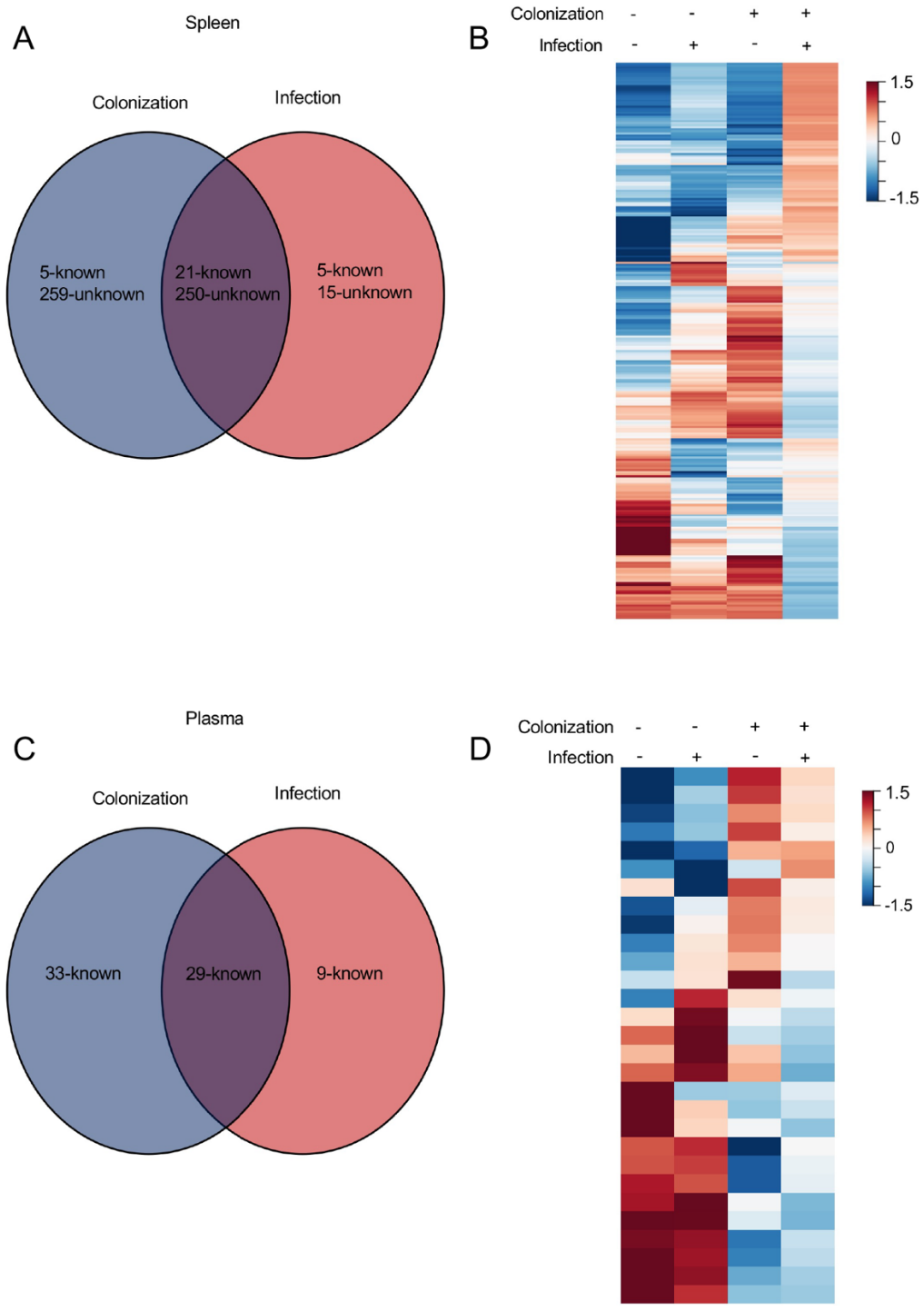

Figure 4.3. Abundances of certain metabolites is altered by colonization and MuLV infection.
(A, C) Venn-diagrams illustrating the numbers of metabolites significantly altered by colonization, infection, or both in the spleen **(A)** or plasma **(C)**. **(B, D)** Heatmaps demonstrating metabolites whose abundances are influence by colonization, MuLV infection, or both in the spleen **(B)** or plasma **(D)**. Each row is a metabolite.

3'-O-Methylinosine	Alanine	N,N-Dimethylarginine
Threonine	Pyridoxal	Tyrosine
Histidine	Cytidine	Pseudouridine
Uracil	Galactitol	N-Acetyl-D-glucosamine
PC 32:1	Uracil	Cytidine
Sphinganine	Threonic acid	Tryptophan
1-Stearoyl-2-arachidonoyl-sn-glycero-3-phosphoserine	1-Oleoyl-2-myristoyl-sn-glycero-3-phosphocholine	2-Docosahexaenoyl-1-stearoyl-sn-glycero-3-phosphoserine

Table 4.5. Metabolites whose abundance are significantly altered by colonization and infection in the spleen.
Spleens from GF, GF infected, *L. murinus* colonized, and *L. murinus* colonized and infected mice were subjected to metabolomics. Two-way ANOVA was used to determine metabolites whose abundances were significantly different in the spleens of colonized infected mice compared to only colonized or infected mice.

Ornithine	Isoleucine	Cytidine	Citric acid	Hypotaurine
Nicotinamide	Arabitol	Delta-Hydroxylysine	Citrulline	Proline
7,8-Dihydrobiopterin	2-Hydroxypalmitic acid	Methioninesulfoxide	Leucine	Asparagine
Cytidine	Hypotaurine	Cystathionine	Valine	Guanidinoacetic acid
N6,N6-dimethyllysine	N-Acetylhistidine	Palmitoyl sphingomyelin	Methioninesulfoxide [M+H]+	1,2-dioleoyl-sn-glycero-3-phosphatidylcholine
1-(1Z-Octadecenyl)-2-(5Z,8Z,11Z,14Z-eicosatetraenoyl)-sn-glycero-3-phosphocholine	1-(1Z-Octadecenyl)-2-(4Z,7Z,10Z,13Z,16Z,19Z-docosahexaenoyl)-sn-glycero-3-phosphocholine	1-O-Hexadecyl-2-O-(5Z,8Z,11Z,14Z,17Z-eicosapentaenoyl)-sn-glyceryl-3-phosphorylcholine	N-Oleoyl-D-erythro-sphingosylphosphorylcholine	

Table 4.6. Metabolites from the plasma whose abundance is significantly modified in the presence of L. murinus and MuLV.
Spleens from GF, GF infected, *L. murinus* colonized, and *L. murinus* colonized and infected mice were subjected to metabolomics. To determine metabolites in the plasma whose abundances were significantly altered in colonized infected mice, two-way ANOVA was used.

whereas infection altered abundance of 7. Two-way ANOVA identified 37 metabolites whose abundance was significantly changed in colonized and infected mice (Figures 4.3A-B and Table 4.2).

As stated above, metabolites can be directly produced by bacteria or induced by bacteria but produced by the host. The former suggests that metabolites would be produced by bacteria in the gut and disseminate into peripheral organs to exert their leukemia promoting properties. If this was the case, we would expect to find the same metabolites with similar expression profiles in both the plasma and the spleen. Within the spleen and plasma, eight metabolites were significantly altered by colonization and infection. However, only two exhibited similar expression patterns between the plasma and spleen. 2'-deoxycytidine and 2'-deoxyuridine are both deoxyribonucleosides which function as nucleotide precursors for DNA/RNA synthesis (Patejko et al., 2018). While nucleoside analogs have been used to target viruses as well as cancer (Patejko et al., 2018), the biological significance of these nucleosides in MuLV induced leukemia development is unknown. Furthermore, we do not observe increased permeability of the gut in SPF infected mice compared to uninfected mice (Figure 4.4). Suggesting metabolites found in the periphery in *L. murinus* colonized mice are small enough to diffuse across the intestinal epithelia or are produced by the host in response to bacterial colonization.

Utilizing an unbiased metabolomics approach, we identified a large list of metabolites influenced by *L. murinus* colonization and MuLV infection separately and together. However, whether any metabolite(s) influence leukemia development remains unanswered. To address this question, we would need to conduct one of the following experiments. 1) perturb the metabolite synthesis pathway in *L. murinus,* colonize GF mice with the mutant bacteria, and infect the mice with MuLV to determine whether this metabolite contributes to MuLV induced leukemia development. Or 2) generate a mouse unable to synthesize these metabolites after being colonized with *L. murinus* and infected with MuLV, then monitor the mouse for MuLV

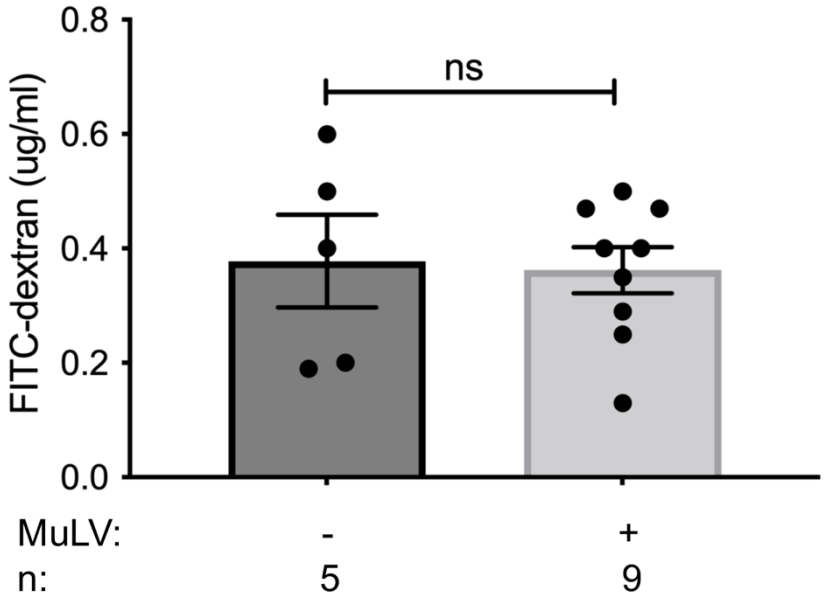

Figure 4.4. Intestinal permeability is unaffected my MuLV infection.
FITC permeability assay was used to determine the permeability of the intestines in SPF BALB/cJ infected and uninfected mice. n, number of mice used. *p* value calculated using unpaired *t* test.

induced leukemia development. The option taken would depend upon the origin of the metabolite. However, determining whether metabolites are produced by bacteria or induced by bacteria and produced by the host is not a trivial task. Furthermore, the immense number of metabolites that exhibit differential abundances in infected colonized mice, the bulk of which are unknown, makes it difficult to select metabolites for further analysis. Overall, using metabolomics to identify compounds responsible for a particular phenotype is a relatively new field. Therefore, expanding the metabolites within the reference library and accruing additional knowledge related to the synthesis pathways of metabolites will likely be required before we can address the biological significance of any particular compound in MuLV induced leukemia development.

CHAPTER 5: MICROBIOTA DOES NOT AFFECT TUMOR DEVELOPMENT IN TWO MODELS OF HERITABLE CANCER

Preface

I performed most of the experiments described in this chapter. S.G. scored sections of tumors that developed in Trp53-deficient and Wnt1 transgenic mice and contributed to experimental design.

Abstract

Tumors can arise from either spontaneous or inborn mutations (Roukos et al., 2007). The effect of the microbiota on spontaneous mutations arising from chemical carcinogens and viruses has been well documented by us and other researchers (Reddy et al., 1975; Sabit et al., 2019; Spring et al., 2022). However, whether the microbiota plays a role in cancers that develop distal from the gut and are driven by inborn mutations is not well understood. Here, we show that in the absence of the microbiota, tumor incidence in *Trp53*-deficient and Wnt1 transgenic mice is unaltered compared to the same mice housed in the SPF setting.

Introduction

In addition to spontaneous tumors, familial cancers arise from inherited mutations occurring in tumor suppressor genes or oncogenes. Development and progression of hereditary colorectal cancer, in which certain tumor suppressor genes such as APC are mutated, is influenced by the microbiota (de la Chapelle, 2004; Sabit et al., 2019). To test whether the microbiota affects tumors resulting from predisposing genetic defects, we used two other animal models. Mutations in the *TRP53* tumor-suppressor gene are the most frequently observed genetic lesions in human cancers (Kandoth et al., 2013). In addition, germ-line mutations in the *TRP53* gene are associated with Li-Fraumeni syndrome, a cancer with familial predisposition

(Malkin et al., 1990). Tumor suppressor p53 (encoded by *TRP53 or Trp53* in mice) plays a critical role in response to cell stress, such as DNA damage, by arresting cell-cycling or inducing apoptosis (Zilfou & Lowe, 2009). A possibility that the microbiota played a role in lymphomagenesis driven by p53 deficiency was suggested by a previous study of ataxia telangiectasia, mutated (ATM) deficient mice (Yamamoto et al., 2013). ATM is activated by a double stranded DNA breaks and induces cell cycle arrest or initiates apoptosis by phosphorylating a tumor-suppressor protein, p53 (Xu & Baltimore, 1996). ATM-deficient mice had reduced lymphoma incidence when they were housed under SPF conditions but supplied with sterile food, water, and bedding compared to mice housed with non-autoclaved supplies or when they were colonized with 'reduced flora' arising from Abx exposure (Yamamoto et al., 2013).

Results and discussion

Thus, we used *Trp53*-deficient mice as a model to validate the possibility that commensal bacteria may facilitate tumor development in a model of genetic predisposition. GF *Trp53*-deficient mice developed tumors at a frequency very similar to that observed in SPF *Trp53*-deficient mice (Figure 5.1A). In accordance with previously published data, most of both SPF and GF Trp53-deficient mice developed lymphomas or sarcomas (Donehower, 1996) (Figure 5.1B and Figure 5.1C). However, some GF mice developed carcinomas (Figure 5.1C), indicating that the microbiota may be protective rather than promotive of that type of tumor.

Using the same rationale, we tested Wnt1 transgenic mice (a transgenic model for mammary carcinoma development). Wnt1 signaling stabilizes and increases cytosolic levels of β-catenin, which then translocates to the nucleus activating numerous genes including regulators of cell cycle c-myc and cyclin D1 (Li et al., 2000). Aberrant Wnt1 expression under the promoter of mammary tumor virus (MMTV-Wnt1) leads to the development of mammary adenocarcinomas (Li et al., 2000). We found rates of tumor induction to be the same between

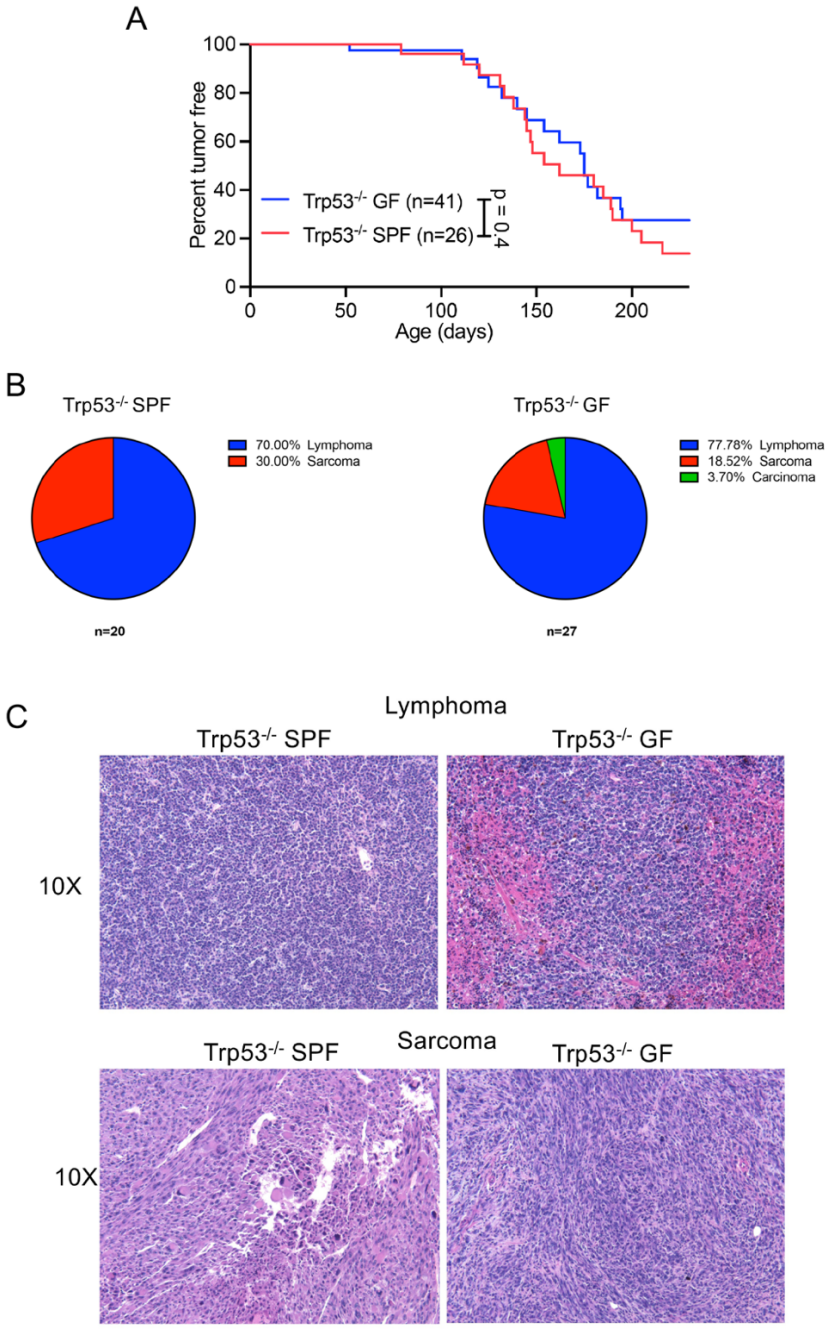

Figure 5.1. Microbiota does not impact the tumorigenesis nor tumor etiology in mice deficient in p53.
(A) C57BL/6 Trp53$^{-/-}$ SPF and GF mice were monitored for tumor development. **(B)** Proportion of SPF Trp53$^{-/-}$ mice that develop various forms of tumors in SPF (left) and GF (right) setting. **(C)** Tumors were excised from the surrounding tissue, fixed, sectioned, and stained with hematoxylin-and eosin. Representative hematoxylin-and eosin stained lymphomas (top) and sarcomas (bottom) from Trp53$^{-/-}$ SPF (left) and GF (right) mice. 10X magnification. n, number of mice used. *p* values calculated using Mantel-Cox test **(A)**.

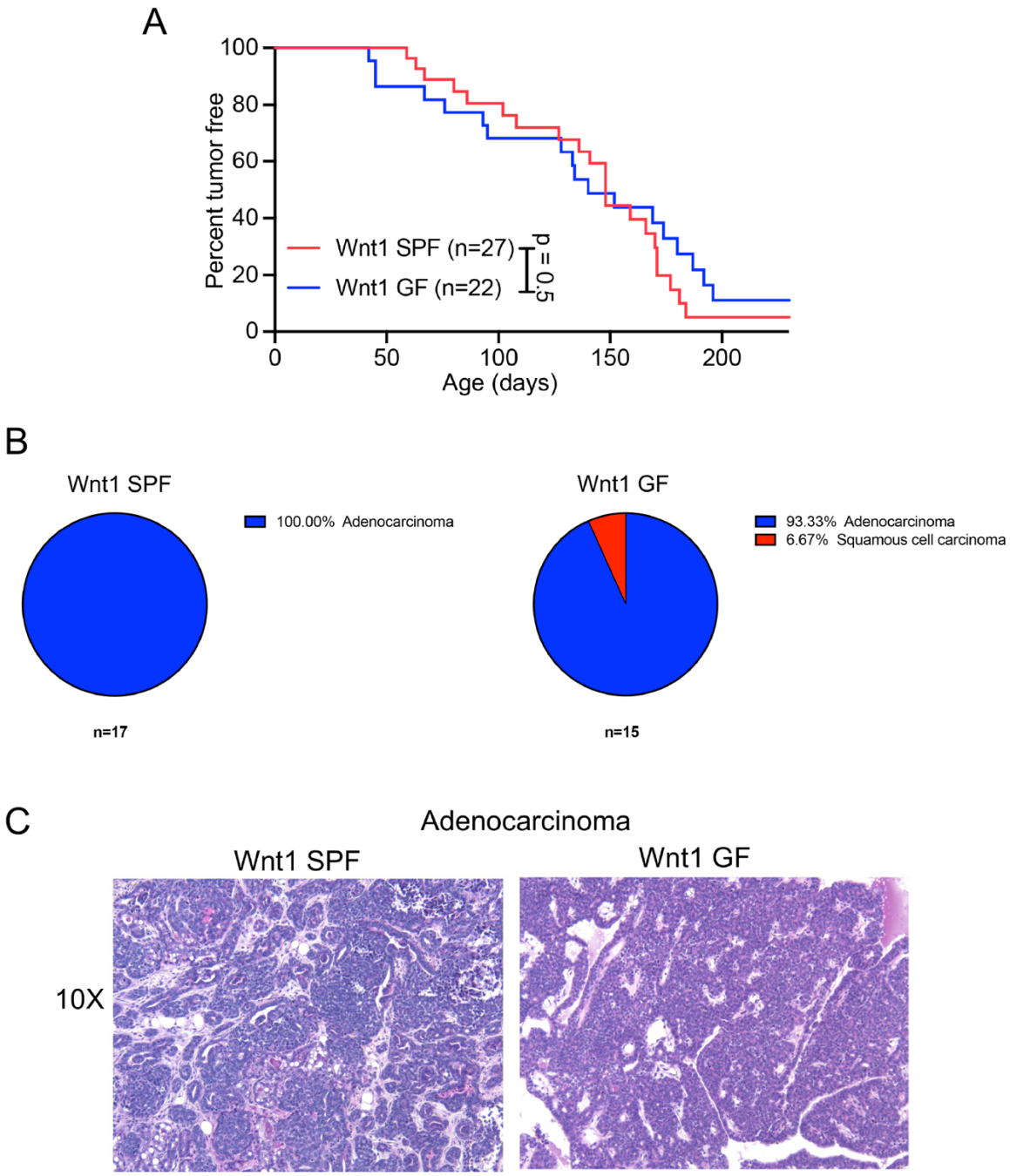

Figure 5.2. The microbiota does not influence tumor development or type in mice transgenic for Wnt1.
(A) FVB Wnt1 transgenic SPF and GF mice were monitored for tumor development. **(B)** Proportion of Wnt1 transgenic mice that develop various types of tumors in SPF (left) and GF (right) setting. **(C)** Tumors were excised from the surrounding tissue, fixed, sectioned, and stained with hematoxylin-and eosin. Example hematoxylin-and eosin stained adenocarcinomas from Wnt1 transgenic SPF (left) and GF (right) mice. 10X magnification. n, number of mice used. *p* values calculated using Mantel-Cox test **(A)**.

SPF and GF MMTV-Wnt1 transgenic mice (Figure 5.2A). Wnt1 transgenic SPF and GF mice both primarily developed adenocarcinomas typical of this model (Figures 5.2B and Figure 5.2C), but a few GF mice developed squamous cell carcinomas (Figures 5.2B and Figure 5.2C), again indicating that the microbiota may be protective against certain types of tumors.

Thus, unlike spontaneous malignancies, such as MuLV-induced leukemia, incidence and latency of hereditary lymphoma/sarcoma and mammary gland tumor in *Trp53*$^{-/-}$ and Wnt1-transgenic mice, respectively, were not affected by the absence of the microbiota (Figures 5.1A and 5.2A). These data suggest that commensal microbes may not influence development of tumors of gut distant organs arising from genetic predisposition. This discordance could be explained by differences in the nature of retrovirally-induced tumors and tumors that develop in *Trp53*$^{-/-}$ and Wnt1-transgenic mice. Retrovirally induced tumors (as do all spontaneous tumors) appear from unique cells in which oncogenes have been upregulated by the integrated proviruses or other events. These cells also express viral antigens or neoantigens that are foreign for the host and may activate an immune response targeting these cells. That puts a strong pressure on tumor cells to escape this response. In heritable cancer models, the oncogene expression or loss of a tumor suppressor are ubiquitous in all cells of the body or a tissue (in case of conditional expression). Lack of foreign antigens at the initiation of tumor development may stifle the induction of a robust immune response. Combined with wide expression of the mutation enhancing the chance for tumor development, this may lead to immunological ignorance or exhaustion early in tumor development as a means to evade the immune response (Ochsenbein, 2002). One observation made in our studies may shed light on exceptions from these rules: in both *Trp53*-deficient and Wnt-transgenic mice (Figures 5.1B and 5.2B), the absence of microbiota led to a higher frequency of development of certain type of carcinomas. Thus, it is possible that microbiota has a negative effect on the development of epithelial tumors.

REFERENCES

Achiwa, K., Ishigami, M., Ishizu, Y., Kuzuya, T., Honda, T., Hayashi, K., Hirooka, Y., Katano, Y., & Goto, H. (2016). DSS colitis promotes tumorigenesis and fibrogenesis in a choline-deficient high-fat diet-induced NASH mouse model. *Biochemical and Biophysical Research Communications*, *470*(1), 15-21. https://doi.org/https://doi.org/10.1016/j.bbrc.2015.12.012

Adams, J. M., & Cory, S. (1991). Transgenic models of tumor development. *Science*, *254*(5035), 1161-1167. https://doi.org/10.1126/science.1957168

Anandasabapathy, N., Ford, G. S., Bloom, D., Holness, C., Paragas, V., Seroogy, C., Skrenta, H., Hollenhorst, M., Fathman, C. G., & Soares, L. (2003). GRAIL: an E3 ubiquitin ligase that inhibits cytokine gene transcription is expressed in anergic CD4+ T cells. *Immunity*, *18*(4), 535-547. https://www.ncbi.nlm.nih.gov/pubmed/12705856

Andrews, S. (2017). FastQC: a quality control tool for high throughput sequence data. 2010. In.

Arthur, J. C., Perez-Chanona, E., Muhlbauer, M., Tomkovich, S., Uronis, J. M., Fan, T. J., Campbell, B. J., Abujamel, T., Dogan, B., Rogers, A. B., Rhodes, J. M., Stintzi, A., Simpson, K. W., Hansen, J. J., Keku, T. O., Fodor, A. A., & Jobin, C. (2012). Intestinal inflammation targets cancer-inducing activity of the microbiota [Research Support, N.I.H., Extramural Research Support, Non-U.S. Gov't]. *Science*, *338*(6103), 120-123. https://doi.org/10.1126/science.1224820

Bai, X.-S., Zhang, C., Peng, R., Jiang, G.-Q., Jin, S.-J., Wang, Q., Ke, A.-W., & Bai, D.-S. (2020). RNF128 Promotes Malignant Behaviors via EGFR/MEK/ERK Pathway in Hepatocellular Carcinoma. *OncoTargets and therapy*, *13*, 10129-10141. https://doi.org/10.2147/OTT.S269606

Baldridge, M. T., Nice, T. J., McCune, B. T., Yokoyama, C. C., Kambal, A., Wheadon, M., Diamond, M. S., Ivanova, Y., Artyomov, M., & Virgin, H. W. (2015). Commensal microbes and interferon-lambda determine persistence of enteric murine norovirus infection. *Science*, *347*(6219), 266-269. https://doi.org/10.1126/science.1258025

Bäumler, A. J., & Sperandio, V. (2016). Interactions between the microbiota and pathogenic bacteria in the gut. *Nature*, *535*(7610), 85-93. https://doi.org/10.1038/nature18849

Bolouri, H., Farrar, J. E., Triche, T., Jr., Ries, R. E., Lim, E. L., Alonzo, T. A., Ma, Y., Moore, R., Mungall, A. J., Marra, M. A., Zhang, J., Ma, X., Liu, Y., Liu, Y., Auvil, J. M. G., Davidsen, T. M., Gesuwan, P., Hermida, L. C., Salhia, B., . . . Meshinchi, S. (2018). The molecular landscape of pediatric acute myeloid leukemia reveals recurrent structural alterations and age-specific mutational interactions. *Nat Med*, *24*(1), 103-112. https://doi.org/10.1038/nm.4439

Bots, M., Kolfschoten, I. G., Bres, S. A., Rademaker, M. T., de Roo, G. M., Krüse, M., Franken, K. L., Hahne, M., Froelich, C. J., Melief, C. J., Offringa, R., & Medema, J. P. (2005). SPI-CI and SPI-6 cooperate in the protection from effector cell-mediated cytotoxicity. *Blood*, *105*(3), 1153-1161. https://doi.org/10.1182/blood-2004-03-0791

Bray, N. L., Pimentel, H., Melsted, P., & Pachter, L. (2016). Near-optimal probabilistic RNA-seq quantification. *Nat Biotechnol*, *34*(5), 525-527. https://doi.org/10.1038/nbt.3519

Brinkman, B. M., Hildebrand, F., Kubica, M., Goosens, D., Del Favero, J., Declercq, W., Raes, J., & Vandenabeele, P. (2011). Caspase deficiency alters the murine gut microbiome. *Cell Death & Disease*, *2*(10), e220-e220. https://doi.org/10.1038/cddis.2011.101

Buffett, R. F., Grace, J. T., Jr., DiBerardino, L. A., & Mirand, E. A. (1969). Vertical transmission of murine leukemia virus through successive generations. *Cancer Res*, *29*(3), 596-602.

Buffie, C. G., Bucci, V., Stein, R. R., McKenney, P. T., Ling, L., Gobourne, A., No, D., Liu, H., Kinnebrew, M., Viale, A., Littmann, E., van den Brink, M. R., Jenq, R. R., Taur, Y., Sander, C., Cross, J. R., Toussaint, N. C., Xavier, J. B., & Pamer, E. G. (2015). Precision microbiome reconstitution restores bile acid mediated resistance to Clostridium difficile. *Nature*, *517*(7533), 205-208. https://doi.org/10.1038/nature13828

Callahan, B. J., McMurdie, P. J., Rosen, M. J., Han, A. W., Johnson, A. J. A., & Holmes, S. P. (2016). DADA2: High-resolution sample inference from Illumina amplicon data. *Nature Methods*, *13*(7), 581-583. https://doi.org/10.1038/nmeth.3869

Carmody, Rachel N., Gerber, Georg K., Luevano, Jesus M., Gatti, Daniel M., Somes, L., Svenson, Karen L., & Turnbaugh, Peter J. (2015). Diet Dominates Host Genotype in Shaping the Murine Gut Microbiota. *Cell host & microbe*, *17*(1), 72-84. https://doi.org/https://doi.org/10.1016/j.chom.2014.11.010

Caruso, R., Warner, N., Inohara, N., & Núñez, G. (2014). NOD1 and NOD2: signaling, host defense, and inflammatory disease. *Immunity*, *41*(6), 898-908. https://doi.org/10.1016/j.immuni.2014.12.010

Casasanta, M. A., Yoo, C. C., Udayasuryan, B., Sanders, B. E., Umaña, A., Zhang, Y., Peng, H., Duncan, A. J., Wang, Y., Li, L., Verbridge, S. S., & Slade, D. J. (2020). Fusobacterium nucleatum host-cell binding and invasion induces IL-8 and CXCL1 secretion that drives colorectal cancer cell migration. *Science signaling*, *13*(641), eaba9157. https://doi.org/10.1126/scisignal.aba9157

Case, L. K., Petell, L., Yurkovetskiy, L., Purdy, A., Savage, K. J., & Golovkina, T. V. (2008). Replication of beta- and gammaretroviruses is restricted in I/LnJ mice via the same genetic mechanism. *J Virol*, *82*(3), 1438-1447. https://doi.org/JVI.01991-07 [pii] 10.1128/JVI.01991-07

Chen, J., Crispin, J. C., Dalle Lucca, J., & Tsokos, G. C. (2011). A novel inhibitor of the alternative pathway of complement attenuates intestinal ischemia/reperfusion-induced injury. *J Surg Res*, *167*(2), e131-136. https://doi.org/10.1016/j.jss.2009.05.041

Chen, M., Muckersie, E., Luo, C., Forrester, J. V., & Xu, H. (2010). Inhibition of the alternative pathway of complement activation reduces inflammation in experimental autoimmune uveoretinitis. *Eur J Immunol*, *40*(10), 2870-2881. https://doi.org/10.1002/eji.201040323

Chervonsky, A. V. (2013). Microbiota and autoimmunity. *Cold Spring Harbor perspectives in biology*, *5*(3), a007294-a007294. https://doi.org/10.1101/cshperspect.a007294

Chirgwin, J. M., Przybyla, A. E., MacDonald, R. J., & Rutter, W. J. (1979). Isolation of biologically active ribonucleic acid from sources enriched in ribonuclease. *Biochemistry*, *18*(24), 5294-5299. https://doi.org/10.1021/bi00591a005

Coffelt, S. B., & de Visser, K. E. (2015). Immune-mediated mechanisms influencing the efficacy of anticancer therapies. *Trends in Immunology*, *36*(4), 198-216. https://doi.org/https://doi.org/10.1016/j.it.2015.02.006

Coffin, J., Hughes, S., & Varmus, H. (1997). *Retroviruses*.

Compere, S. J., Baldacci, P., & Jaenisch, R. (1988). Oncogenes in transgenic mice. *Biochimica et Biophysica Acta (BBA) - Reviews on Cancer*, *948*(2), 129-149. https://doi.org/https://doi.org/10.1016/0304-419X(88)90008-X

Crowe, N. Y., Smyth, M. J., & Godfrey, D. I. (2002). A critical role for natural killer T cells in immunosurveillance of methylcholanthrene-induced sarcomas. *The Journal of Experimental Medicine*, *196*(1), 119-127. https://doi.org/10.1084/jem.20020092

D'Alessandro, G., Antonangeli, F., Marrocco, F., Porzia, A., Lauro, C., Santoni, A., & Limatola, C. (2020). Gut microbiota alterations affect glioma growth and innate immune cells involved in tumor immunosurveillance in mice. *Eur J Immunol*, *50*(5), 705-711. https://doi.org/10.1002/eji.201948354

David, L. A., Materna, A. C., Friedman, J., Campos-Baptista, M. I., Blackburn, M. C., Perrotta, A., Erdman, S. E., & Alm, E. J. (2014). Host lifestyle affects human microbiota on daily timescales. *Genome Biology*, *15*(7), R89. https://doi.org/10.1186/gb-2014-15-7-r89

de la Chapelle, A. (2004). Genetic predisposition to colorectal cancer. *Nature Reviews Cancer*, *4*(10), 769-780. https://doi.org/10.1038/nrc1453

de Oliviera Nascimento, L., Massari, P., & Wetzler, L. (2012). The Role of TLR2 in Infection and Immunity [Review]. *Frontiers in Immunology*, *3*(79). https://doi.org/10.3389/fimmu.2012.00079

Demon, D., Kuchmiy, A., Fossoul, A., Zhu, Q., Kanneganti, T. D., & Lamkanfi, M. (2014). Caspase-11 is expressed in the colonic mucosa and protects against dextran sodium sulfate-induced colitis. *Mucosal Immunology*, *7*(6), 1480-1491. https://doi.org/10.1038/mi.2014.36

Dethlefsen, L., Huse, S., Sogin, M. L., & Relman, D. A. (2008). The Pervasive Effects of an Antibiotic on the Human Gut Microbiota, as Revealed by Deep 16S rRNA Sequencing. *PLOS Biology*, *6*(11), e280. https://doi.org/10.1371/journal.pbio.0060280

Dewhirst, F. E., Chien, C. C., Paster, B. J., Ericson, R. L., Orcutt, R. P., Schauer, D. B., & Fox, J. G. (1999). Phylogeny of the defined murine microbiota: altered Schaedler flora. *Appl Environ Microbiol*, *65*(8), 3287-3292. http://www.ncbi.nlm.nih.gov/entrez/query.fcgi?cmd=Retrieve&db=PubMed&dopt=Citation&list_uids=10427008

Dittmer, U., He, H., Messer, R. J., Schimmer, S., Olbrich, A. R., Ohlen, C., Greenberg, P. D., Stromnes, I. M., Iwashiro, M., Sakaguchi, S., Evans, L. H., Peterson, K. E., Yang, G., & Hasenkrug, K. J. (2004). Functional impairment of CD8(+) T cells by regulatory T cells during persistent retroviral infection. *Immunity*, *20*(3), 293-303. https://www.ncbi.nlm.nih.gov/pubmed/15030773

Dittmer, U., Sutter, K., Kassiotis, G., Zelinskyy, G., Bánki, Z., Stoiber, H., Santiago, M. L., & Hasenkrug, K. J. (2019). Friend retrovirus studies reveal complex interactions between intrinsic, innate and adaptive immunity. *FEMS Microbiology Reviews*, *43*(5), 435-456. https://doi.org/10.1093/femsre/fuz012

Dobin, A., Davis, C. A., Schlesinger, F., Drenkow, J., Zaleski, C., Jha, S., Batut, P., Chaisson, M., & Gingeras, T. R. (2013). STAR: ultrafast universal RNA-seq aligner. *Bioinformatics*, *29*(1), 15-21. https://doi.org/10.1093/bioinformatics/bts635

Donehower, L. A. (1996). The p53-deficient mouse: a model for basic and applied cancer studies. *Semin Cancer Biol*, *7*(5), 269-278. https://doi.org/10.1006/scbi.1996.0035

Donohoe, D. R., Holley, D., Collins, L. B., Montgomery, S. A., Whitmore, A. C., Hillhouse, A., Curry, K. P., Renner, S. W., Greenwalt, A., Ryan, E. P., Godfrey, V., Heise, M. T., Threadgill, D. S., Han, A., Swenberg, J. A., Threadgill, D. W., & Bultman, S. J. (2014). A gnotobiotic mouse model demonstrates that dietary fiber protects against colorectal tumorigenesis in a microbiota- and butyrate-dependent manner. *Cancer Discov*, *4*(12), 1387-1397. https://doi.org/10.1158/2159-8290.CD-14-0501

Duggan, J., Okonta, H., & Chakraborty, J. (2006). Transmission of Moloney murine leukemia virus (ts-1) by breast milk. *The Journal of general virology*, *87*(Pt 9), 2679-2684. https://doi.org/10.1099/vir.0.82015-0

Eslami-S, Z., Majidzadeh-A, K., Halvaei, S., Babapirali, F., & Esmaeili, R. (2020). Microbiome and Breast Cancer: New Role for an Ancient Population [Review]. *Frontiers in Oncology*, *10*. https://doi.org/10.3389/fonc.2020.00120

Fox, J. G., Feng, Y., Theve, E. J., Raczynski, A. R., Fiala, J. L. A., Doernte, A. L., Williams, M., McFaline, J. L., Essigmann, J. M., Schauer, D. B., Tannenbaum, S. R., Dedon, P. C., Weinman, S. A., Lemon, S. M., Fry, R. C., & Rogers, A. B. (2010). Gut microbes define liver cancer risk in mice exposed to chemical and viral transgenic hepatocarcinogens. *Gut*, *59*(01), 88-97. https://doi.org/10.1136/gut.2009.183749

Fu, W., Wojtkiewicz, G., Weissleder, R., Benoist, C., & Mathis, D. (2012). Early window of diabetes determinism in NOD mice, dependent on the complement receptor CRIg, identified by noninvasive imaging. *Nat Immunol*, *13*(4), 361-368. https://doi.org/10.1038/ni.2233

Garrett, W. S. (2015). Cancer and the microbiota. *Science*, *348*(6230), 80-86. http://dx.doi.org/10.1126/science.aaa4972 http://www.ncbi.nlm.nih.gov/pubmed/25838377

Gensollen, T., Iyer, S. S., Kasper, D. L., & Blumberg, R. S. (2016). How colonization by microbiota in early life shapes the immune system. *Science*, *352*(6285), 539-544. https://doi.org/doi:10.1126/science.aad9378

Gonzalez, H., Hagerling, C., & Werb, Z. (2018). Roles of the immune system in cancer: from tumor initiation to metastatic progression. *Genes Dev*, *32*(19-20), 1267-1284. https://doi.org/10.1101/gad.314617.118

Goodrich, Julia K., Waters, Jillian L., Poole, Angela C., Sutter, Jessica L., Koren, O., Blekhman, R., Beaumont, M., Van Treuren, W., Knight, R., Bell, Jordana T., Spector, Timothy D., Clark,

Andrew G., & Ley, Ruth E. (2014). Human Genetics Shape the Gut Microbiome. *Cell*, *159*(4), 789-799. https://doi.org/https://doi.org/10.1016/j.cell.2014.09.053
Graveline, R., Segura, M., Radzioch, D., & Gottschalk, M. (2007). TLR2-dependent recognition of Streptococcus suis is modulated by the presence of capsular polysaccharide which modifies macrophage responsiveness. *International Immunology*, *19*(4), 375-389. https://doi.org/10.1093/intimm/dxm003

Grivennikov, S. I., Greten, F. R., & Karin, M. (2010). Immunity, inflammation, and cancer [Research Support, N.I.H., Extramural
Research Support, Non-U.S. Gov't
Review]. *Cell*, *140*(6), 883-899. https://doi.org/10.1016/j.cell.2010.01.025

Groves, H. T., Higham, S. L., Moffatt, M. F., Cox, M. J., Tregoning, J. S., & Bomberger, J. M. (2020). Respiratory Viral Infection Alters the Gut Microbiota by Inducing Inappetence. *mBio*, *11*(1), e03236-03219. https://doi.org/doi:10.1128/mBio.03236-19

Guerin, M. V., Finisguerra, V., Van den Eynde, B. J., Bercovici, N., & Trautmann, A. (2020). Preclinical murine tumor models: a structural and functional perspective. *Elife*, *9*. https://doi.org/10.7554/eLife.50740

Guidi, R., Guerra, L., Levi, L., Stenerlöw, B., Fox, J. G., Josenhans, C., Masucci, M. G., & Frisan, T. (2013). Chronic exposure to the cytolethal distending toxins of Gram-negative bacteria promotes genomic instability and altered DNA damage response. *Cell Microbiol*, *15*(1), 98-113. https://doi.org/10.1111/cmi.12034

Han, S., Van Treuren, W., Fischer, C. R., Merrill, B. D., DeFelice, B. C., Sanchez, J. M., Higginbottom, S. K., Guthrie, L., Fall, L. A., Dodd, D., Fischbach, M. A., & Sonnenburg, J. L. (2021). A metabolomics pipeline for the mechanistic interrogation of the gut microbiome. *Nature*, *595*(7867), 415-420. https://doi.org/10.1038/s41586-021-03707-9

Han, S. H., Kim, J. H., Martin, M., Michalek, S. M., & Nahm, M. H. (2003). Pneumococcal lipoteichoic acid (LTA) is not as potent as staphylococcal LTA in stimulating Toll-like receptor 2. *Infection and immunity*, *71*(10), 5541-5548. https://doi.org/10.1128/IAI.71.10.5541-5548.2003

Hanna, M. G., Jr., Walburg, H. E., Jr., Tyndall, R. L., & Snodgrass, M. J. (1970). Histoproliferative effect of Rauscher leukemia virus on lymphatic tissue. II. Antigen-stimulated germfree and conventional BALB-c mice. *Proceedings of the Society for Experimental Biology and Medicine. Society for Experimental Biology and Medicine*, *134*(4), 1132-1141. http://www.ncbi.nlm.nih.gov/pubmed/5457739

Haymaker, C., Yang, Y., Wang, J., Zou, Q., Sahoo, A., Alekseev, A., Singh, D., Ritthipichai, K., Hailemichael, Y., Hoang, O. N., Qin, H., Schluns, K. S., Wang, T., Overwijk, W. W., Sun, S. C., Bernatchez, C., Kwak, L. W., Neelapu, S. S., & Nurieva, R. (2017). Absence of Grail promotes CD8(+) T cell anti-tumour activity. *Nat Commun*, *8*(1), 239. https://doi.org/10.1038/s41467-017-00252-w

He, Z., Gharaibeh, R. Z., Newsome, R. C., Pope, J. L., Dougherty, M. W., Tomkovich, S., Pons, B., Mirey, G., Vignard, J., Hendrixson, D. R., & Jobin, C. (2019). Campylobacter jejuni promotes colorectal tumorigenesis through the action of cytolethal distending toxin. *Gut*, *68*(2), 289-300. https://doi.org/10.1136/gutjnl-2018-317200

Hezaveh, K., Shinde, R. S., Klötgen, A., Halaby, M. J., Lamorte, S., Ciudad, M. T., Quevedo, R., Neufeld, L., Liu, Z. Q., Jin, R., Grünwald, B. T., Foerster, E. G., Chaharlangi, D., Guo, M., Makhijani, P., Zhang, X., Pugh, T. J., Pinto, D. M., Co, I. L., . . . McGaha, T. L. (2022). Tryptophan-derived microbial metabolites activate the aryl hydrocarbon receptor in tumor-associated macrophages to suppress anti-tumor immunity. *Immunity*, *55*(2), 324-340.e328. https://doi.org/10.1016/j.immuni.2022.01.006

Hicklin, D. J., Marincola, F. M., & Ferrone, S. (1999). HLA class I antigen downregulation in human cancers: T-cell immunotherapy revives an old story. *Mol Med Today*, *5*(4), 178-186. https://doi.org/10.1016/s1357-4310(99)01451-3

Hook, L. M., Jude, B. A., Ter-Grigorov, V. S., Hartley, J. W., Morse, H. C., 3rd, Trainin, Z., Toder, V., Chervonsky, A. V., & Golovkina, T. V. (2002). Characterization of a novel murine retrovirus mixture that facilitates hematopoiesis. *J Virol*, *76*(23), 12112-12122. http://www.ncbi.nlm.nih.gov/entrez/query.fcgi?cmd=Retrieve&db=PubMed&dopt=Citation&list_uids=12414952

Hope, M. E., Hold, G. L., Kain, R., & El-Omar, E. M. (2005). Sporadic colorectal cancer--role of the commensal microbiota [Research Support, Non-U.S. Gov't Review]. *FEMS Microbiol Lett*, *244*(1), 1-7. https://doi.org/10.1016/j.femsle.2005.01.029

Huang, X., Feng, Y., Xiong, G., Whyte, S., Duan, J., Yang, Y., Wang, K., Yang, S., Geng, Y., Ou, Y., & Chen, D. (2019). Caspase-11, a specific sensor for intracellular lipopolysaccharide recognition, mediates the non-canonical inflammatory pathway of pyroptosis. *Cell & Bioscience*, *9*(1), 31. https://doi.org/10.1186/s13578-019-0292-0

Ichinohe, T., Pang, I. K., & Iwasaki, A. (2010). Influenza virus activates inflammasomes via its intracellular M2 ion channel. *Nat Immunol*, *11*(5), 404-410. https://doi.org/ni.1861 [pii] 10.1038/ni.1861

Imai, K., Inoue, H., Tamura, M., Cueno, M. E., Inoue, H., Takeichi, O., Kusama, K., Saito, I., & Ochiai, K. (2012). The periodontal pathogen Porphyromonas gingivalis induces the Epstein-Barr virus lytic switch transactivator ZEBRA by histone modification. *Biochimie*, *94*(3), 839-846. https://doi.org/10.1016/j.biochi.2011.12.001

Isaak, D. D., Bartizal, K. F., & Caulfield, M. J. (1988). Decreased pathogenicity of murine leukemia virus-Moloney in gnotobiotic mice. *Leukemia*, *2*(8), 540-544. http://www.ncbi.nlm.nih.gov/entrez/query.fcgi?cmd=Retrieve&db=PubMed&dopt=Citation&list_uids=3261822

Jacobs, J. F., Nierkens, S., Figdor, C. G., de Vries, I. J., & Adema, G. J. (2012). Regulatory T cells in melanoma: the final hurdle towards effective immunotherapy? *Lancet Oncol*, *13*(1), e32-42. https://doi.org/10.1016/S1470-2045(11)70155-3

Jain, T., Sharma, P., Are, A. C., Vickers, S. M., & Dudeja, V. (2021). New Insights Into the Cancer–Microbiome–Immune Axis: Decrypting a Decade of Discoveries [Review]. *Frontiers in Immunology*, *12*. https://doi.org/10.3389/fimmu.2021.622064

Jandhyala, S. M., Talukdar, R., Subramanyam, C., Vuyyuru, H., Sasikala, M., & Nageshwar Reddy, D. (2015). Role of the normal gut microbiota. *World journal of gastroenterology*, *21*(29), 8787-8803. https://doi.org/10.3748/wjg.v21.i29.8787

Jiang, L., Wang, Y. J., Zhao, J., Uehara, M., Hou, Q., Kasinath, V., Ichimura, T., Banouni, N., Dai, L., Li, X., Greiner, D. L., Shultz, L. D., Zhang, X., Sun, Z. J., Curtin, I., Vangos, N. E., Yeoh, Z. C., Geffken, E. A., Seo, H. S., . . . Abdi, R. (2020). Direct Tumor Killing and Immunotherapy through Anti-SerpinB9 Therapy. *Cell*, *183*(5), 1219-1233.e1218. https://doi.org/10.1016/j.cell.2020.10.045

Johnsen, A. K., Templeton, D. J., Sy, M., & Harding, C. V. (1999). Deficiency of transporter for antigen presentation (TAP) in tumor cells allows evasion of immune surveillance and increases tumorigenesis. *J Immunol*, *163*(8), 4224-4231. https://www.ncbi.nlm.nih.gov/pubmed/10510359

Kandoth, C., McLellan, M. D., Vandin, F., Ye, K., Niu, B., Lu, C., Xie, M., Zhang, Q., McMichael, J. F., Wyczalkowski, M. A., Leiserson, M. D. M., Miller, C. A., Welch, J. S., Walter, M. J., Wendl, M. C., Ley, T. J., Wilson, R. K., Raphael, B. J., & Ding, L. (2013). Mutational landscape and significance across 12 major cancer types. *Nature*, *502*(7471), 333-339. https://doi.org/10.1038/nature12634

Kane, M., Case, L. K., Kopaskie, K., Kozlova, A., MacDearmid, C., Chervonsky, A. V., & Golovkina, T. V. (2011). Successful transmission of a retrovirus depends on the commensal microbiota. *Science*, *334*(6053), 245-249. https://doi.org/10.1126/science.1210718

Kane, M., Deiss, F., Chervonsky, A., & Golovkina, T. V. (2018). A Single Locus Controls Interferon Gamma-Independent Antiretroviral Neutralizing Antibody Responses. *J Virol*, *92*(16). https://doi.org/10.1128/JVI.00725-18

Khan, A. A., Yurkovetskiy, L., O'Grady, K., Pickard, J. M., de Pooter, R., Antonopoulos, D. A., Golovkina, T., & Chervonsky, A. (2019). Polymorphic Immune Mechanisms Regulate Commensal Repertoire. *Cell Reports*, *29*(3), 541-550.e544. https://doi.org/https://doi.org/10.1016/j.celrep.2019.09.010

Kim, R., Emi, M., & Tanabe, K. (2007). Cancer immunoediting from immune surveillance to immune escape. *Immunology*, *121*(1), 1-14. https://doi.org/10.1111/j.1365-2567.2007.02587.x

Kim, S., Covington, A., & Pamer, E. G. (2017). The intestinal microbiota: Antibiotics, colonization resistance, and enteric pathogens. *Immunol Rev*, *279*(1), 90-105. https://doi.org/10.1111/imr.12563

Kobayashi, K. S., Chamaillard, M., Ogura, Y., Henegariu, O., Inohara, N., Nuñez, G., & Flavell, R. A. (2005). Nod2-Dependent Regulation of Innate and Adaptive Immunity in the Intestinal Tract. *Science*, *307*(5710), 731-734. https://doi.org/doi:10.1126/science.1104911

Kouttab, N. M., & Jutila, J. W. (1972). Friend leukemia virus infection in germfree mice following antigen stimulation. *J Immunol*, *108*(3), 591-595.

Kriegel, M. A., Rathinam, C., & Flavell, R. A. (2009). E3 ubiquitin ligase GRAIL controls primary T cell activation and oral tolerance. *Proc Natl Acad Sci U S A*, *106*(39), 16770-16775. https://doi.org/10.1073/pnas.0908957106

Kuss, S. K., Best, G. T., Etheredge, C. A., Pruijssers, A. J., Frierson, J. M., Hooper, L. V., Dermody, T. S., & Pfeiffer, J. K. (2011). Intestinal microbiota promote enteric virus replication

and systemic pathogenesis. *Science*, *334*(6053), 249-252. http://dx.doi.org/10.1126/science.1211057 http://www.ncbi.nlm.nih.gov/pubmed/21998395

Lee, E. Y. H. P., & Muller, W. J. (2010). Oncogenes and tumor suppressor genes. *Cold Spring Harbor perspectives in biology*, *2*(10), a003236-a003236. https://doi.org/10.1101/cshperspect.a003236

Li, Y., Hively, W. P., & Varmus, H. E. (2000). Use of MMTV-Wnt-1 transgenic mice for studying the genetic basis of breast cancer. *Oncogene*, *19*(8), 1002-1009. https://doi.org/10.1038/sj.onc.1203273

Liao, Y., Smyth, G. K., & Shi, W. (2014). featureCounts: an efficient general purpose program for assigning sequence reads to genomic features. *Bioinformatics*, *30*(7), 923-930. https://doi.org/10.1093/bioinformatics/btt656

Lind, M. H., Rozell, B., Wallin, R. P., van Hogerlinden, M., Ljunggren, H. G., Toftgard, R., & Sur, I. (2004). Tumor necrosis factor receptor 1-mediated signaling is required for skin cancer development induced by NF-kappaB inhibition. *Proc Natl Acad Sci U S A*, *101*(14), 4972-4977. https://doi.org/10.1073/pnas.0307106101

Lineberry, N. B., Su, L. L., Lin, J. T., Coffey, G. P., Seroogy, C. M., & Fathman, C. G. (2008). Cutting edge: The transmembrane E3 ligase GRAIL ubiquitinates the costimulatory molecule CD40 ligand during the induction of T cell anergy. *J Immunol*, *181*(3), 1622-1626. https://doi.org/10.4049/jimmunol.181.3.1622

Liou, G.-Y., & Storz, P. (2010). Reactive oxygen species in cancer. *Free radical research*, *44*(5), 479-496. https://doi.org/10.3109/10715761003667554

Lippitz, B. E. (2013). Cytokine patterns in patients with cancer: a systematic review. *Lancet Oncol*, *14*(6), e218-228. https://doi.org/10.1016/s1470-2045(12)70582-x

Littman, D. R., & Pamer, E. G. (2011). Role of the commensal microbiota in normal and pathogenic host immune responses. *Cell host & microbe*, *10*(4), 311-323. https://doi.org/10.1016/j.chom.2011.10.004

Lopez, L. R., Bleich, R. M., & Arthur, J. C. (2021). Microbiota Effects on Carcinogenesis: Initiation, Promotion, and Progression. *Annual Review of Medicine*, *72*(1), 243-261. https://doi.org/10.1146/annurev-med-080719-091604

Love, M. I., Huber, W., & Anders, S. (2014). Moderated estimation of fold change and dispersion for RNA-seq data with DESeq2. *Genome Biology*, *15*(12), 550. https://doi.org/10.1186/s13059-014-0550-8

Maeda, N., Fan, H., & Yoshikai, Y. (2008). Oncogenesis by retroviruses: old and new paradigms. *Rev Med Virol*, *18*(6), 387-405. https://doi.org/10.1002/rmv.592

Malkin, D., Li, F. P., Strong, L. C., Fraumeni, J. F., Jr., Nelson, C. E., Kim, D. H., Kassel, J., Gryka, M. A., Bischoff, F. Z., Tainsky, M. A., & et al. (1990). Germ line p53 mutations in a familial syndrome of breast cancer, sarcomas, and other neoplasms. *Science*, *250*(4985), 1233-1238. https://www.ncbi.nlm.nih.gov/pubmed/1978757

Mantovani, A., Sozzani, S., Locati, M., Allavena, P., & Sica, A. (2002). Macrophage polarization: tumor-associated macrophages as a paradigm for polarized M2 mononuclear phagocytes. *Trends in Immunology*, *23*(11), 549-555. https://doi.org/https://doi.org/10.1016/S1471-4906(02)02302-5

McMurdie, P. J., & Holmes, S. (2013). phyloseq: An R Package for Reproducible Interactive Analysis and Graphics of Microbiome Census Data. *PLOS ONE*, *8*(4), e61217. https://doi.org/10.1371/journal.pone.0061217

Medema, J. P., de Jong, J., Peltenburg, L. T. C., Verdegaal, E. M. E., Gorter, A., Bres, S. A., Franken, K. L. M. C., Hahne, M., Albar, J. P., Melief, C. J. M., & Offringa, R. (2001). Blockade of the granzyme B/perforin pathway through overexpression of the serine protease inhibitor PI-9/SPI-6 constitutes a mechanism for immune escape by tumors. *Proceedings of the National Academy of Sciences*, *98*(20), 11515-11520. https://doi.org/10.1073/pnas.201398198

Medzhitov, R. (2008). Origin and physiological roles of inflammation. *Nature*, *454*(7203), 428-435. https://doi.org/nature07201 [pii]
10.1038/nature07201

Meisel, M., Hinterleitner, R., Pacis, A., Chen, L., Earley, Z. M., Mayassi, T., Pierre, J. F., Ernest, J. D., Galipeau, H. J., Thuille, N., Bouziat, R., Buscarlet, M., Ringus, D. L., Wang, Y., Li, Y., Dinh, V., Kim, S. M., McDonald, B. D., Zurenski, M. A., . . . Jabri, B. (2018). Microbial signals drive pre-leukaemic myeloproliferation in a Tet2-deficient host. *Nature*, *557*(7706), 580-584. https://doi.org/10.1038/s41586-018-0125-z

Metelitsa, L. S., Naidenko, O. V., Kant, A., Wu, H. W., Loza, M. J., Perussia, B., Kronenberg, M., & Seeger, R. C. (2001). Human NKT cells mediate antitumor cytotoxicity directly by recognizing target cell CD1d with bound ligand or indirectly by producing IL-2 to activate NK cells. *J Immunol*, *167*(6), 3114-3122. https://doi.org/10.4049/jimmunol.167.6.3114

Mirand, E. A., & Grace, J. T., Jr. (1963). Responses of Germ-Free Mice to Friend Virus. *Nature*, *200*, 92-93. https://www.ncbi.nlm.nih.gov/pubmed/14074649

Mishra, R., Rajsiglová, L., Lukáč, P., Tenti, P., Šima, P., Čaja, F., & Vannucci, L. (2021). Spontaneous and Induced Tumors in Germ-Free Animals: A General Review. *Medicina (Kaunas, Lithuania)*, *57*(3), 260. https://doi.org/10.3390/medicina57030260

Moore, K. W., de Waal Malefyt, R., Coffman, R. L., & O'Garra, A. (2001). Interleukin-10 and the interleukin-10 receptor. *Annu Rev Immunol*, *19*, 683-765. https://doi.org/10.1146/annurev.immunol.19.1.683

Morris, T. L., Arnold, R. R., & Webster-Cyriaque, J. (2007). Signaling cascades triggered by bacterial metabolic end products during reactivation of Kaposi's sarcoma-associated herpesvirus. *J Virol*, *81*(11), 6032-6042. https://doi.org/10.1128/jvi.02504-06

Nagata, S., & Golstein, P. (1995). The Fas death factor. *Science*, *267*(5203), 1449-1456. https://doi.org/10.1126/science.7533326

Natividad, J. M. M., & Verdu, E. F. (2013). Modulation of intestinal barrier by intestinal microbiota: Pathological and therapeutic implications. *Pharmacological Research*, *69*(1), 42-51. https://doi.org/https://doi.org/10.1016/j.phrs.2012.10.007

Nurieva, R. I., Zheng, S., Jin, W., Chung, Y., Zhang, Y., Martinez, G. J., Reynolds, J. M., Wang, S. L., Lin, X., Sun, S. C., Lozano, G., & Dong, C. (2010). The E3 ubiquitin ligase GRAIL regulates T cell tolerance and regulatory T cell function by mediating T cell receptor-CD3 degradation. *Immunity*, *32*(5), 670-680. https://doi.org/10.1016/j.immuni.2010.05.002

Ochsenbein, A. F. (2002). Principles of tumor immunosurveillance and implications for immunotherapy. *Cancer Gene Ther*, *9*(12), 1043-1055. https://doi.org/10.1038/sj.cgt.7700540

Olson, B., Li, Y., Lin, Y., Liu, E. T., & Patnaik, A. (2018). Mouse Models for Cancer Immunotherapy Research. *Cancer Discovery*, *8*(11), 1358-1365. https://doi.org/10.1158/2159-8290.Cd-18-0044

Pasche, B. (2001). Role of transforming growth factor beta in cancer. *J Cell Physiol*, *186*(2), 153-168. https://doi.org/10.1002/1097-4652(200002)186:2<153::AID-JCP1016>3.0.CO;2-J

Patejko, M., Struck-Lewicka, W., Siluk, D., Waszczuk-Jankowska, M., & Markuszewski, M. J. (2018). Chapter One - Urinary Nucleosides and Deoxynucleosides. In G. S. Makowski (Ed.), *Advances in Clinical Chemistry* (Vol. 83, pp. 1-51). Elsevier. https://doi.org/https://doi.org/10.1016/bs.acc.2017.10.001

Perdiguero, E. G., & Geissmann, F. (2016). The development and maintenance of resident macrophages. *Nat Immunol*, *17*(1), 2-8. https://doi.org/10.1038/ni.3341

Petnicki-Ocwieja, T., Hrncir, T., Liu, Y.-J., Biswas, A., Hudcovic, T., Tlaskalova-Hogenova, H., & Kobayashi, K. S. (2009). Nod2 is required for the regulation of commensal microbiota in the intestine. *Proceedings of the National Academy of Sciences*, *106*(37), 15813-15818. https://doi.org/10.1073/pnas.0907722106

Poltorak, A., He, X., Smirnova, I., Liu, M.-Y., Huffel, C. V., Du, X., Birdwell, D., Alejos, E., Silva, M., Galanos, C., Freudenberg, M., Ricciardi-Castagnoli, P., Layton, B., & Beutler, B. (1998). Defective LPS Signaling in C3H/HeJ and C57BL/10ScCr Mice: Mutations in Tlr4 Gene. *Science*, *282*(5396), 2085-2088. https://doi.org/doi:10.1126/science.282.5396.2085

Quast, C., Pruesse, E., Yilmaz, P., Gerken, J., Schweer, T., Yarza, P., Peplies, J., & Glöckner, F. O. (2013). The SILVA ribosomal RNA gene database project: improved data processing and web-based tools. *Nucleic acids research*, *41*(Database issue), D590-D596. https://doi.org/10.1093/nar/gks1219

Quezada, S. A., Simpson, T. R., Peggs, K. S., Merghoub, T., Vider, J., Fan, X., Blasberg, R., Yagita, H., Muranski, P., Antony, P. A., Restifo, N. P., & Allison, J. P. (2010). Tumor-reactive CD4(+) T cells develop cytotoxic activity and eradicate large established melanoma after transfer into lymphopenic hosts. *J Exp Med*, *207*(3), 637-650. https://doi.org/10.1084/jem.20091918

Rakoff-Nahoum, S., & Medzhitov, R. (2007). Regulation of spontaneous intestinal tumorigenesis through the adaptor protein MyD88 [Research Support, N.I.H., Extramural

Research Support, Non-U.S. Gov't]. *Science*, *317*(5834), 124-127. https://doi.org/10.1126/science.1140488

Raskov, H., Orhan, A., Christensen, J. P., & Gögenur, I. (2021). Cytotoxic CD8+ T cells in cancer and cancer immunotherapy. *British Journal of Cancer*, *124*(2), 359-367. https://doi.org/10.1038/s41416-020-01048-4

Reddy, B. S., Narisawa, T., Wright, P., Vukusich, D., Weisburger, J. H., & Wynder, E. L. (1975). Colon carcinogenesis with azoxymethane and dimethylhydrazine in germ-free rats [Comparative Study
Research Support, U.S. Gov't, Non-P.H.S.
Research Support, U.S. Gov't, P.H.S.]. *Cancer Res*, *35*(2), 287-290. http://www.ncbi.nlm.nih.gov/pubmed/162868

Rehman, A., Sina, C., Gavrilova, O., Häsler, R., Ott, S., Baines, J. F., Schreiber, S., & Rosenstiel, P. (2011). Nod2 is essential for temporal development of intestinal microbial communities. *Gut*, *60*(10), 1354-1362. https://doi.org/10.1136/gut.2010.216259

Riquelme, E., Zhang, Y., Zhang, L., Montiel, M., Zoltan, M., Dong, W., Quesada, P., Sahin, I., Chandra, V., San Lucas, A., Scheet, P., Xu, H., Hanash, S. M., Feng, L., Burks, J. K., Do, K. A., Peterson, C. B., Nejman, D., Tzeng, C. D., . . . McAllister, F. (2019). Tumor Microbiome Diversity and Composition Influence Pancreatic Cancer Outcomes. *Cell*, *178*(4), 795-806.e712. https://doi.org/10.1016/j.cell.2019.07.008

Robertson, S. J., Ammann, C. G., Messer, R. J., Carmody, A. B., Myers, L., Dittmer, U., Nair, S., Gerlach, N., Evans, L. H., Cafruny, W. A., & Hasenkrug, K. J. (2008). Suppression of acute anti-friend virus CD8+ T-cell responses by coinfection with lactate dehydrogenase-elevating virus. *J Virol*, *82*(1), 408-418. https://doi.org/10.1128/jvi.01413-07

Robertson, S. J., Messer, R. J., Carmody, A. B., & Hasenkrug, K. J. (2006). In vitro suppression of CD8+ T cell function by Friend virus-induced regulatory T cells. *J Immunol*, *176*(6), 3342-3349. https://www.ncbi.nlm.nih.gov/pubmed/16517701

Robinson, H. L. (1982). Retroviruses and Cancer. *Reviews of Infectious Diseases*, *4*(5), 1015-1025. https://doi.org/10.1093/clinids/4.5.1015

Rossi, T., Vergara, D., Fanini, F., Maffia, M., Bravaccini, S., & Pirini, F. (2020). Microbiota-Derived Metabolites in Tumor Progression and Metastasis. *Int J Mol Sci*, *21*(16). https://doi.org/10.3390/ijms21165786

Roukos, D. H., Murray, S., & Briasoulis, E. (2007). Molecular genetic tools shape a roadmap towards a more accurate prognostic prediction and personalized management of cancer. *Cancer Biology & Therapy*, *6*(3), 308-312. https://doi.org/10.4161/cbt.6.3.3994

Rowe, W. P., Pugh, W. E., & Hartley, J. W. (1970). Plaque assay techniques for murine leukemia viruses. *Virology*, *42*(4), 1136-1139.

Ruedl, C., & Jung, S. (2018). DTR-mediated conditional cell ablation-Progress and challenges. *Eur J Immunol*, *48*(7), 1114-1119. https://doi.org/10.1002/eji.201847527

Sabit, H., Cevik, E., & Tombuloglu, H. (2019). Colorectal cancer: The epigenetic role of microbiome. *World journal of clinical cases*, *7*(22), 3683-3697. https://doi.org/10.12998/wjcc.v7.i22.3683

Sarma-Rupavtarm, R. B., Ge, Z., Schauer, D. B., Fox, J. G., & Polz, M. F. (2004). Spatial distribution and stability of the eight microbial species of the altered schaedler flora in the mouse gastrointestinal tract. *Appl Environ Microbiol*, *70*(5), 2791-2800. http://www.ncbi.nlm.nih.gov/pubmed/15128534

Shankaran, V., Ikeda, H., Bruce, A. T., White, J. M., Swanson, P. E., Old, L. J., & Schreiber, R. D. (2001). IFNgamma and lymphocytes prevent primary tumour development and shape tumour immunogenicity. *Nature*, *410*(6832), 1107-1111. https://doi.org/10.1038/35074122

Singh, R. K., Chang, H.-W., Yan, D., Lee, K. M., Ucmak, D., Wong, K., Abrouk, M., Farahnik, B., Nakamura, M., Zhu, T. H., Bhutani, T., & Liao, W. (2017). Influence of diet on the gut microbiome and implications for human health. *Journal of translational medicine*, *15*(1), 73-73. https://doi.org/10.1186/s12967-017-1175-y

Sivan, A., Corrales, L., Hubert, N., Williams, J. B., Aquino-Michaels, K., Earley, Z. M., Benyamin, F. W., Lei, Y. M., Jabri, B., Alegre, M. L., Chang, E. B., & Gajewski, T. F. (2015). Commensal Bifidobacterium promotes antitumor immunity and facilitates anti-PD-L1 efficacy. *Science*, *350*(6264), 1084-1089. https://doi.org/10.1126/science.aac4255

Sonnenburg, E. D., Smits, S. A., Tikhonov, M., Higginbottom, S. K., Wingreen, N. S., & Sonnenburg, J. L. (2016). Diet-induced extinctions in the gut microbiota compound over generations. *Nature*, *529*(7585), 212-215. https://doi.org/10.1038/nature16504

Spring, J., Lara, S., Khan, A. A., O'Grady, K., Wilks, J., Gurbuxani, S., Erickson, S., Fischbach, M., Jacobson, A., Chervonsky, A., & Golovkina, T. (2022). Gut commensal bacteria enhance pathogenesis of a tumorigenic murine retrovirus. *bioRxiv*, 2022.2002.2002.478820. https://doi.org/10.1101/2022.02.02.478820

Staveley-O'Carroll, K., Sotomayor, E., Montgomery, J., Borrello, I., Hwang, L., Fein, S., Pardoll, D., & Levitsky, H. (1998). Induction of antigen-specific T cell anergy: An early event in the course of tumor progression. *Proc Natl Acad Sci U S A*, *95*(3), 1178-1183. https://doi.org/10.1073/pnas.95.3.1178

ten Berge, R. L., Meijer, C. J., Dukers, D. F., Kummer, J. A., Bladergroen, B. A., Vos, W., Hack, C. E., Ossenkoppele, G. J., & Oudejans, J. J. (2002). Expression levels of apoptosis-related proteins predict clinical outcome in anaplastic large cell lymphoma. *Blood*, *99*(12), 4540-4546. https://doi.org/10.1182/blood.v99.12.4540

Thursby, E., & Juge, N. (2017). Introduction to the human gut microbiota. *The Biochemical journal*, *474*(11), 1823-1836. https://doi.org/10.1042/BCJ20160510

Toes, R. E., Ossendorp, F., Offringa, R., & Melief, C. J. (1999). CD4 T cells and their role in antitumor immune responses. *The Journal of experimental medicine*, *189*(5), 753-756. https://doi.org/10.1084/jem.189.5.753

Topping, D. L., & Clifton, P. M. (2001). Short-Chain Fatty Acids and Human Colonic Function: Roles of Resistant Starch and Nonstarch Polysaccharides. *Physiological Reviews*, *81*(3), 1031-1064. https://doi.org/10.1152/physrev.2001.81.3.1031

Uchiyama, R., Chassaing, B., Zhang, B., & Gewirtz, A. T. (2014). Antibiotic treatment suppresses rotavirus infection and enhances specific humoral immunity. *The Journal of infectious diseases*, *210*(2), 171-182. https://doi.org/10.1093/infdis/jiu037

Uhlen, M., Zhang, C., Lee, S., Sjöstedt, E., Fagerberg, L., Bidkhori, G., Benfeitas, R., Arif, M., Liu, Z., Edfors, F., Sanli, K., von Feilitzen, K., Oksvold, P., Lundberg, E., Hober, S., Nilsson, P., Mattsson, J., Schwenk, J. M., Brunnström, H., . . . Ponten, F. (2017). A pathology atlas of the human cancer transcriptome. *Science*, *357*(6352). https://doi.org/10.1126/science.aan2507

Vetizou, M., Pitt, J. M., Daillere, R., Lepage, P., Waldschmitt, N., Flament, C., Rusakiewicz, S., Routy, B., Roberti, M. P., Duong, C. P., Poirier-Colame, V., Roux, A., Becharef, S., Formenti, S., Golden, E., Cording, S., Eberl, G., Schlitzer, A., Ginhoux, F., . . . Zitvogel, L. (2015). Anticancer immunotherapy by CTLA-4 blockade relies on the gut microbiota. *Science*, *350*(6264), 1079-1084. https://doi.org/10.1126/science.aad1329

Vinay, D. S., Ryan, E. P., Pawelec, G., Talib, W. H., Stagg, J., Elkord, E., Lichtor, T., Decker, W. K., Whelan, R. L., Kumara, H. M., Signori, E., Honoki, K., Georgakilas, A. G., Amin, A., Helferich, W. G., Boosani, C. S., Guha, G., Ciriolo, M. R., Chen, S., . . . Kwon, B. S. (2015). Immune evasion in cancer: Mechanistic basis and therapeutic strategies. *Semin Cancer Biol*, *35 Suppl*, S185-198. https://doi.org/10.1016/j.semcancer.2015.03.004

Vogt, L., Schmitz, N., Kurrer, M. O., Bauer, M., Hinton, H. I., Behnke, S., Gatto, D., Sebbel, P., Beerli, R. R., Sonderegger, I., Kopf, M., Saudan, P., & Bachmann, M. F. (2006). VSIG4, a B7 family-related protein, is a negative regulator of T cell activation. *J Clin Invest*, *116*(10), 2817-2826. https://doi.org/10.1172/JCI25673

Vogt, P. K. (2012). Retroviral oncogenes: a historical primer. *Nat Rev Cancer*, *12*(9), 639-648. https://doi.org/10.1038/nrc3320

White, M. K., Pagano, J. S., & Khalili, K. (2014). Viruses and Human Cancers: a Long Road of Discovery of Molecular Paradigms. *Clinical Microbiology Reviews*, *27*(3), 463-481. https://doi.org/doi:10.1128/CMR.00124-13

Whiteside, T. L. (2008). The tumor microenvironment and its role in promoting tumor growth. *Oncogene*, *27*(45), 5904-5912. https://doi.org/10.1038/onc.2008.271

Wickham, H. (2009). *ggplot2: Elegant Graphics for Data Analysis*. Springer Publishing Company, Incorporated.

Wikoff, W. R., Anfora, A. T., Liu, J., Schultz, P. G., Lesley, S. A., Peters, E. C., & Siuzdak, G. (2009). Metabolomics analysis reveals large effects of gut microflora on mammalian blood metabolites. *Proceedings of the National Academy of Sciences*, *106*(10), 3698-3703. https://doi.org/doi:10.1073/pnas.0812874106

Wilks, J., Beilinson, H., & Golovkina, T. V. (2013). Dual role of commensal bacteria in viral infections. *Immunological reviews*, *255*(1), 222-229. https://doi.org/10.1111/imr.12097

Wilks, J., Beilinson, H., Theriault, B., Chervonsky, A., & Golovkina, T. (2014). Antibody-mediated immune control of a retrovirus does not require the microbiota. *J Virol*, *88*(11), 6524-6527. https://doi.org/10.1128/JVI.00251-14
Wilks, J., & Golovkina, T. (2012). Influence of Microbiota on Viral Infections. *PLOS Pathogens*, *8*(5), e1002681. https://doi.org/10.1371/journal.ppat.1002681

Wilks, J., Lien, E., Jacobson, A. N., Fischbach, M. A., Qureshi, N., Chervonsky, A. V., & Golovkina, T. V. (2015). Mammalian Lipopolysaccharide Receptors Incorporated into the Retroviral Envelope Augment Virus Transmission. *Cell host & microbe*, *18*(4), 456-462. https://doi.org/10.1016/j.chom.2015.09.005

Xie, Y., Akpinarli, A., Maris, C., Hipkiss, E. L., Lane, M., Kwon, E.-K. M., Muranski, P., Restifo, N. P., & Antony, P. A. (2010). Naive tumor-specific CD4+ T cells differentiated in vivo eradicate established melanoma. *Journal of Experimental Medicine*, *207*(3), 651-667. https://doi.org/10.1084/jem.20091921

Xu, H., Liu, M., Cao, J., Li, X., Fan, D., Xia, Y., Lu, X., Li, J., Ju, D., & Zhao, H. (2019). The Dynamic Interplay between the Gut Microbiota and Autoimmune Diseases. *Journal of immunology research*, *2019*, 7546047-7546047. https://doi.org/10.1155/2019/7546047

Xu, S., Sun, Z., Li, L., Liu, J., He, J., Song, D., Shan, G., Liu, H., & Wu, X. (2010). Induction of T cells suppression by dendritic cells transfected with VSIG4 recombinant adenovirus. *Immunol Lett*, *128*(1), 46-50. https://doi.org/10.1016/j.imlet.2009.11.003

Xu, Y., & Baltimore, D. (1996). Dual roles of ATM in the cellular response to radiation and in cell growth control. *Genes Dev*, *10*(19), 2401-2410. https://www.ncbi.nlm.nih.gov/pubmed/8843193

Yamamoto, M. L., Maier, I., Dang, A. T., Berry, D., Liu, J., Ruegger, P. M., Yang, J. I., Soto, P. A., Presley, L. L., Reliene, R., Westbrook, A. M., Wei, B., Loy, A., Chang, C., Braun, J., Borneman, J., & Schiestl, R. H. (2013). Intestinal bacteria modify lymphoma incidence and latency by affecting systemic inflammatory state, oxidative stress, and leukocyte genotoxicity. *Cancer Res*, *73*(14), 4222-4232. https://doi.org/10.1158/0008-5472.CAN-13-0022

Yoshimoto, S., Loo, T. M., Atarashi, K., Kanda, H., Sato, S., Oyadomari, S., Iwakura, Y., Oshima, K., Morita, H., Hattori, M., Honda, K., Ishikawa, Y., Hara, E., & Ohtani, N. (2013). Obesity-induced gut microbial metabolite promotes liver cancer through senescence secretome [Research Support, Non-U.S. Gov't]. *Nature*, *499*(7456), 97-101. https://doi.org/10.1038/nature12347

Yu, L. X., & Schwabe, R. F. (2017). The gut microbiome and liver cancer: mechanisms and clinical translation. *Nat Rev Gastroenterol Hepatol*, *14*(9), 527-539. https://doi.org/10.1038/nrgastro.2017.72

Zeng, Z., Surewaard, B. G., Wong, C. H., Geoghegan, J. A., Jenne, C. N., & Kubes, P. (2016). CRIg Functions as a Macrophage Pattern Recognition Receptor to Directly Bind and Capture Blood-Borne Gram-Positive Bacteria. *Cell Host Microbe*, *20*(1), 99-106. https://doi.org/10.1016/j.chom.2016.06.002

Zilfou, J. T., & Lowe, S. W. (2009). Tumor suppressive functions of p53. *Cold Spring Harb Perspect Biol*, *1*(5), a001883. https://doi.org/10.1101/cshperspect.a001883

Zitvogel, L., Galluzzi, L., Viaud, S., Vétizou, M., Daillère, R., Merad, M., & Kroemer, G. (2015). Cancer and the gut microbiota: an unexpected link. *Science translational medicine*, *7*(271), 271ps271-271ps271. https://doi.org/10.1126/scitranslmed.3010473